QUENCH OF CYLINDRICAL TUBES DURING TRANSITION FROM FILM TO NUCLEATE BOILING HEAT TRANSFER

QUENCH OF CYLINDRICAL TUBES DURING TRANSITION FROM FILM TO NUCLEATE BOILING HEAT TRANSFER IN CANDU REACTOR CORE

By

KIFAH J. TAKROURI, Msc.

A Thesis

Submitted to the School of Graduate Studies

in Partial Fulfillment of the Requirements for the Degree of

Doctoral In Engineering Physics

McMaster University

Doctoral Degree (2011)
(Engineering Physics)

McMaster University
Hamilton, Ontario

TITLE: QUENCH OF CYLINDRICAL TUBES DURING TRANSITION FROM FILM TO NUCLEATE BOILING HEAT TRANSFER IN CANDU REACTOR CORE

AUTHER: Kifah J. Takrouri, MSc. (Jordan University of Science and Technology)

SUPERVISOR: Dr. John Luxat

NUMBER OF PAGES: xvii, 139

Abstract

Study of quench cooling is very important in nuclear reactor safety for limiting the extent of core damage during the early stages of severe accidents after Loss of Coolant Accidents (LOCA). Quench of a hot dry surface involves the rapid decrease in surface temperature resulting from bringing the hot surface into sudden contact with a coolant at a lower temperature. The quench temperature is the onset of the rapid decrease in the surface temperature and corresponds to the onset of destabilization of a vapor film that exists between the hot surface and the coolant. Re-wetting the surface is the establishment of direct contact between the surface and the liquid at the so-called re-wetting temperature. Re-wetting is characterized by the formation of a wet patch on the surface which then spreads to cover the entire surface. Situations involving quench and re-wetting heat transfer are encountered in a number of postulated accidents in Canada Deuterium Uranium (CANDU) reactors, such as re-wetting of a hot dry calandria tube in a critical break LOCA. This accident results in high heat transfer from the calandria tube to the surrounding moderator liquid which can cause the calandria tube surface to experience dryout and a subsequent escalation in the surface temperature. If the calandria tube temperature is not reduced by initiation of quench heat transfer, then this may lead to subsequent fuel channel failure. In literature very limited knowledge is available on quench and re-wetting of hot curved surfaces like the calandria tubes.

In this study, a Water Quench Facility (WQF) has been constructed and a series of experiments were conducted to investigate the quench and re-wetting of hot horizontal tubes by a vertical rectangular water multi-jet system. The tubes were heated to a temperature between 380-800°C in a controlled temperature furnace then cooled to the jet temperature. The temperature variation with time in the circumferential and the axial directions of the tubes has been measured. The two-phase flow behavior and the propagation of the re-wetting front around and along the tubes were simultaneously observed by using a high-speed camera. The effects of several parameters on the cooling process have been investigated. These parameters include: initial surface temperature, water subcooling (in the range 15-80°C), jet velocity (in the range 0.15-1.60 m/s), tube solid material (brass, steel and Alumina), surface curvature, tube wall thickness, jet orientation and number of jets. The variables studied include the re-wetting delay time (time to quench after initiating the cooling process), the re-wetting front propagation velocity, the quench and re-wetting temperatures, the quench cooling rates and the boiling region size. The quench and the re-wetting temperatures as well as the re-wetting delay time were found to be a strong function of water subcooling. The quench and re-wetting temperatures increase with increasing water subcooling. The re-wetting delay time decreases with increasing the water subcooling, decreasing initial surface temperature, increasing liquid velocity and decreasing the surface curvature. The re-wetting front velocity is mainly dependent on the initial surface

temperature and water subcooling. The re-wetting velocity increases by decreasing the initial surface temperature and by increasing the water subcooling. Decreasing the surface curvature was found to also increase the re-wetting front velocity. Correlations of the phenomena studied have been developed and provided good prediction of the experimental data collected in this study and data available from literature. The results of this study provide novel knowledge and an experimental database for mechanistic modeling of quench heat transfer on calandria tube surfaces that experience dryout and film boiling.

Acknowledgements

I would like to thank Dr. John Luxat, Dr. Mohamed Hamed, Dr. David Novog and Dr. Alaa Hassan for supervising this work and for their support and encouragement.

I would like to thank the technicians at The Student Workshops for their suggestions and advice during the design and construction of the experimental setup.

I would like to thank all friends and colleagues at the departments of Engineering Physic and Mechanical Engineering.

Special thanks to all my family members for their continuous support and many thanks to everyone helped throughout this work.

Table of Contents

Nomenclature

Symbol	Unit	Description
t	sec	Time
t_d	sec	Re-wetting delay time
T_{wall}	°C	Wall temperature
T_{in}	°C	Initial surface temperature
T_{sat}	°C	Liquid saturation temperature
T_{water}	°C	Water temperature
T_{mfb}	°C	Minimum film boiling temperature
T_{rw}	°C	Re-wetting temperature
T_q	°C	Quench temperature
q	$J/m^2.°C$	Heat flux
d	m	Tube diameter
r	m	Radial position
d_{jet}	m	Jet diameter
w_{jet}	m	Width of the jet
V_{jet}	m/sec	Jet velocity
u_{rw}	m/sec	Re-wetting front velocity
k	W/m.K	Thermal conductivity
x	m	Distance in x direction
γ	-	Proportionality constant
h	$W/m^2.K$	Heat transfer coefficient
ΔT_{sub}	°C	Degree of liquid subcooling
ρ	kg/m^3	Density
C	J/kg.°C	Specific heat capacity
a	$cm/sec.°C^b$	Constant in re-wetting front velocity correlation
b	-	Constant in re-wetting front velocity correlation
B	sec/cm	Constant in re-wetting front velocity correlation
n	sec/cm	Constant in re-wetting front velocity correlation
R	°C/sec	Cooling rate
R_{vapor}	°C/sec	Cooling rate of vapor film boiling
$R_{nucleate}$	°C/sec	Cooling rate of nucleate boiling region

Subscripts

in	Initial	vapor	Vapor film boiling
solid	Solid material	nucleate	Nucleate boiling
sub	Subcooling	rw	Re-wetting
sat	Saturation	mfb	Minimum film boiling
water	Water		

Abbreviations

Abbreviation	Meaning
LOCA	Loss of Coolant Accident
CANDU	Canada Deuterium Uranium
ECCS	Emergency Core Cooling System
WQF	Water Quench Facility
DAQ	Data Acquisition System
NB	Nucleate Boiling
TB	Transition Boiling
TC	Thermocouple
fps	Frames per second
Leid	Leidenfrost

List of Figures

List of Tables

Chapter One

Introduction

1.1 Background: Boiling and Quench Cooling

Quench cooling of a hot dry surface involves the rapid decrease in surface temperature resulting from bringing the hot surface into sudden contact with a coolant at a lower temperature prior to the hot surface being re-wetted by the coolant. Quench temperature can be defined as the onset of the rapid decrease in the surface temperature and corresponds to the onset of destabilization of a vapor film that exists between the hot surface and the coolant. Situations involving quench heat transfer are encountered in a number of postulated accidents in Canada Deuterium Uranium (CANDU) reactors, such as quenching of hot fuel elements experiencing post – dryout conditions during a loss of flow accident or quenching of a hot calandria tube in certain loss of coolant accidents (LOCA) in which a pressure tube balloons (deforms) into contact with its calandria tube. A great deal of knowledge on quench phenomena has originated from the field of nuclear power engineering. Other situations involving quench heat transfer include hardening of metals in metallurgical industries, start-up of liquid natural gas pipe lines, microelectronic device production and filling of cryogenic vessels [1].

The core of a CANDU reactor is contained within a large horizontal cylindrical tank called the calandria vessel. The calandria vessel is 6 m long and 7.6 m in diameter in a CANDU-6 reactor and 8.5 m in diameter in a 900MW CANDU reactor. The core contains 380 horizontal fuel channels (CANDU-6) or 480 horizontal fuel channels (900MW CANDU) surrounded by heavy water moderator. Each fuel channel consists of an inner tube (pressure tube) which contains fuel bundles, and an outer tube (calandria tube) which is approximately 130 mm in diameter. One of the scenarios that can lead to the progression to a severe accident following a LOCA, accompanied by the impairment of the Emergency Core Cooling System ECCS, is the early and sustained overheating of a pressure tube for a time sufficient to cause failure of the fuel channel (i.e. failure of both a pressure tube and its calandria tube). However, an accident of greater interest that does not involve impairment of the emergency core cooling system is a loss of coolant accident referred to as a critical break LOCA in which the fuel channel integrity may be challenged by a pressure tube ballooning and a potential key of the calandria tube low subcooling of the moderator. This accident is of interest since it involves potential dry out and quench of an overheated calandria tube.

Another scenario of interest is cooling of the calandria tubes outer surface in the Pickering A reactor during reactor operation with a reduced moderator level or following infrequent moderator dump. Under such conditions, the calandria tubes are not in continuous contact with the moderator and are subject to heating. To prevent overheating of the calandria tubes, cooling water is provided by spray nozzles located at the top of the calandria shell.

In a critical break LOCA the coolant flow in a fuel channel can become very low for a sustained period of time while the heat transport system pressure is still high. During this period of low coolant flow the fuel heats up causing the pressure to increase sufficiently resulting in ballooning deformation of the pressure tube into contact with its calandria tube. Contact between the hot pressure tube and the cold calandria tube results in high heat transfer between the two contacting tubes. In turn, this results in high heat transfer from the calandria tube to the surrounding moderator liquid. This can cause the calandria tube surface to experience dry out and a subsequent escalation in the temperature of the calandria tube [2, 3]. If the calandria tube temperature is not reduced by initiation of quench heat transfer, then it is possible that both the pressure tube and the calandria tube can continue to experience ballooning deformation leading to subsequent fuel channel failure. The extent and duration of dry out on the calandria tube surface is governed by both the heat flux from the pressure tube and the subcooling of the moderator liquid [3]. Quenching of the calandria tube surface is dependent on de-superheating the vapor film that forms on the tube following the onset of dry out. After some time, the vapor film starts to destabilize at a critical thickness when the vapor generation is not sufficient to sustain the vapor film [2, 4]. Then, a rapid decrease in surface temperature starts to take place (at the quench temperature) after which the liquid re-establishes contact with the surface at the so-called "re-wetting temperature". The re-wetting temperature can be defined as the maximum surface temperature at which liquid-solid contact occurs and can be obtained from measurement of the surface temperature and simultaneous observation of the liquid-surface interface. The quench temperature, as well as the re-wetting temperature, are not constant and depend on fluid properties, surface material and the surrounding environment [5]. After re-wetting is established, a wet patch is initiated which spreads and results in the formation of a re-wetting front. The re-wetting front travels in the direction of liquid flow (a rebound in the re-wetting front motion has been observed in this study; this observation is discussed in Chapter Five: Results and Discussion). Upstream of the re-wetting front, single-phase forced convection and nucleate boiling exist, and film boiling prevails downstream [6]. At the front itself, transition and nucleate boiling co-exist and liquid drops of several sizes are ejected from the surface and a cloud of steam is generated due to vigorous boiling. One of the observations of this study, which was reported by few researchers [7, 8], is lifting a thin sheet of liquid from the hot surface at the re-wetting front. This lifting is most likely due to rapid vapor generation at the outer boundary of the re-wetting front. Due to surface tension,

the sheet breaks down to a large number of droplets further downstream [8]. Re-wetting may also be initiated when a two-phase region, and not only a single-phase region, is put into contact with a hot surface given that the region contains sufficient liquid [3].

If the time to reach the moment of vapor film destabilization is long enough, the calandria surface temperature may increase excessively due to the stored and decay heats in the fuel elements and, in the worst case, this may lead to failure of the fuel channel.

The determination of the quench and re-wetting temperatures in the reactor is very important for limiting the extent of core damage during the early stages of severe accidents and is essential for predicting the rate at which the coolant quenches an overheated core.

Due to the wide application of quenching in industry, many analytical and experimental studies have been carried out to obtain better understanding of the quench phenomena. These studies can be divided into two main categories depending on the interest of the study: the first category interests in understanding the mechanism of heat transfer and fluid flow during the quench process. The second category interests in the mechanical properties of the quenched surface, such as strength, toughness and hardness, where the product quality greatly depends on the cooling method employed during the manufacturing process, as in metallurgical industry. This study belongs to the first category. Research in this area is of great importance and great practical value since, for example, in reactor safety analysis, the initial temperature around which quench cooling is initiated is typically 700°C and in metallurgical industry, is typically 800°C for steel production and 450°C for aluminum alloys [8].

1.2 Definition and Estimation of Quench and Re-Wetting Temperatures

In literature, there is still no single unique definition of the quench temperature. Some researchers use both terms (quench and re-wetting temperatures) to describe the temperature at which the liquid coolant re-establishes wetted contact with the hot dry surface [10, 11]. Others [12, 13, 14, and 15] define the quench temperature as the onset of the rapid decrease in surface temperature and the re-wetting temperature as the direct liquid-solid contact temperature. This later definition has been adopted in this study and therefore, the quench temperature is generally higher than the re-wetting temperature. Some researchers define the re-wetting temperature as the Leidenfrost temperature [16, 17] and others considered it as the minimum film boiling temperature [18]. F. Gunnerson [12] defined re-wetting as the direct liquid-solid contact and the establishment of a liquid-solid-vapor triple interface. Barnea [40] considered the re-wetting temperature as the

highest temperature at which the slope of the cooling curve exceeds an arbitrary value of 500°C/sec.

As the surface quenches, very complex heat transfer and two-phase flow phenomena occur. The quenching process involves many sub-processes which are complicated themselves. Quenching consists of two simultaneous processes: the first process is rapid transition from film boiling to nucleate boiling and convective heat transfer through a transition boiling region. All these modes of heat transfer can exist simultaneously at different spatial locations on the surface. The second process is rapid heat conduction within the solid. More details of the quench process can be obtained by looking at the boiling curve.

1.3 Boiling Curve

The boiling heat transfer process is usually represented by plotting the surface heat flux, q", as a function of the wall superheat (difference between wall temperature and the liquid saturation temperature) yielding the boiling curve shown in Figure 1. The two-phase flow pattern in each boiling zone is also shown. The following paragraphs describe the various terms included in the boiling curve which will be used extensively throughout this study.

1.3.1 Single-Phase Forced Convection Region

In this region, heat transfer to a fluid flowing past a hot surface occurs in the absence of boiling. This region is governed by Newton's law of cooling and usually extends to wall temperatures exceeding that of liquid saturation by few degrees and continues till the Onset of Nucleate Boiling Point shown in Figure 1.

1.3.2 Nucleate Boiling Region

This region starts at the Onset of Nucleate Boiling Point, A, and continues till point B, the maximum heat flux point. Point A is usually a few degrees (~5°C) higher than the saturation point, where vapor may form in surface cavities. These few degrees are required for the vapor to emerge from cavities and form stable discrete bubbles that can detach from the surface. Isolated bubbles form at the beginning of this region and many larger bubbles form as the wall temperature increases. This region is characterized by a large increase in heat transfer induced by relatively small changes in wall temperature. This region is attractive for many high-heat-flux cooling applications provided that the maximum heat flux point is known.

1.3.3 Transition Region

Beyond point B, bubble formation is so rapid such that the vapour forms an unstable film at the surface, with intermittent liquid-surface contacts, which causes the heat transfer to decline. At a certain point on the surface, oscillation between nucleate and film boiling may occur. This region continues till point C, the minimum heat flux and minimum heat flux temperature point.

1.3.4 Film Boiling Region

Beyond point C, the vapour forms a stable film that completely covers the surface. This is the region which has to be avoided during normal operation of water-cooled nuclear reactors. It is well accepted now that the thickness of this film increases as the surface temperature increases or as the coolant subcooling decreases. The primary heat transfer mode in this region is forced convection through the vapour film augmented by radiation heat transfer at higher surface temperatures. The nature of the vapour/liquid interface also has an effect on the rate of heat transfer in film boiling. As the disturbances in the vapour/liquid interface increases, the area of convection heat transfer to the liquid increases.

After quenching, direct liquid-solid contact may occur. Observations of this study showed that, for certain combinations of wall and coolant temperatures, there is a possibility of the vapour film to re-appear after collapsing.

1.3.5 Heat Transfer Coefficient

Experimental studies have shown that during quenching the effective surface heat transfer coefficient varies more than two orders of magnitude with surface temperature [19]. The accuracy of theoretical analysis of quench phenomena greatly depends on the boundary conditions provided. It was pointed out that the most significant factor limiting theoretical studies of quenching is the uncertainty in the surface boundary conditions and the heat transfer coefficient is the most important boundary condition required [8]. The heat transfer coefficient in quenching was found to be affected by initial surface temperature, surface roughness, surface geometry, surface orientation, coolant subcooling and flow velocity [19].

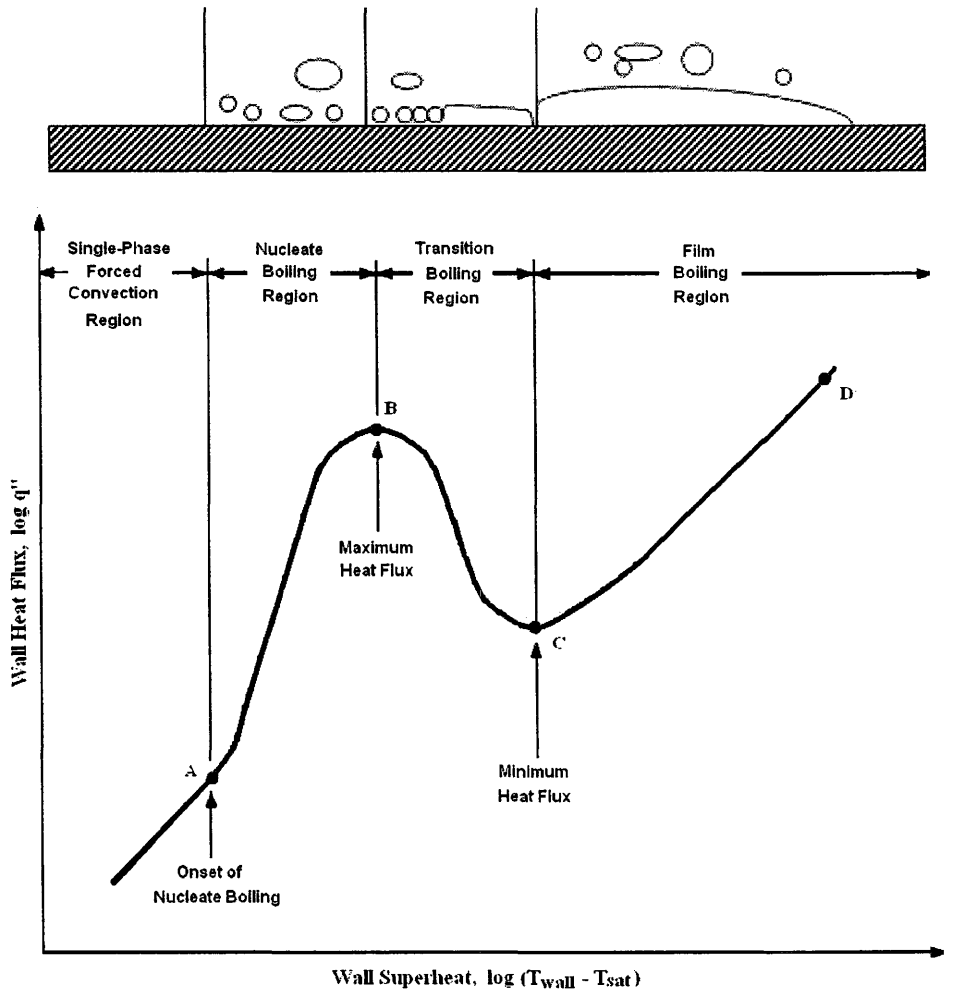

Figure 1: Typical Pool Boiling Curve.

1.4 Cooling Profile

More information on quench phenomena can be obtained by examining the temperature history of the surface being quenched. A typical cooling profile during quenching is shown in Figure 2. The figure shows the temperature at a specific location on the hot surface as a function of time. The different flow patterns are also shown. In quench studies, the cooling profile is used more frequently than the boiling curve.

As shown in Figure 2, the film boiling region is characterized by slow cooling rate where the vapor film separates the liquid from contact with the surface. However, liquid-surface contact drastically increases the cooling rate in the transition and nucleate boiling regions. The cooling time from the minimum heat

flux point to the end of boiling is generally short in comparison with the duration of film boiling.

The quench temperature can be determined from this profile by determining the intersection point between the tangent lines drawn at the profile before and after the region of the rapid decrease in temperature. Specifically, the quench temperature can be defined as the temperature at the intersection between the tangent line to the cooling profile in the film boiling region, with the tangent line at the point where the profile's slope is steepest, as shown in Figure 3. This definition does not assume surface re-wetting. The re-wetting temperature is difficult to be determined from the measured cooling profile alone and, usually, experimental observation is needed. Generally, its location is as shown in Figure 3 and might be approximated by the point where a slope change in the cooling profile occurs [12].

In this study, five distinct cooling profiles were obtained depending on the operating conditions of water temperature, initial surface temperature and solid material. These profiles will be discussed in Section 4.1 in Chapter Four.

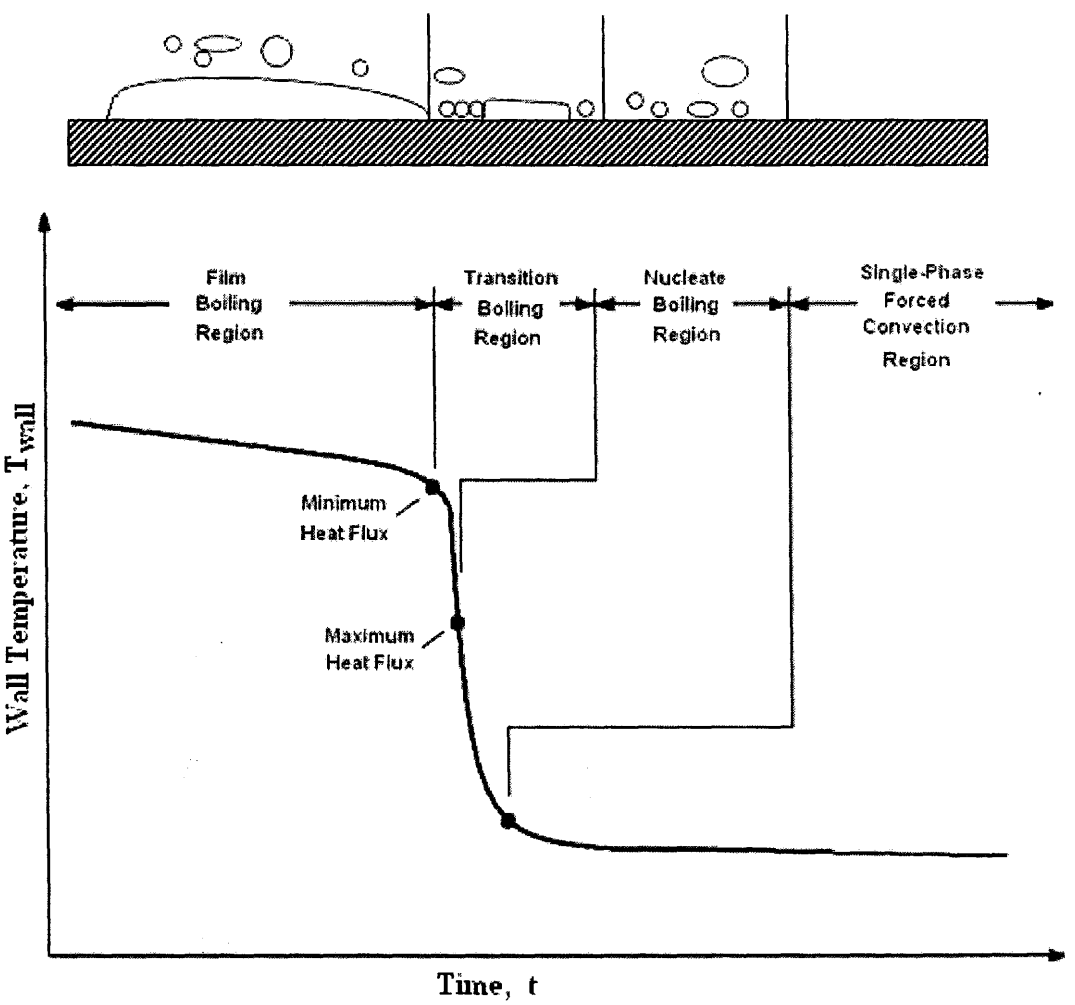

Figure 2: Typical Cooling Profile.

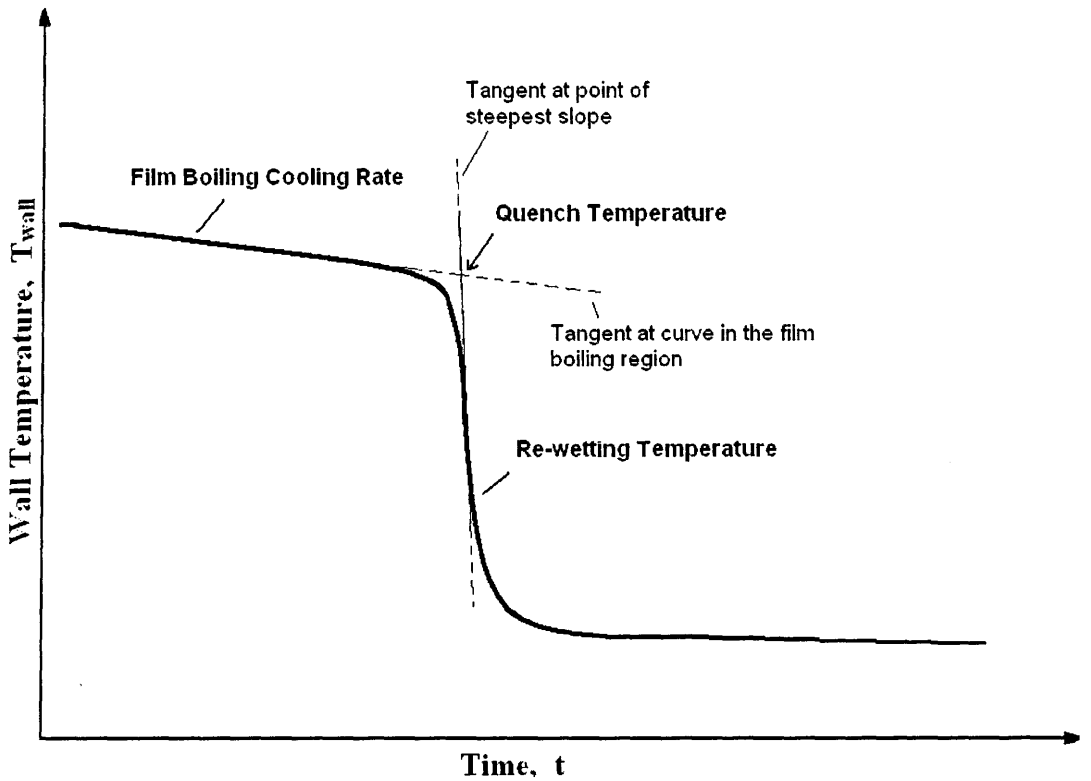

Figure 3: Typical cooling profile with quench and re-wetting temperatures defined.

1.5 Jet Impingement Quenching

Jet impingement quenching is one of the most attractive methods of high-heat-flux removal applications. When a high temperature dry surface is exposed to an impinging jet of evaporable liquid, the liquid may undergo the different boiling modes discussed above. Heat transfer by jet impingement is influenced by surface properties, surface condition, coolant properties, jet size and type (circular, slot, etc.) and other factors.

Multiple-jet systems are usually advantageous for higher rates of heat transfer in a wide area. Heat and flow behavior in multiple-jet quenching is expected to be more complicated than single-jet quenching due to interactions between flows from the adjoining jets [20].

1.5.1 Delay Time

When a jet of coolant is incident on a hot dry surface a period of stable vapor film boiling exists before quenching is initiated. In this period, the liquid forms a sheet above the vapor film. At the quench temperature, the vapor film starts to destabilize and the water then becomes able to contact the surface with

intermittent liquid-solid contacts. The onset of re-wetting is characterized by a strong disruption of the liquid sheet around the stagnation point. Transition and nucleate boiling are now possible. Before the re-wetting front starts to proceed, an initial wet patch is formed. The size of the initial wet patch stays almost constant for a while and then starts to increase as the re-wetting front proceeds. The time interval from when the jet first strikes the hot surface and the spreading of the wet patch is called the delay time [7, 21]. In jet impingement quenching, the delay time is an important phenomenon and estimating this time is of great importance when analyzing the consequences of a LOCA. A long delay time can lead to excessive calandria surface temperature which may cause failure of the fuel channels. Despite its great importance, the delay time have been studied in only a few studies. One of the objectives of this study is to investigate this relatively unexplored phenomenon.

The delay time has been defined as the time from when the jet first strikes the surface to the time of spreading the wet patch and not to time when the film collapses. This is due to the fact that in many applications, the spread of the wet patch is more important than the collapse of the vapor film. However, both delay times were investigated in this study because the time to vapor film destabilization is of importance in rector safety. The delay times were found to be very close to each other as the wet patch starts to spread immediately after the vapor film collapses. The delay time was found to vary from fraction of a second to tens of seconds depending on the operating conditions.

1.5.2 Velocity of the Re-Wetting Front

As indicated above, when a liquid is close to a hot surface, there exists a maximum temperature (the re-wetting temperature) at which the liquid is in actual contact with the surface. Similarly, when a wet patch is established at a specified location on the surface, its edge (the re-wetting front) can proceed in the direction of flow only if the surface ahead of it cools down to the re-wetting temperature. During the motion of the re-wetting front, heat is removed by transition and nucleate boiling at the front and by conduction within the surface from the dry to the wet region. The prediction of the re-wetting front velocity has been the main goal of many researchers. However, there is still confusion in literature in determining the location of the re-wetting front edge. Locating the re-wetting edge is not an easy task as the large generation of vapour prevents clear visibility of the re-wetting front [13].

One final note in this subsection is that the quench process is not always characterized by propagation of a re-wetting front, but can occur after a vapour film collapse at the whole surface (or part of it) at once, as may occur when a hot sphere is immersed in subcooled water or as in bottom re-flooding of a hot vertical surface [12, 22, 23].

1.5.3 Width of the Boiling Region

In jet impingement quenching, and when the re-wetting front propagates, the wetted area is observed to be divided into two regions: fully wetted central region (the wet patch) with no apparent boiling and an outer thin annular region with vigorous nucleate (and transition) boiling. The width of the boiling region usually ranges from 0.5 mm to few millimeters and is important because the heat flux tends to be higher in this region. The inner edge of this region represents the boundary between the single-phase liquid convection region and the combined nucleate and transition boiling region. The outer edge represents the re-wetting front line where actual surface-liquid contact starts to take place. Previous studies showed that the boiling width increases with surface thermal conductivity, and decreases with coolant subcooling. The initial surface temperature was also reported to have an effect: the width decreases by increasing the initial surface temperature [24]. This region has a white appearance due to vigorous boiling as seen in visualization tests. The most effective heat transfer in jet quenching takes place within this narrow annular moving region.

Figure 4 shows a typical image of the re-wetting front and the boiling region obtained in this study. Figure 5 shows a series of typical images captured in this study showing the film boiling heat transfer mode, the moment just after the collapse of the vapor film and the spread of the wet patch during quench cooling of a hot horizontal tube by a subcooled water jet.

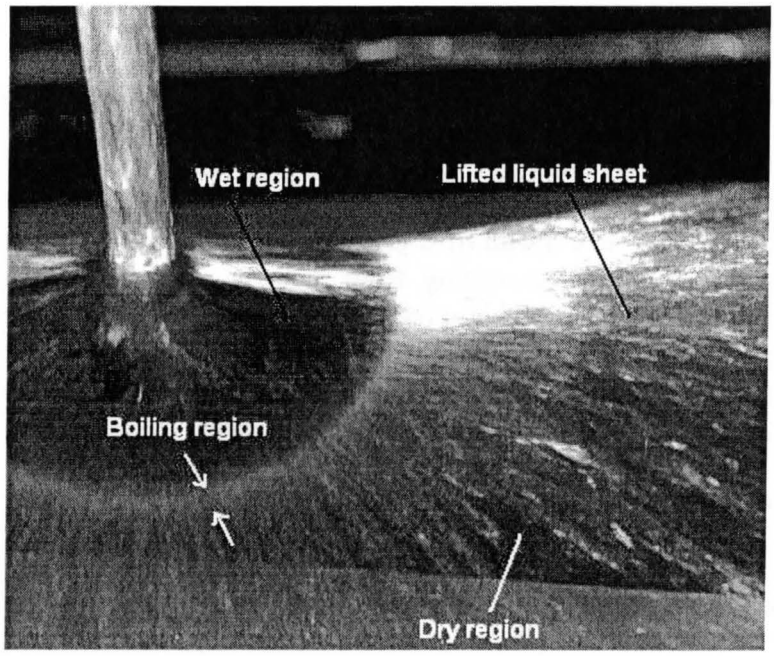

Figure 4: Typical image of jet impingement on a hot tube.

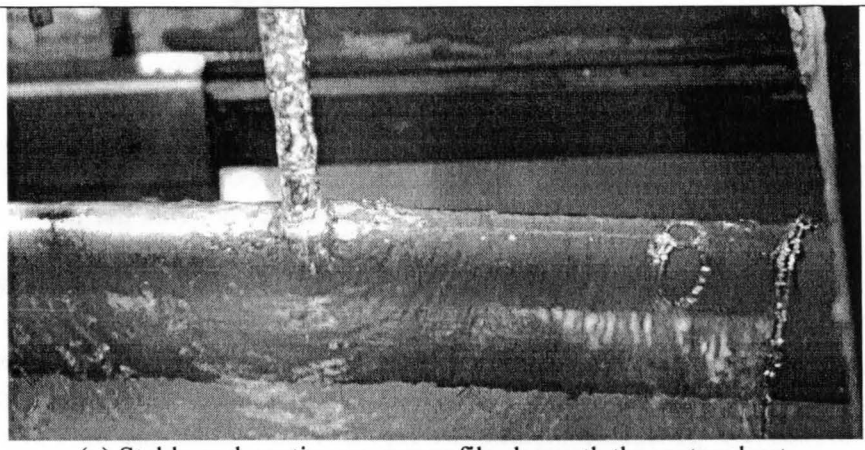

(a) Stable and continuous vapor film beneath the water sheet.

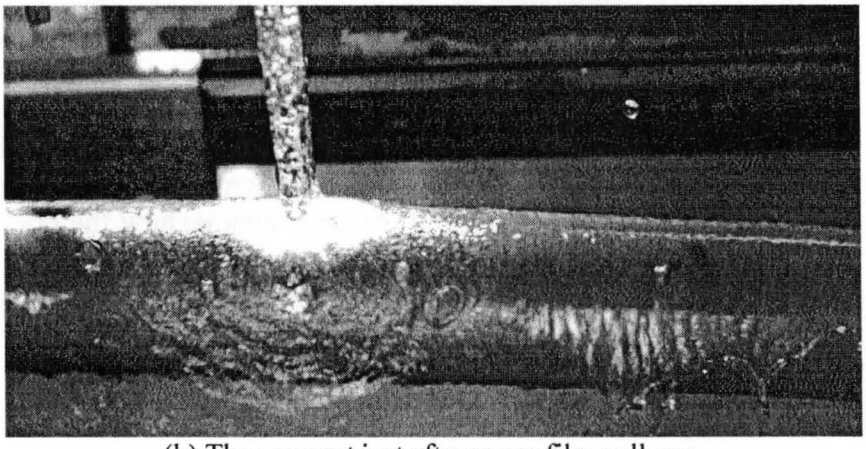

(b) The moment just after vapor film collapse.

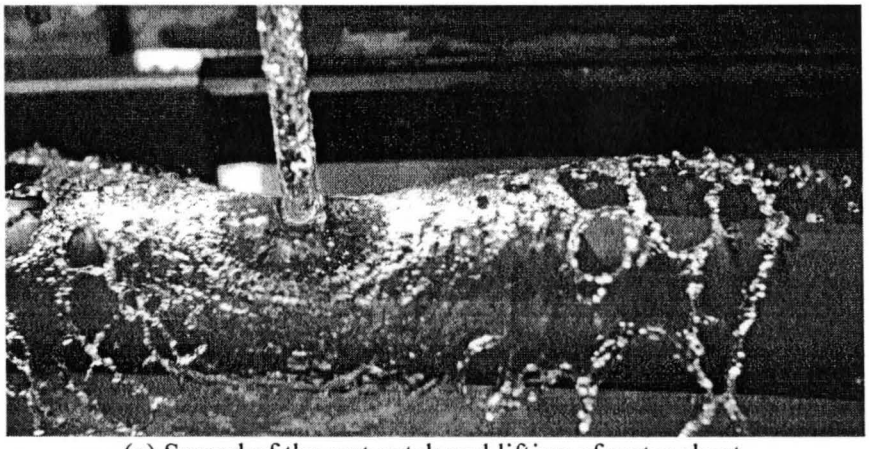

(c) Spread of the wet patch and lifting of water sheet.

Figure 5: (a) Vapor film boiling, (b) vapor film collapse and (c) spread of the wet patch.

1.6 Quench and Re-Wetting of Horizontal Tubes

Figure 6 shows sketches of a hot horizontal tube quenched by jet impingement as observed in this study. Sketch (a) shows the re-wetting front as it moves along the tube axis. The movement of the re-wetting front in this direction is similar to that of a flat plate. The sputtering droplets are moved downstream by the rapidly generated vapor and may touch the surface and re-wet it when the jet flow rate is high enough. Sketches (b) and (c) show re-wetting of the upper and lower parts of the tube; respectively. In re-wetting the upper part, a liquid sheet moves above the re-wetting front. Due to the jet hydrodynamic pressure exerted above the re-wetting front, nucleate and transition boiling region (the boiling region) is narrow on the upper part. On the lower part, and due to smaller effect of jet pressure, more bubbles are generated within the liquid. Also, when the re-wetting front moves on the lower part, the surface there would be cooled to a lower temperature than the initial surface temperature by conduction to the upper part, and thus the size of the boiling region increases. Furthermore, the water gets hotter while moving on the tube which again causes the boiling region size to increase.

Finally, upon re-wetting the lower part, the liquid may not get into full contact with the region around the bottom point especially when the tube diameter is large and the jet velocity is high. The two flow streams, approaching the bottom point from both sides of the tube, may eventually get into contact with the point at the bottom and form one stream beneath the tube and fall down. In this case, the region around the bottom point cools mainly by conduction. Much more details on the boiling size, re-wetting front velocity and re-wetting temperature are included in Chapter Five: Results and Discussion.

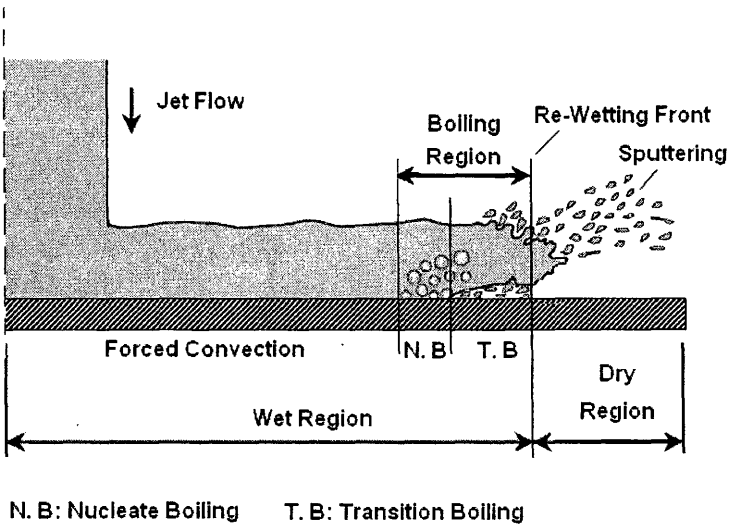

(a) Tube axial view.

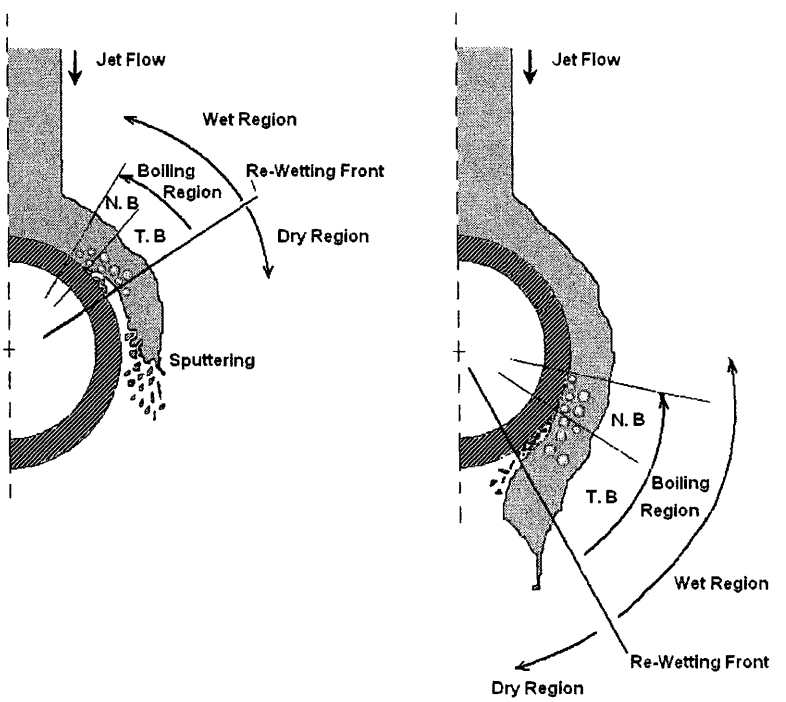

(b) Re-wetting the upper part of a hot tube.

(c) Re-wetting the lower part of a hot tube.

Figure 6: Sketch of jet impingement on a hot horizontal tube (sketches are not to scale).

1.7 Objectives

A significant body of experimental data has been accumulated for flat surfaces as will be discussed in Chapter Two: Literature Review. However, very limited knowledge of liquid jet impingement on hot curved surfaces is available. Few studies have analyzed quench heat transfer on tube and rod geometries and to the best knowledge of the author, the quench temperature distribution and the re-wetting front propagation around the perimeter of hot cylindrical tubes have not been investigated. Also, observation of two-phase flow behavior and vapor film collapse and measurement of the boiling region size on cylindrical tubes have not been reported in the literature. Chapter Two summarizes the studies found in literature where quench cooling was used to cool heated tubes, rods, spheres and cylindrical blocks. Also, literature on quench of other geometries, where some interesting findings are believed to give insight on the quench phenomena, is presented.

The objective of this study is to contribute to the understanding of heat transfer during quench of curved surfaces. This is an experimental work and the aims in specific are to:

1. Experimentally measure the surface temperature in the circumferential and axial directions of hot horizontal cylindrical tubes during quench cooling using a vertical water multiple-jet system in a transient mode. Effects of initial surface temperature, water jet velocity, jet temperature, jet orientation, number of jets, tube diameter and solid material on the quench process have been investigated.

2. Visualize the two phase flow behavior around the tubes, simultaneously with the temperature measurement, using a high speed camera in order to study the complex dynamics accompanying the quench process. This includes: quench temperature, re-wetting temperature, film collapse and delay time, re-wetting front velocity, rebound of the re-wetting front, size of boiling region and the quench cooling rate.

3. Develop correlations of the phenomena studied with respect to the parameters investigated.

4. Compare the experimental results with experimental and theoretical predictions obtained or developed by other researches, when available.

The results of this study provide novel information and knowledge and an experimental database for mechanistic modeling of quench heat transfer on calandria tube surfaces that experience film boiling due to pressure tube contact during critical break LOCA in CANDU reactors. This mechanistic modeling can

be used to support safety analysis methodology that has been developed to demonstrate fuel channel integrity during loss of coolant accidents in CANDU reactors.

1.8 Scope of the Dissertation

This dissertation includes seven chapters containing the following:

Chapter One:	This chapter, an introduction to quench phenomenon and its applications, fundamental definitions of different terms in quench and boiling heat transfer and, finally, the objectives of this study.
Chapter Two:	A literature review on quench heat transfer, mainly on curved surfaces.
Chapter Three:	Description of the experimental setup designed and constructed in this study, part specifications and procedure followed to run the tests and to collect the data. It also includes experimental operating conditions, parameter ranges and measurement uncertainty.
Chapter Four:	Raw data description and processing.
Chapter Five:	The results and discussion. It contains temperature measurements, visual observations, analysis and discussion.
Chapter Six:	Conclusions of this study.
Chapter Seven:	Recommendations for further work.
Appendices:	More details on the experimental setup.

Chapter Two

Literature Review

In this chapter a literature review on quench studies is presented. The chapter is divided into the following sections: literature on quench of cylindrical tubes and rods, literature on quench of spheres, literature on size of boiling region, literature on quench of other geometries, literature on unusual phenomena reported in literature during quench cooling. Most of the literature is focused on experimental studies. However, some literature on quench modeling is also provided where some results give an insight and description of the quench phenomena.

2.1 Literature on Quench of Cylindrical Tubes and Rods

2.1.1 Horizontal Tubes

F. Gunnerson et al. [12] discussed the definitions of the quench and re-wetting temperatures and reported that the two terms are distinctly different and are often incorrectly assumed to be synonymous. They defined quench as the rapid cooling of a hot solid surface resulting from enhanced heat transfer conditions. In their study (water-fuel rod system) they considered quenching to occur when the cooling profile attains a slope of -200K/sec (which coincides with the intersection point of the two tangents shown in Figure 3). Re-wetting was defined as the direct liquid-solid contact and the establishment of liquid-solid-vapor triple interface. Re-wetting was considered a complex process influenced by many factors acting simultaneously like time, temperature, surface geometry and surface condition. They also distinguished between the re-wetting temperature and the Leidenfrost temperature and concluded that these temperatures are not necessarily the same as transient liquid-solid contacts could exist during boiling at temperatures higher than the Leidenfrost temperature. Finally, they reported that the geometry of the surface significantly influences the quenching process.

B. Piggott et al. [7] investigated cooling of hot horizontal rods by circular water jets. In their experiments, initial surface temperature was varied between 500-800°C, water subcooling between 2-20°C and jet flow rate between 1.5-15 g/sec. Three solid materials were used: gold, Inconel and Silica and rod size was varied between outer diameters of 6.3-18 mm. Three surface conditions were investigated; ground finish, shot blasted and silver plated. The delay time (time between jet being incident on the rod and onset of re-wetting) was found to be a very strong function of water subcooling. Jet velocity, surface temperature and surface thermal conductivity were also found to have a strong effect on the delay time. The delay time decreased by increasing water subcooling, increasing jet velocity and decreasing surface temperature. Using a high-speed camera, three

heat transfer regimes were observed: film, transition, and nucleate boiling. Surface finish and rod size were found to have no effect. However, M. Cumo [27] conducted experiments on droplet heat transfer and concluded that re-wetting depends on surface roughness. He reported that surface roughness promotes the contact between the liquid and the surface.

M. Akmal et al. [28] studied the re-wetting front propagation during cooling of hot horizontal tube using impinging circular water jet. The tube was made of stainless steel with 2.54 cm outer diameter. Effects of jet velocity, jet diameter, cooling water temperature and initial surface temperature on the re-wetting front velocity in the axial direction were investigated. The initial surface temperatures were 250, 500 and 800°C, water temperature was varied between 20-80°C and jet velocity between 5-7.75 m/sec. Two jet diameters were used; 3 and 4 mm. The re-wetting front location was correlated using a power law function of time. It was found that the re-wetting front velocity is strongly dependent on water temperature. At low water temperatures and high jet velocities the re-wetting front was found to grow fast. By increasing jet diameter, the velocity of the re-wetting front increased mainly at low water temperature, low surface temperature and high jet velocities. Finally, by comparing their results with other researchers, surface curvature was found to increase the re-wetting front velocity by about 26%.

K. Takrouri, the author of this study, et al. [29] studied the effects of water subcooling and initial surface temperature on the re-wetting front propagation along the circumferential direction on a 2.54 cm outer diameter horizontal brass tube. The tube initial surface temperature was varied between 300-700°C and was cooled using a 3-mm circular water jet with 3 m/s jet velocity. It was found that the re-wetting front slows down as the temperature difference between the hot tube and the jet decreases.

A. Abdul-Razzak et al. [4] conducted an experimental and analytical study on refilling and re-wetting of hot horizontal Zircaloy tubes. The tubes were 25.4 mm in diameter, 3 m long and 1 mm and 2 mm thick. They proposed a re-wetting criterion based on vapor film collapse and suggested that surface re-wetting is initiated when the thickness of the vapor film decreases to a value equal to the sum of the amplitude of the fluctuations at the liquid-vapor interface and the wall surface roughness. Their proposed model predicted the experimentally observed thermal-hydraulic transients during the re-wetting process.

J. Luxat [3] developed a mechanistic model to describe the heat transfer and thermal-mechanical processes associated with ballooning deformation of a pressure tube into contact with its calandria tube in the CANDU reactor. It was stated that the extent and duration of film boiling heat transfer mode on the outer surface of the calandria tube is dependent on the heat flux from the pressure tube

and the subcooling of the water surrounding the calandria tube. The model was validated by comparison with experimental data and the minimum film boiling temperature estimated by the model agreed with those predicted by several correlations available from the literature.

A mechanistic model of convection film boiling on the outer surface of a hot horizontal tube cooled by water has been developed and validated by Jiang et al. [2]. The tube diameter was relevant to the CANDU calandria tube. The effects of coolant subcooling, surface temperature and incident heat flux on the vapor film thickness were investigated. The model was compared to experimental data and provided good predictions of the outer surface heat flux and the effective heat transfer coefficient of film boiling.

2.1.2 Vertical Tubes

F. Kaminaga et al. [14] investigated the quench temperature and the propagation of the re-wetting front on a hot vertical cylindrical tube exposed to water moving in the upward direction. The tube was made of stainless steel and was 10 mm in diameter. Initial surface temperature was varied between 250-800°C, water temperature between 16-86°C and water velocity between 1.2-10.3 cm/sec. The quench temperature was defined as the onset of the rapid decrease in surface temperature and was shown to decrease with increasing elevation along the tube and decreased with increasing water temperature. The re-wetting front was found to advance upward at a constant speed for low water temperatures. For water temperatures higher than 80°C, the re-wetting front velocity was very low at the lower part of the tube but increased as the re-wetting front advanced and reached a nearly constant value. Film, transition, and nucleate boiling modes as well as forced convection were visualized during the quench process. The heat transfer coefficient of nucleate boiling was found to be around ten times higher than that of film boiling.

T. Ueda [30] experimentally studied the re-wetting of a hot vertical tube by Freon 113 liquid film at atmospheric pressure. The tube was made of stainless steel with 16 mm outer diameter and 400 mm length. Liquid subcooling was 5°C with Reynolds number ranging between 700-7000. Effects of liquid flow rate and initial surface temperature on the re-wetting front velocity were investigated. They observed that the moment of the re-wetting front covering a thermocouple location in the wall coincided well with the onset of the sharp decrease in the wall temperature. Therefore, they defined the re-wetting temperature as the wall temperature at the re-wetting front. They found that the wall superheat at the re-wetting location scattered in the range 34-47 K with a slight trend to increase with increasing initial wall temperature. The liquid flow rate was found to have no effect on the re-wetting temperature. The re-wetting front velocity decreased by increasing initial wall temperature and was correlated by a power law with initial

wall temperature. The re-wetting front velocity was only slightly affected by the liquid flow rate. Finally, they reported that the effect of liquid flow rate is not clear for high liquid temperatures close to the liquid saturation temperature.

B. Piggot [16] investigated re-wetting of a vertical 1.27 cm diameter Inconel tube 20 cm long by upward water flow. Surface temperature was varied between 400-700°C, water subcooling between 14-78°C and flow velocity between 1-40 g/sec. They showed that for high flow rates and subcoolings the re-wetting front velocity was proportional to the product of flow rate and inlet water subcooling. At low flow rates and inlet subcoolings the re-wetting front velocity tended to be constant.
A. Kim [15] developed a correlation to estimate the quench temperature as a function of wall properties, wall thickness, wall initial temperature, coolant inlet temperature and water flow rate. The correlation was developed using experimental data of bottom re-flooding of hot fuel rods and the quench temperature was defined as the onset of the rapid decrease in surface temperature estimated by the intersection point of the tangents line as shown in Chapter One: Introduction.

Y. Murao [20] developed a correlation to estimate the quench temperature of Zircaloy and stainless steel tubes as a function of water properties using data from bottom re-flooding of a vertical tube. From the experiments, it was found that the quench temperature was in the range 320-510°C for water subcoolings between 0-30°C and water flow rates between 5-25 cm/sec.

2.2 Literature on Quench of Spherical Objects

It is of great importance to look at quench cooling as well as the various boiling modes on spherical objects when studying the quench of cylindrical objects. Liu et al. [31] reported that film boiling on spheres and on cylinders are quite similar to each other with respect to vapor film configurations and in the ways that the heat transfer data are correlated. However, the boundaries around a sphere are axial symmetric instead of two-dimensional as for a cylinder. Observations of this study, when compared to published results, showed that the motion of the re-wetting front in the axial direction on cylindrical tubes is similar to that on a flat plate but similar to that of a sphere in the azimuthal direction. No study of quench by jet impingement on spherical objects was found in literature. However, several researchers studied the quench of either: hot spheres moving in a bath of stationary liquid or stationary hot spheres with liquid moving around.

C. Liu [31] used four diameter brass and stainless steel spheres to investigate the effect of sphere diameter on the film boiling heat transfer under saturated forced convection film boiling. The sphere outer diameters were 6.35, 9.53, 12.7 and 19.1 mm and were immersed in a bath of flowing water at flow velocity ranging between 0-2.3 m/sec at surface temperatures between 350°C-900°C. No effect of

sphere diameter was noticed under the operating conditions of their study. They conducted experiments with distilled water, de-ionized water, tap water, and de-ionized water with salt additions. The experiments showed that the kind of water used had no effect on the heat transfer data obtained. For a 12.7 mm stainless steel sphere, the quench temperature was reported to be about 250°C for saturated pool film boiling and increased gradually with water flow velocity. For 20°C subcooled water, the quench temperature was found to be about 300°C in still water and increased slowly with the water velocity when the velocity was small (less than 0.5 m/sec), and increased quickly for higher velocities. The quench temperatures were found to be much higher than those obtained at saturated flow conditions. Brass spheres had a little lower quench temperatures than the stainless steel spheres, especially for high water velocities.

Recently, A. Jouhara et al. [22] conducted a study of transient film boiling cooling on spheres (20 mm and 35 mm in diameter), cylinders (10 mm and 20 mm in diameter) and plane surfaces (two flat plates 10 mm thick, 35 mm wide and 70 mm/140 mm height). All specimens were made of copper and heated up to 450°C and then lowered into a bath of flowing water at velocities ranging between 2-18 cm/sec. Water temperature was varied between 75.7-97.5°C. It was found that the film boiling period increased with decreasing water subcooling for all specimens. The heat transfer coefficient was found to increase as the specimens cooled and the vapor film thickness became thinner. Except for cylinders in cross flow, water velocity was found not to have a great impact on the heat transfer coefficient. Heat transfer coefficient was found to be affected by sphere diameter, plate length but less significantly by cylinder length. That was explained to be due to a more turbulent vapor/liquid interface for the spheres and the plane plates. The more turbulent the vapor/liquid interface the bigger the area of heat transfer convection into the water flow. For cylinders in parallel flow, a thicker vapor film cancelled the effect of the turbulence at the vapor/liquid interface.

A. Jouhara et al. in another study [23] observed three modes of film collapse on spherical surfaces heated up to 600°C: explosive collapse (destabilizing the film instantly at the whole surface in an explosive way) at relatively high water subcoolings, progressive collapse (destabilizing the film instantly at a small region and movement of the re-wetting front) at relatively low water subcoolings and explosive-progressive collapse (initial collapse of the film on the whole surface, then reforming of the film to start a progressive mode) at intermediate water subcoolings. Typical values of the critical vapor film thickness was reported to be in the range 80-110 μm. Water velocity did not influence the heat transfer coefficient significantly. They attributed this behavior to the mean vapor velocity within the film being larger than the water velocity employed. Finally, at given water subcoolings, higher minimum film boiling temperatures were reported for spheres than for plane specimens.

The effect of the surface geometry on the re-wetting temperature was investigated by F. Gunnerson et al. [12]. Higher quench temperatures were observed for small diameter spheres. It was found that, as the sphere diameter increases, the surface can be considered as a flat surface with less dependence on the geometry.

2.3 Literature on Boiling Region Size during Quenching

M. Akmal [28] in his previously mentioned study on quench of horizontal steel tube reported that for initial surface temperature of 500°C, the size of the boiling zone varied from less than 0.5 mm to a maximum of 5 mm in the tube axial direction. It was observed that the size was affected by initial surface temperature, water temperature and jet velocity but the data was not correlated.

In a recent study, P. Woodfield et al. [32] studied the flow behavior and boiling region size during water jet quenching of a high temperature cylindrical block 94 mm in diameter and 59 mm height. In their experimental work, a 2 mm diameter circular water jet was directed upwards towards the flat bottom of the cylinder. Three blocks made of copper, brass and steel were used with initial surface temperature varied between 250-600°C. Water subcooling was varied between 5-45°C with two jet velocities; 3 and 5 m/sec. The size of the boiling region was found to increase with material conductivity and decrease with jet subcooling and velocity. The width of the boiling region was found to shrink with increasing initial surface temperature. In another study, P. Woodfield et al. [8] studied the flow behavior and boiling sound of water jet impinging on the high temperature copper block during a quench process. For cases where the initial surface temperature was below 300°C a liquid sheet flow structure was observed. However, for temperatures higher than 300°C, almost explosive pattern was observed when the jet first strikes the surface. The phase change was accompanied by a sudden change in the boiling sound.

A. Mozumder [9] experimentally investigated the boiling width using the above experimental setup used by Woodfield [32] with water subcooling varied between 5-80°C and jet velocity between 3-15 m/sec. He reported an increase in the boiling width with increasing the radial position during the motion of the re-wetting front. The boiling width was greatly influenced by the radial temperature gradient; the higher the radial gradient, smaller was the boiling width.

M. Mitsutake et al. [21] considered the decrease in the boiling region width with increasing subcooling to be governed by combination of the heat removal by the liquid and the heat transferred in the solid by conduction. They reported that the maximum heat flux at a certain position on the surface would take place when nucleate boiling occurred there.

From the literature of this sub-section, it is concluded that few researchers studied the boiling width during quench experiments. Furthermore, the boiling width on curved surfaces has not been investigated. One of the objectives of this study is to investigate this relatively unexplored field.

2.4 Literature on Quench of Other Geometries

J. Hammad [13] studied the flow behavior during water jet quenching of a high temperature cylindrical block 94 mm in diameter and 59 mm height. A 2 mm diameter circular water jet was directed upwards towards the flat bottom of the cylinder. Three blocks made of copper, brass and steel were used with initial surface temperature of 250 and 300°C. Water temperature was varied between 20-95°C and jet velocity between 3-15 m/sec. The delay time was found to increase with increasing initial surface temperature and thermal conductivity of the surface and with decreasing jet velocity and water subcooling. Re-wetting front velocity decreased with increasing initial surface temperature and thermal conductivity of the surface and with decreasing jet velocity and water subcooling.
M. Mitsutake et al. [21] conducted an experimental study of transient boiling heat transfer using the experimental setup used by Woodfield [32]. In their experimental work, water subcooling was varied between 20-80°C and jet velocity between 5-15 m/sec. They observed the motion of the wetting front and correlated its position as a power law function of time. They observed that, for carbon steel specimen, the sudden drop in surface temperature at a specific location starts at the moment when the re-wetting front reaches that location. For brass and copper specimens, gradual decrease in temperature started before the re-wetting front reaches the location. One important observation they reported was that the time delay between the temperatures estimated at the surface and those measured 1 mm in depth was less than 0.01 sec even for carbon steel surface; being the poorest thermal conductance they investigated.

J. Hammad et al. [33] studied the characteristics of heat transfer and re-wetting front motion during quenching the high temperature brass cylindrical block mentioned in the study of Woodfield [32]. Water subcooling was varied between 5-80°C, jet velocities between 3-15 m/sec. They estimated the surface temperature and the heat flux using a two-dimensional inverse solution. They found that the maximum heat flux occurs neither at the re-wetting front, nor within the boiling region but in the fully wetted region. They also showed that the maximum heat flux occurred when the surface temperature decreased to a value less than 170°C.

A. Hauksson et al. [34] investigated the heat flux during subcooled quenching of horizontal flat plate by water jet impingement. Water subcooling was varied between 30-50°C and jet velocity between 5.5-6.0 m/sec. The plate was made of steel and was 280 mm long, 280 mm wide and 7 mm thick and the nozzle-to-plate distance was constant at 1500 mm. Higher heat fluxes were reported for lower

water temperatures close to the stagnation point. This effect was shown to diminish with increasing distance from the stagnation point as the water temperature rises as it flows over the plate. The maximum heat flux was found to decrease by decreasing jet velocity. However, the effect of jet velocity was reported to be not clear at several locations on the plate especially at low flow rates.

2.5 Literature on Unusual Quench Phenomena

N. Hatta et al. [35] used a 10 mm diameter water jet to quench hot flat stainless steel plate (200 mm in side length and 10 mm in thickness) heated up to 900°C. The temperature of the cooling water was varied between 18°C and 21°C and the flow rate between 0.1 and 7 L/min. They correlated the re-wetting front to time by a power law relation. Depending on their visual observation, and contrary to all jet impingement quench studies, they reported that as soon as the water jet strikes the hot red plate the plate and the water were not insulated with a vapor film, but they were in direct contact as the initially hot red plate surface immediately began to darken. They demonstrated that, if a vapor film had been formed, such a change in color would not have been observed. In another study, Witte [4] reported that no vapor film boiling was observed around a sphere moving in a bath of liquid sodium although the sphere was 1100°C hotter than the liquid.

The observation of no film boiling in Hatta's previous study, according to the author of this study, could be attributed to a low imaging rate which did not allow observing the vapor film boiling mode and the collapse of the vapor film. In this study, and using a stainless steel tube heated up to 800°C, it was observed that a vapor film does exist which collapses within 16 ms using water jet at 20°C. In their study, no imaging rate was reported.

Also, A. Tuzla et al. [36] experimentally assessed the validity of the no-contact phenomena and the existence of a vapor film between a hot surface and a liquid using a special rapid-response probe. The specimen in their study consisted of a vertical tube of 1.57 cm ID and 172 cm length. Water was used with upward mass flux rate inside the tube ranging between 9 and 31 $kg/m^2.sec$. Their experimental test results indicated that water could only contact the hot surface at wall temperatures up to 400°C. No contact was reported for higher surface temperatures.

D. Hall [18] experimentally studied boiling heat transfer during quench of a 25.4 mm thick copper disk 112 mm in diameter by circular water jet. The disk initial temperature was 650°C and water velocity was varied between 2-4 m/sec. They focused on variations with stream wise location during the cooling process. They defined the re-wetting temperature as the minimum film boiling temperature in the boiling curve and found that it ranges between 180-450°C. The interesting

finding in their study was the increase of the minimum film boiling temperature with the axial location up to $r/d_{jet}=8$ from the stagnation point (where r is the axial distance and d_{jet} is the jet diameter). Beyond this distance, the minimum film boiling temperature started to decrease with r. The normal expectation is a decrease in the minimum film boiling temperature with axial distance as the jet momentum decreases and the local water subcooling increases as water moves along the surface. They attributed the initial increase in the re-wetting temperature to jet deflection from the surface immediately downstream of the quench front. Due to the vigorous boiling at the quench front, water is separated from the surface. As the quench front moves, the momentum of the liquid coming from the jet decreases which causes the velocity of the deflected water to decrease; a condition that enhances film boiling and thus the minimum film boiling temperature increases. After a distance downstream of the jet, the water will no longer be deflected and thus flows over a vapor film. Now, the increase in water temperature and further decrease in water momentum with special distance causes the minimum boiling temperature to decrease; which is the normal expectation.

M. Gadala et al. [37] used a pilot plant test facility to study the heat flux at the stagnation point of a stationary hot steel plate cooled by 19 mm circular water jet. Initial surface temperature was varied between 700-900°C. The plate was made of steel with dimensions of 280 mm length, 280 mm width and 7 (or 10 mm) thickness. Water subcooling was varied between 30-80°C and jet velocity between 5.5-6.0 m/sec. They found that the heat flux is higher for lower water temperatures as increasing water temperature significantly reduces its capability of heat extraction from the surface. Also, they concluded that the duration of film boiling depends mainly on water temperature; the higher the water temperature, the longer the film boiling period. Water flow rate was found to have little effect on heat transfer when water temperatures was 30, 40 70 and 80°C but it has a noticeable effect when the water temperature was 50°C. They reported that this result is, generally, against to the common accepted trend (i.e., the increase of water flow rate does not increase the heat transfer) and recommended further investigation to verify this phenomenon. Furthermore, although the boiling curve for water flow rate of 30 L/min (5.7 m/sec) was found to show the same combination of heat transfer modes (film, transition and nucleate boiling) as those for water flow rate of 15 L/min (5.0 m/sec) or 45 L/min (6.0 m/sec), its magnitude was much less. They did not provide an explanation for this abnormal behavior and attributed it to measurement error or to unknown complex relationship to be explored in future work. As a general conclusion, they found that the heat transfer behavior is greatly affected by water temperature. When the temperature was lower than 60°C the cooling was governed by transition, nucleate and convective boiling modes. When the temperature was higher than 60°C, a film boiling regime existed.

J. Stevens [38] experimentally investigated the film and transition boiling on 1.9 cm diameter copper sphere moving through subcooled water. Water temperature was varied between 24-60°C, sphere velocity between 3-6 m/sec and initial surface temperature between 190-250°C. They observed that the transition from film to nucleate boiling was accompanied with a pulsation of the vapor film. It was found that the minimum film boiling temperature was in the range 175-204°C and increases as a linear function of the initial surface temperature. It was reported by J. Carbajo [10] that this linear relation was not confirmed by other experiments. In their study, they found that the velocity of the sphere had no effect on the minimum film boiling temperature. One other finding they reported, contrary to intuition, was the decrease in the minimum film temperature by decreasing water temperature. They provided no explanation of this behavior but recommended further experimentation.

2.6 Comments on the Literature Review

From the above literature review on quenching it is clear that some of the fundamental aspects of the mechanism of phase change and heat transfer characteristics during quenching are still not well defined at present [8, 13, 34]. There is confusion in the literature in defining the quench and the re-wetting temperatures. Also, a number of unusual phenomena during quenching have been reported by several researchers and, sometimes, contradiction between the reported results exists. The effect of jet velocity and surface roughness are clear examples. Some researchers reported that coolant velocity has no effect on the cooling process up to a critical value, beyond which any increase in liquid velocity increases the rate of heat transfer. Other researchers reported that the velocity affects the process up to a value beyond which no effect was observed. Roughness of the surface was reported by some researchers to increase the re-wetting temperature as it promotes liquid contact with the solid [4, 27] but reported by other researchers to have no effect [7].

From the literature review on the experimental quench studies, one can conclude the following:

1. Most researchers used flat plates and most of those who used tubes, used upper or bottom re-flooding of the tube while being vertical.

2. Few studies investigated the quench phenomena under multiple-jet impingement and for varying jet orientations.

3. Effect of jet velocity in quench experiments needs further experimental investigation.

4. In many of the quench studies available in literature, a lot of noise was observed in the cooling profiles which were not always explained. The noise could be due to misplacement of the thermocouple as a result of repeated rapid surface contractions or due to coolant phase change. Coolant phase change was reported (and found in this study) to have a considerable effect on the shape of the cooling profile [9, 13, 14, 22].

5. There has been a difficulty in observing and determining the position of the re-wetting front leading edge. In most of the studies, the imaging rate and the imaging resolution were not high enough to provide accurate measurements, only approximations.

These comments were taken into consideration in setting the objectives of this study and in designing and constructing the experimental setup. In the next chapter, the experimental setup is described.

Chapter Three

Experimental Setup and Methodology

3.1 Experimental Setup

To achieve the above mentioned objectives, an experimental setup has been designed and built as part of this study. The setup is named the "Water Quench Facility (WQF)" and was constructed at McMaster University student workshops. A schematic and an image of the facility showing the major components are shown in Figure 7 and Figure 8; respectively.

The facility consists of the following main parts:

1. Specimens and Motorized Motion System.
2. Water Circulation System.
3. High Speed Imaging and Data Acquisition Systems.

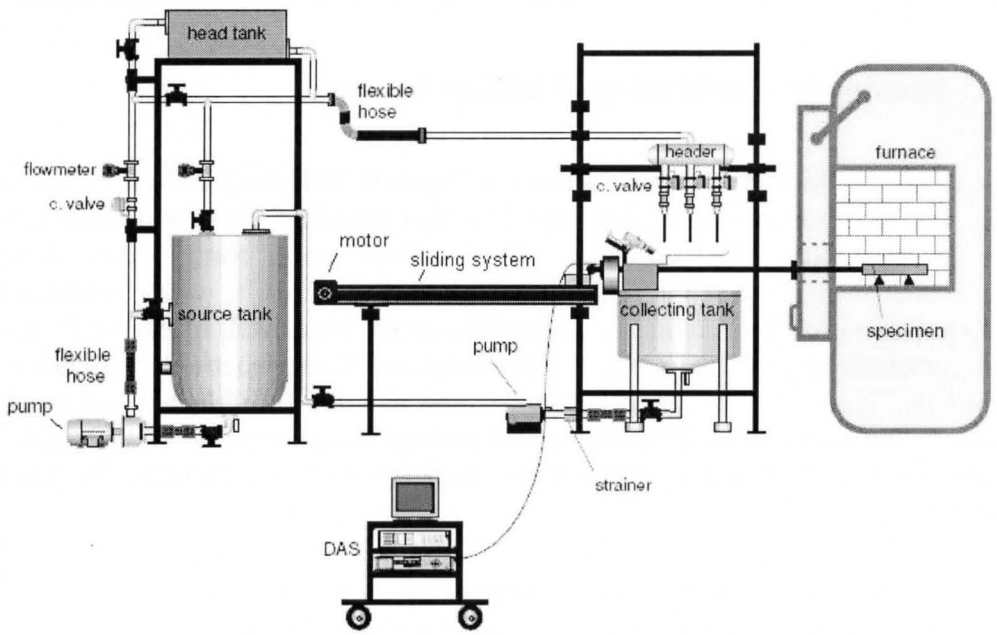

Figure 7: Schematic of the Water Quench Facility (WQF).

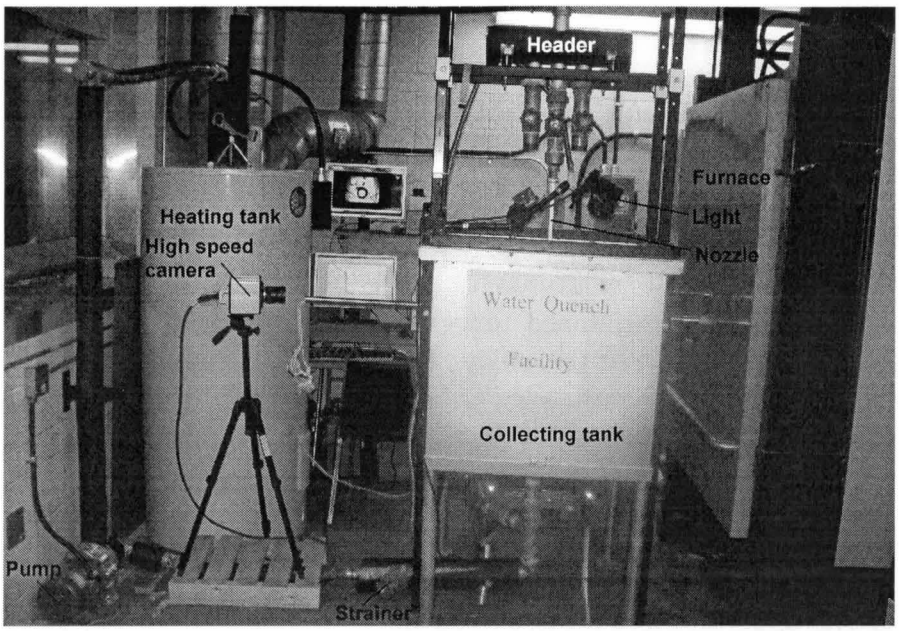

Figure 8: Image of the Water Quench Facility (WQF).

These main components of the setup are described in the following three sections.

3.1.1 Specimens and Motorized Motion System

A schematic of the heated tube is shown in Figure 9. This is a 1-ft long cylindrical tube. The tube was machined from two 1-ft tubes (one half from each tube) milled through the axis with accuracy of ± 0.0005 mm. Nine 1-mm K-type thermocouples with maximum deviation of -0.8°C at 650°C were mounted by silver soldering circumferentially and axially on the inner wall of each half in the hole locations shown in Figure 9. The method of thermocouple mounting is shown in Figure 10. Several silver solder and flux (surface cleaner and binder) materials were tested until the best combinations was found to be: 062-DIA-X-COIL BRAZE 051 and ULTRA Flux; respectively, manufactured by Lucas-Milhaupt Inc.

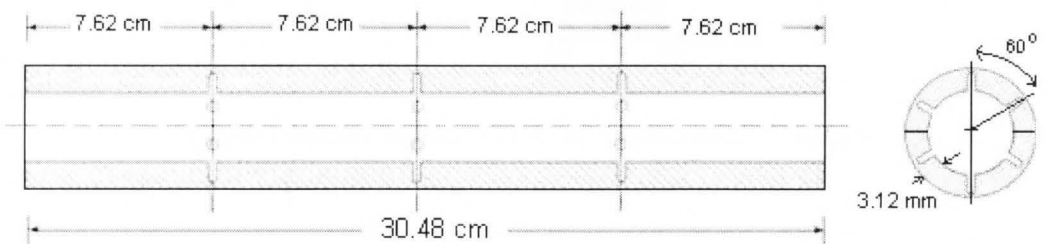

Figure 9: Heated tube and thermocouple locations.

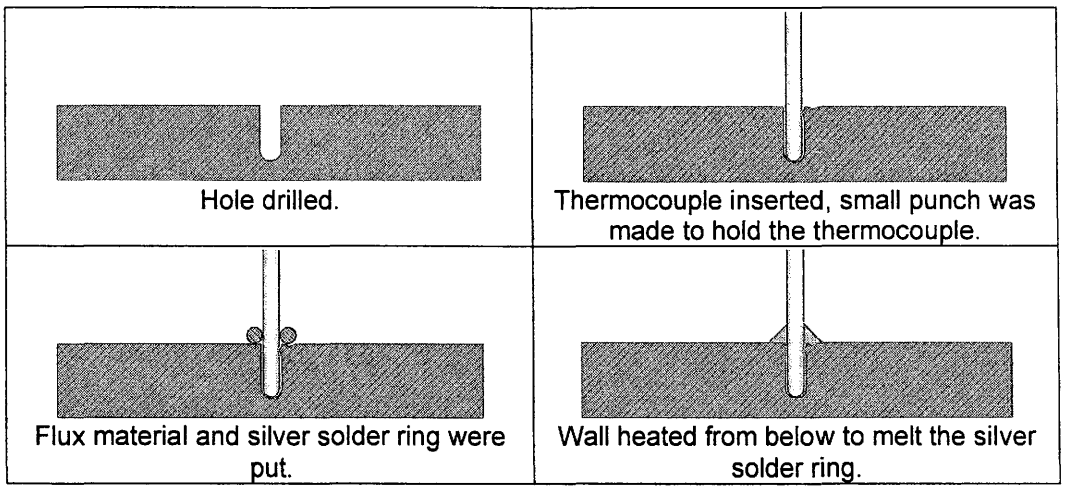

Figure 10: Method of thermocouple mounting in the specimen.

The silver solder has to have a melting point above the maximum surface temperature required for the tests but less than the melting point of the surface. The solder used in this study has a melting point of 850°C; 50°C less than the melting point of the brass tube and 30°C above the maximum surface temperature achieved in this study. Silver solder can perfectly mount the thermocouple and at the same time acts as a high thermal conductance which is necessary to fill any gap between the thermocouple tip and the surface. From initial tests done in this study, it was found that if the thermocouple loses its contact with the surface by 1 mm; it gives a temperature approximately 100°C less than that when it is in full contact with the surface. Several types of high temperature cements were also tested for thermocouple mounting but the rapid contraction during the quench caused them to fragment. Small metallic strips were put on the thermocouple and welded on the surface for additional support (the strips are shown in Figure 13 (d)). Brass strips were used with brass tube and stainless steel strips with stainless steel tube. Direct welding of the thermocouple to the wall was found to damage the thermocouple sheath. Perfect mounting of the thermocouples is very important and critical in quench studies. This is because the transition between the boiling modes may cause significant noise in the temperature profile and one should eliminate any noise caused by the misplacement of the thermocouple. Also, as in most of cooling studies, thermocouples should not be mounted at the outer surface of the specimen in order not to affect the flow behavior at the outside solid surface. F. Gunnerson [12] reported that external thermocouples can affect both quenching and re-wetting phenomena. The two tube halves were then welded to each other through the axial and circumferential directions. Before welding, the edges of the two halves were grooved such that a gap is created between the two parts at the welding locations, as shown in Figure 11. By doing it this way, there is no need for supporting clamps around the tube.

The gaps were then filled by welding using filler made of the same material as that of the tube. This ensures perfect thermal contact between the two parts. The tube outer surface was then cleared by lathe machine to ensure homogenous surface roughness and to prevent any undulations on the surface from affecting the boiling phenomena. Emery paper of 200 Grit was used to polish the outside surface. The surface was polished before every experimental run to maintain the same surface roughness. The tube is heated in a 3 ft x 3ft x 3ft box furnace (maximum furnace temperature is 1000°C). The furnace is provided with a 7-in diameter window at the side door and the specimen is inserted through this window. 1-in diameter brass tube and 2-in diameter 316 stainless steel specimens were prepared in this study.

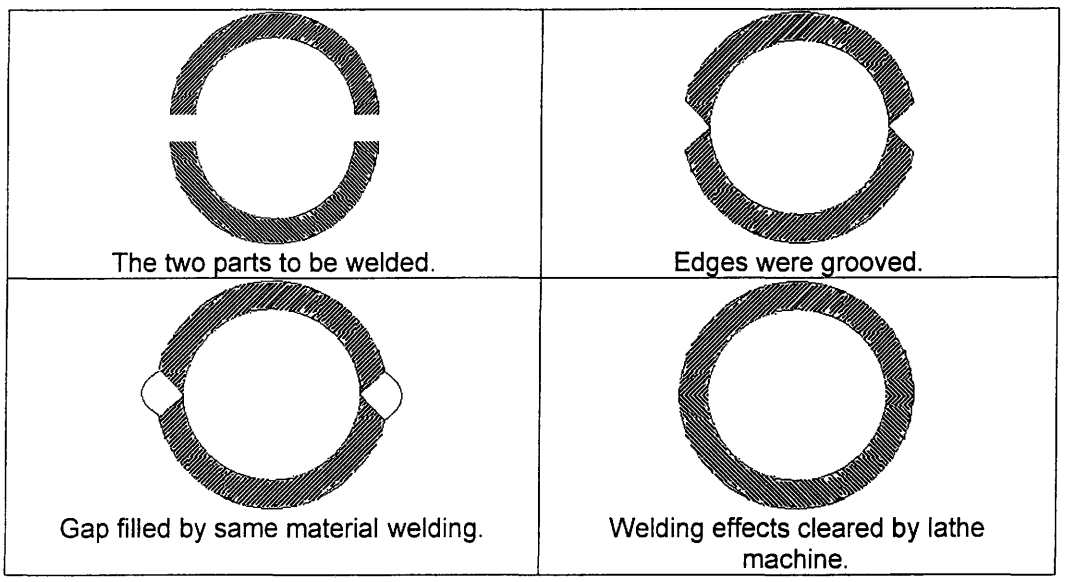

Figure 11: Method of welding the two parts of the specimen.

Doing the experiments with a portable specimen (heated in the furnace and then moved to a cooling location) was one of the challenges in designing the experimental setup. This requires a specimen holding system to hold the specimen while in the furnace and move it quickly, precisely and gently to the prescribed quench location underneath a multiple-jet system. The holding system consists of a poor thermal conductance 1-ft long and 1-in inside diameter Alumina tube with 3 mm wall thickness attached to the hot tube at one end and to a stainless steel tube (1-in diameter and 5-ft long) at the other end acting as a connector. Alumina tubes were found to be best connectors for the tests of this study. Glass, quartz and several types of ceramic were tested as connectors but found to easily break because of the mechanical stresses created by the stainless steel holder or because of the thermo-mechanical stresses due to rapid contraction during the quench process. One more interesting specification of the Alumina tubes is the decrease of its thermal conductivity with increasing temperature. Metallic shell was used to

cover the Alumina tube to protect it as Alumina is fragile. The specimen and the connector are shown in Figure 12.

The hot tube and the holding system (the Alumina tube and the stainless steel tube) are held on two parallel telescopic linear bearings with less than ±0.1 mm misalignment in linear motion. Telescopic linear bearings were chosen due to space limitations. The far end of the stainless steel tube holder is attached to a horizontal motorized linear motion system (Velmex type) which provides a maximum speed of 3 m/s (with less than 0.1 mm misalignment) in order to move the hot tube quickly from the furnace. 12-in long and 3-in wide Aluminum sheet bent 135° in the middle of the long side is positioned coaxially 2-in above the heated tube to act as a guard. The guard is loaded on a spring held by a special piece and can be released when it makes contact by another piece attached to the motion system as soon as the tube reaches the cooling location. When the cooling process is started, the guard is rapidly moved axially by releasing the spring to let the jet/s hit the tube at the prescribed quench location/s. A proximity switch sensor is located close to the guard and sends the measurement signal when the guard just starts to move.

Figure 13 shows the steps followed to prepare the specimen. A similar procedure was followed to prepare the other specimen used in this study. The guard and the loaded spring system are shown in Figure 14. In order to ensure axial symmetry of cooling, the position of the specimen was carefully adjusted such that the specimen center point meets the center of the nozzle at the middle. A "+" shaped laser pointer is used to point to the specimen center point as shown in Figure 14.

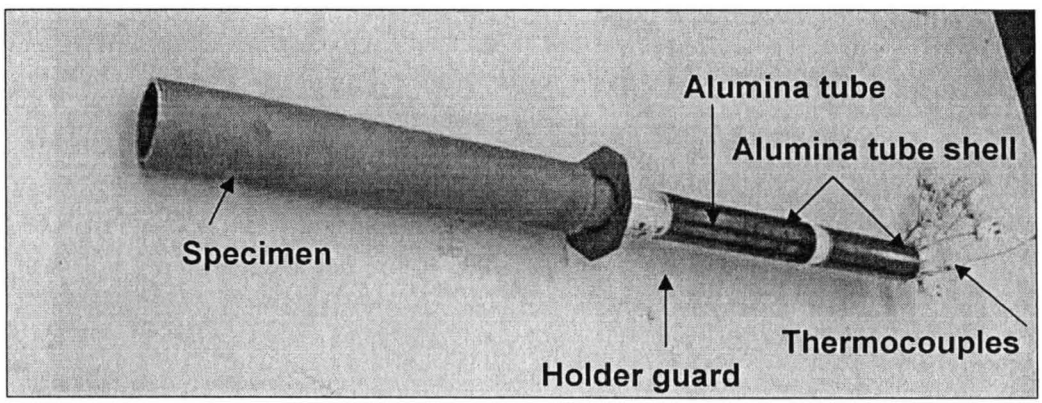

Figure 12: Stainless steel specimen and its holder.

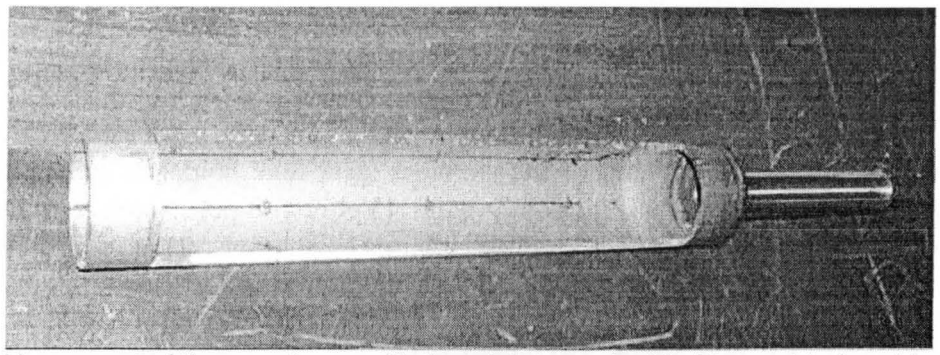

(a) Upper part of the specimen with the stainless steel holder welded and holes drilled.

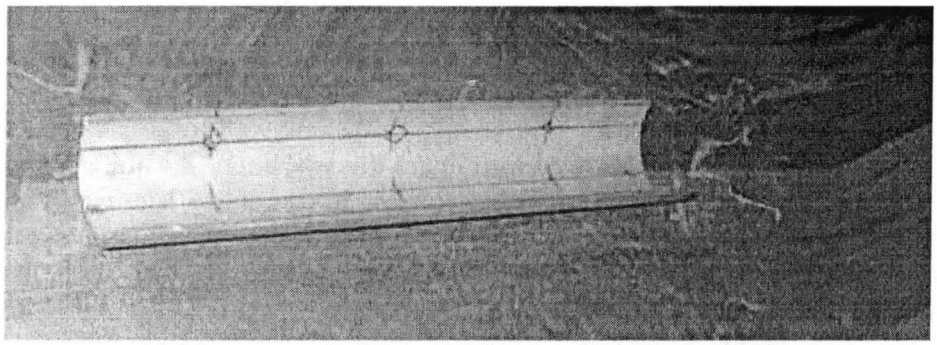

(b) Lower part of the specimen with holes drilled.

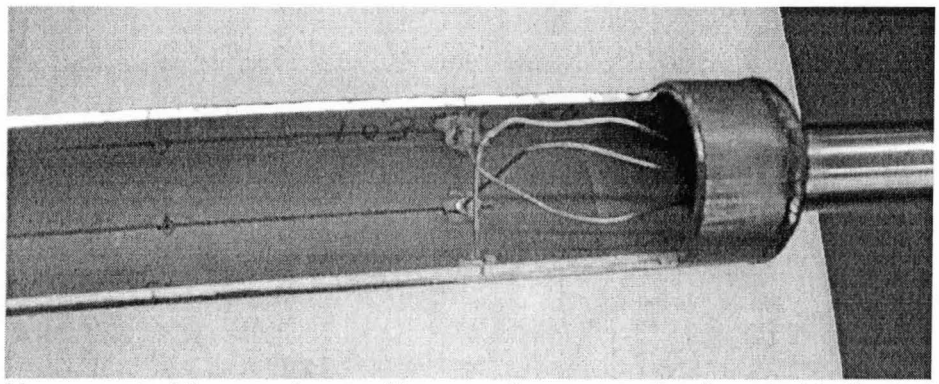

(c) Upper part of the specimen with some thermocouples inserted in the holes, flux added and silver solder rings put around the thermocouples.

Figure 13: Method of preparing the specimen (see next two pages).

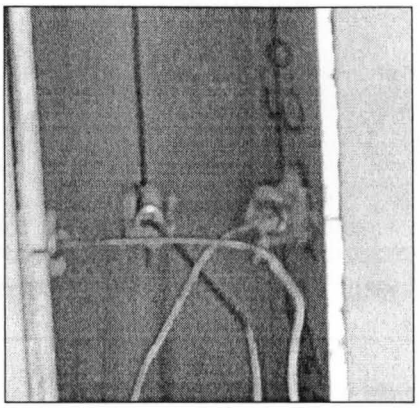

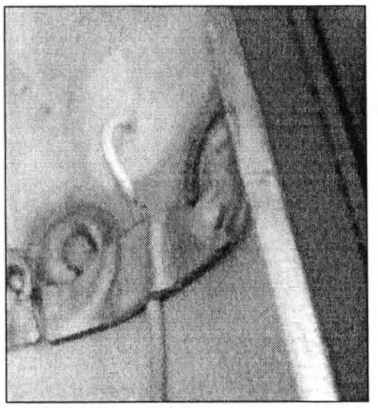

(d)The outer surfaces of the parts were heated to melt the silver solder. Stainless steel strips were welded on each thermocouple for additional thermocouple support.

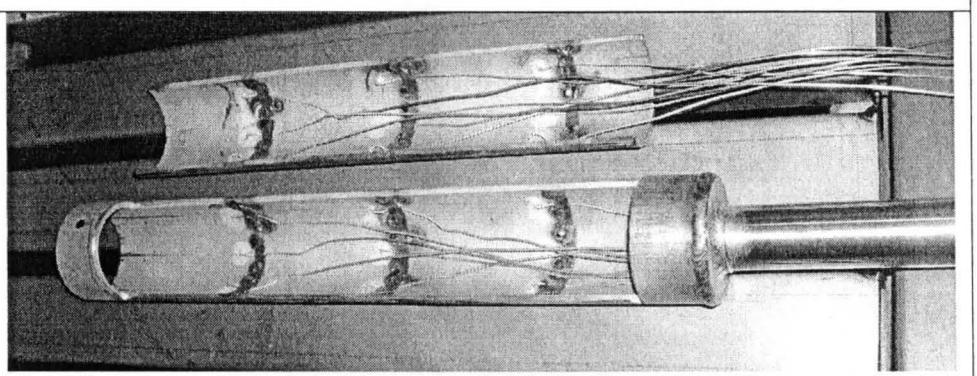

(e) Nine thermocouples were mounted in each part and the parts are to be welded together.

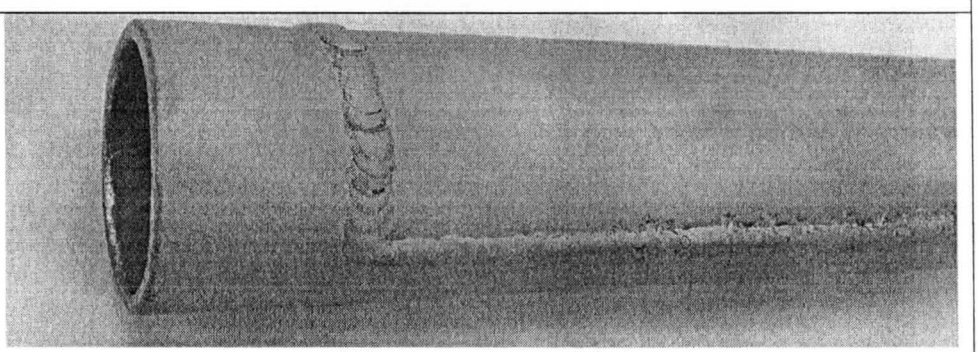

(f)The two parts welded.

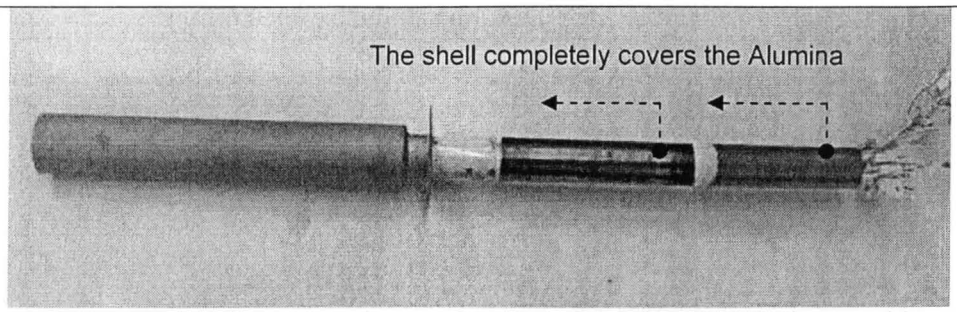

(g) The outer surface was cleared from welding effects by lathe machine. Alumina holder and its metallic shell were connected to the specimen.

Figure 13: Method of preparing the specimen (continued).

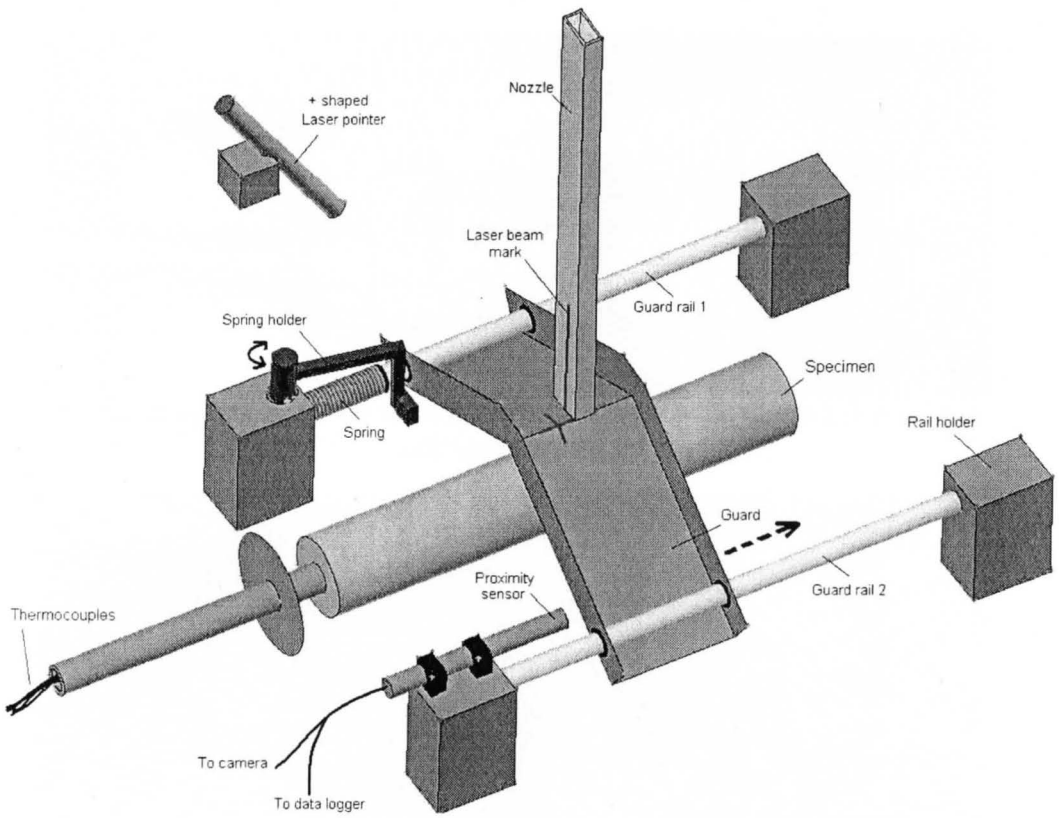

Figure 14: Specimen guard, loaded spring assembly and proximity sensor (three guards were used for the three jets).

3.1.2 Water Circulation System

The whole facility is located as close as possible to the box furnace in order to minimize the heat loss from the tube while it is being transferred to the cooling location. The water used in the cooling process passes through a circuit consisting of a heating tank, flow pump, head tank, distribution flow header and a collecting tank. Water is pumped from the heating tank by a ¾ hp GOULDS 316 SS centrifugal pump operating at 1750 rpm. A Y-strainer with mesh screen No. 165 filters the water before entering the pump in order to trap any incoming impurities and small particulate matter. The heating tank is 450 L Brad Ford White electric water heater with three 15 kW heating elements. The tank is surrounded by a 2-in thick non-CFC foam insulation to minimize heat losses. Fast acting, fully automatic controls are provided for temperature control and to reset energy cut off to prevent overheating. The heating tank is protected from corrosive effects of the hot water by a ceramic porcelain-like coating on the inside surface. A protective magnesium rod inserted through the tank provides additional protection against corrosion. For safety considerations, the tank is provided with a pressure relief valve [29].

Water is pumped to an 80 L head tank at elevation of 3.5 m from where it flows to a three-outlet cylindrical header (4-in diameter and 18-in long) located above the collecting tank. The header dimensions are shown in Figure 15. The header outlets connect to long rectangular nozzles (slots) to provide the rectangular water jets. Each header outlet has a valve to control the flow rate through each nozzle. When using more than one jet, the flow rate in each nozzle was manually adjusted by using a stopwatch and a graduated cylinder. The nozzles are 33.02 cm long; a length sufficient to ensure fully developed flow. The dimensions of the nozzles are shown in Figure 16.

The water flow from the nozzles is collected in the collecting tank (a cubic stainless steel tank) located underneath the nozzles. The flow rate is measured using a 1-in SIMARK turbine flowmeter with accuracy of ± 1% of reading. To minimize the vibrations generated by the pump from being transmitted to the test section, vibration dampers were placed beneath the pump. Also, high temperature hoses (-54-177°C operating range) were used before and after the pump and the specimen holder, as well as the motion system, were installed on supports fully separated from the stands supporting the water circulation system.

Depending on the required flow rate, two configurations of circulating the water in the water circulation system are possible; configuration A and configuration B as shown in Figure 17 and Figure 18; respectively. Configuration A is used for very low to high flow rates, up to 0.3 L/sec. However, the head tank, which is at elevation of 3.5 m, can not provide very high flow rates through the relatively large nozzle opening size, especially when the three jets are in operation. To

achieve higher rates, operation should be switched to Configuration B, where the flow is pumped from the collecting tank into the closed heating tank. This configuration is not possible without the advantage of the heating tank being closed and could be pressurized. The pressure created by the pump pushes the flow into the heating tank and directly from there to the header. This configuration was also found to provide constant flow rates with any effect of pump disturbances cancelled in the large heating tank and in the header itself.

More images of the specimen motion system and specimen guard assembly are shown in Figure 19.

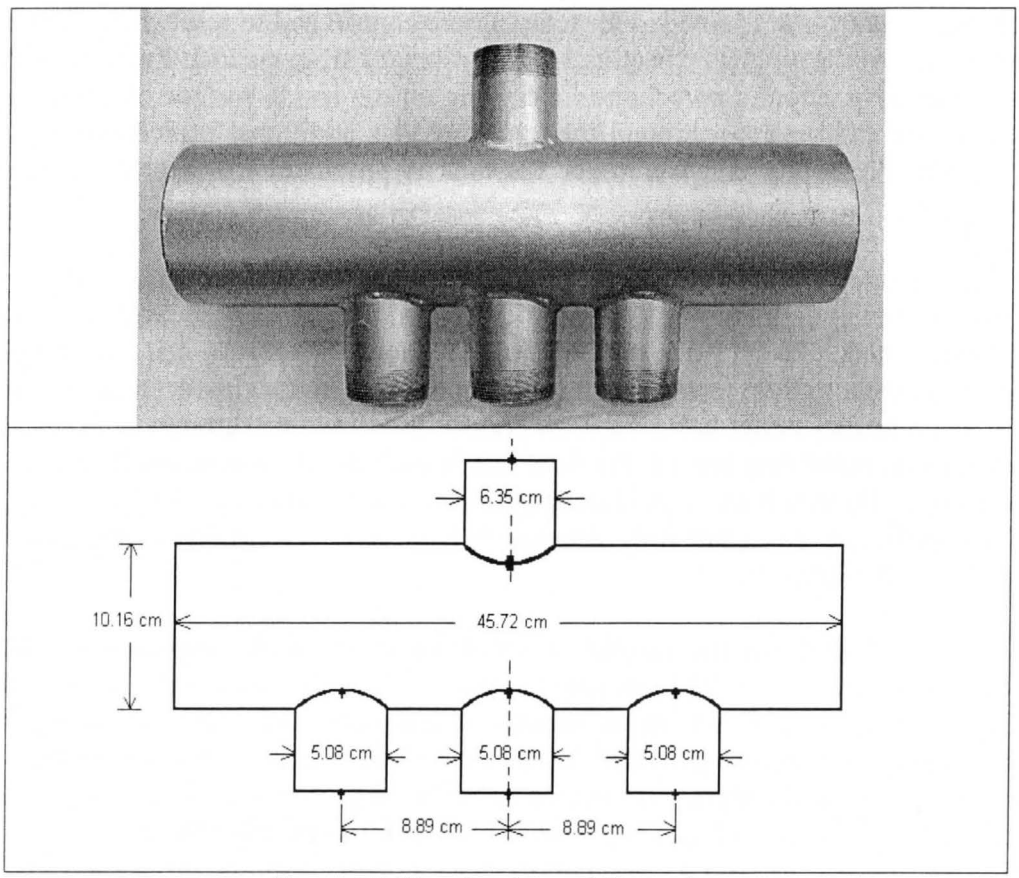

Figure 15: Flow header and dimensions.

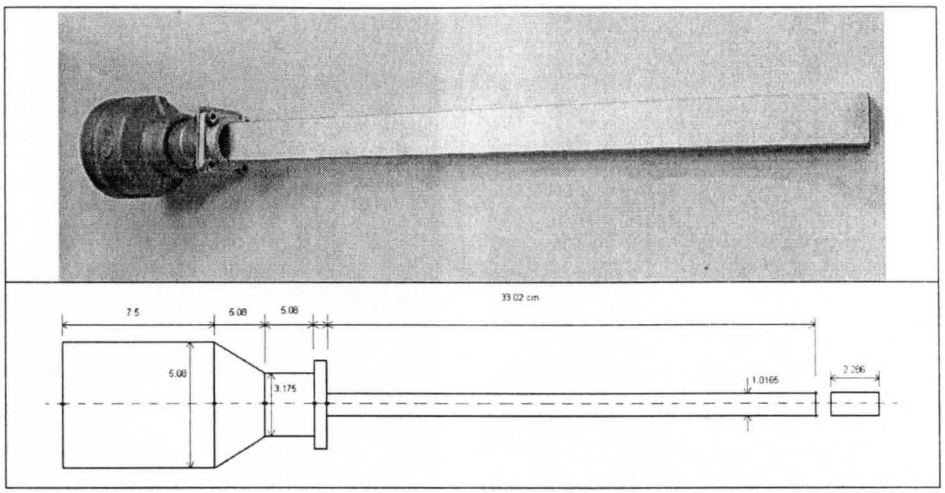

Figure 16: Rectangular nozzle and dimensions (three nozzles were used in this study).

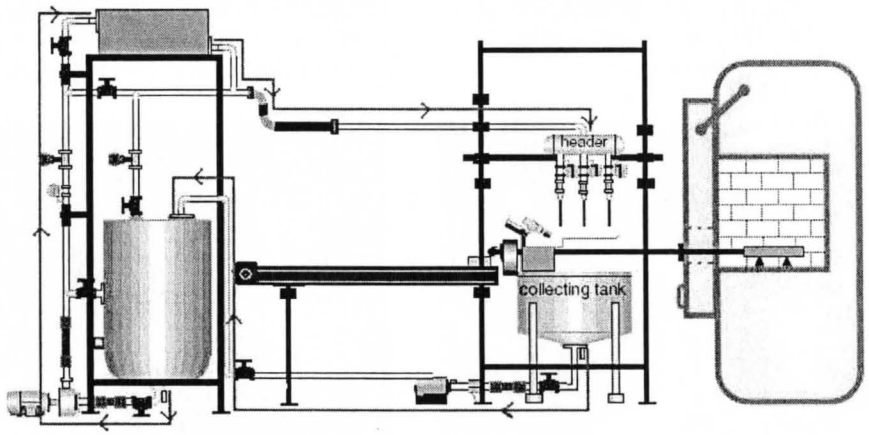

Figure 17: Configuration A of Water Circulation System (for very low to high flow rates).

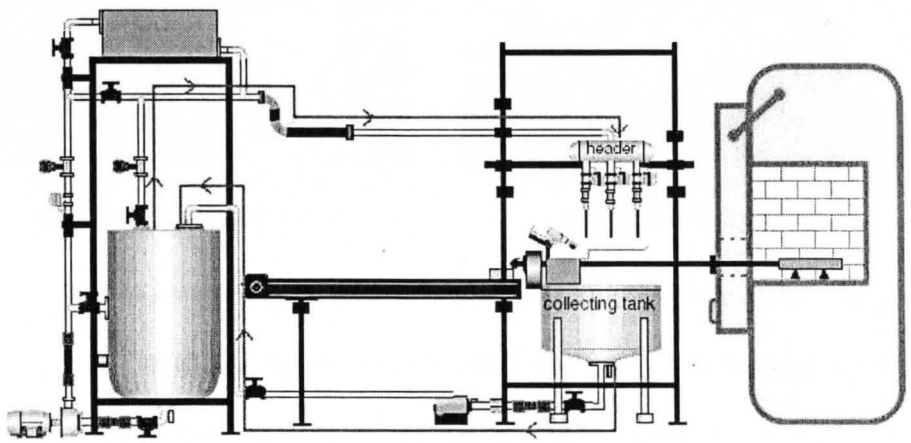

Figure 18: Configuration B of Water Circulation System (for very high flow rates).

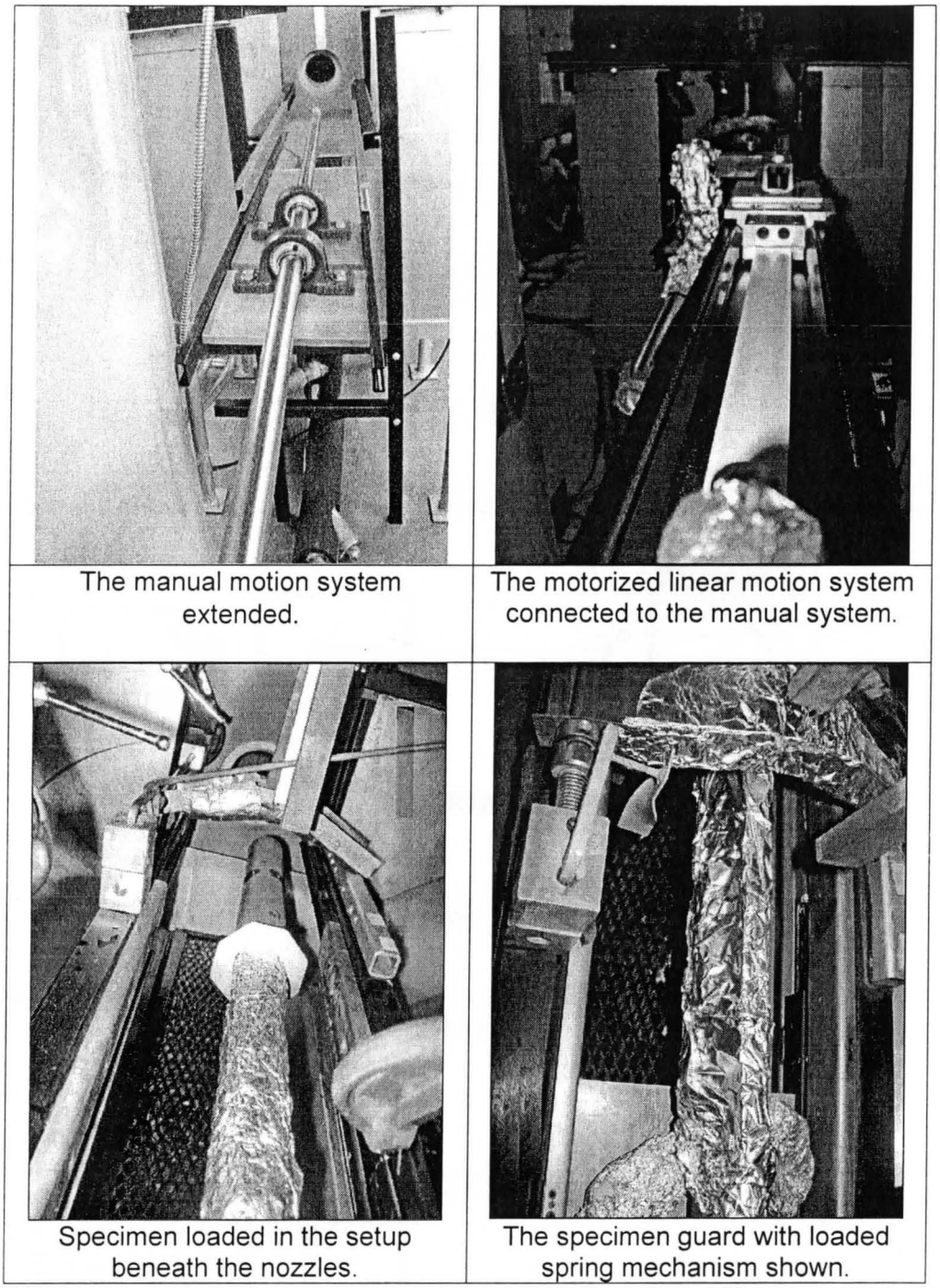

Figure 19: Specimen motion systems and specimen guard assembly.

3.1.3 High Speed Imaging and Data Acquisition System

The two-phase flow behavior around the tubes when quenched were visualized and recorded by a FASTCAM-X PCI 1024 high-speed camera (maximum of 1000

frames/sec at a resolution of 1024×1024 pixels and up to 109,500 frames/sec at a reduced resolution of 128×16 pixels). Lights are located at the back and the front of the tubes for illumination. The temperature at the thermocouple locations in the tubes were recorded by NI SCXI-1000 data acquisition system DAQ with maximum sampling rate of 500 kSample/s. Both measurements start simultaneously by receiving the signal from the proximity switch sensor. The proximity switch sensor could be mounted at the end of the motorized motion system and send the signal just before the specimen reaches the cooling location. It could also be mounted close to the specimen guard and sends the signal when the guard starts to move after releasing the spring as was shown previously.

Table 1 below summarizes the experimental setup main components and their specifications. More details on the experimental setup are included in Appendix A.

Table 1: Specifications of the experimental setup main components.

Equipment	Specifications	Manufacturer
High speed camera	Maximum resolution: 1 M pixel at 1000 fps*. Maximum Speed: 109,500 fps at 128×16 pixels.	Photron
Data acquisition system	Maximum sampling rate: 500 kSample/s.	National Instruments, NI
Heating tank	450 L electric water heater, 45 kW with temperature controller.	Bradford White
Pump	1750 rpm and ¾ hp.	mcKeough
Flowmeter	Flow range: 18.93-189.27 LPM, Temperature range: -100-121°C.	SIMARK
Strainer	165 mesh.	Sure Flow
Manual motion system	Self-alignment capability for mounting on imperfect surfaces, corrosion resistant and strokes to 198 cm.	The Precision Alliance
Motorized motion system	Maximum speed 3 m/s, less than 0.1 mm misalignment.	Velmex
Thermocouples	K- type, maximum deviation: -0.8°C at 650°C.	Omega
Furnace	Size: 92 cm x 92 cm x 92 cm box furnace, maximum temperature: 1000°C.	PSH Kilns and Furnaces
Computer	DELL, 2.33 GHz, 2 GB RAM.	DELL

* fps: frames per second.

3.2 Features of the Experimental Setup

The experimental setup was designed and constructed in such a way that it would be easy to be modified in future to study the effect of other parameters not are of interest in this study. These features include: controlling nozzle opening size and shape (circular, slot, ...), flow type (jet or spray), nozzle-to-surface spacing, jet distribution above or around the specimen, quench of multiple-specimens, cooling a moving specimen at constant or accelerated velocity (resembling steel cooling). Also, the setup can be easily modified for rapid immersion of the hot specimen in a water bath in the collecting tank, programmed motorized rotation of the specimen while in furnace (this is useful to get uniform temperature distribution on larger specimens as there is no heating elements at the furnace lower and upper surfaces but only on the sides). Finally, upper or bottom re-flooding of the specimen can be achieved by further modification.

3.3 Experimental Procedure and Test Matrix

A series of experiments have been conducted to investigate the quench process. The effects of the parameters shown in Figure 20 have been studied. The experimental data was obtained by the following procedure:

1. The outer surface of the tube was polished by Emery paper of 200 Grit before each test.

2. The water in the heating tank was heated to the required water temperature.

3. The tube was then inserted into the furnace and heated to the desired initial surface temperature.

4. When the desired surface temperature was reached, the high speed camera and the DAQ were placed in a ready state for measurement prior to moving the tube from the furnace. Lights were turned on and the specimen guard was armed by loading the spring.

5. The heated water was pumped through the water circulation system at the required water velocity until steady state conditions of jet temperature and jet velocity were reached.

6. The tube was then moved from the furnace by sending a command from the computer to the motorized motion system to start moving. The tube was rapidly moved into position beneath the tube guard which was then moved away quickly allowing the water jets to impinge on the heated tube to start the cooling process. The measurements were recorded using the

high speed camera and the DAQ until the tube's surface temperature reached that of the jet.

7. Most of the tests were repeated at least three times to ensure test repeatability. Some tests were repeated up to five times, if necessary. A few tests were not possible to be repeated due to the difficulty in setting the exact same operating conditions, especially at high water flow rates with water temperature within a "critical water subcooling range": a water subcooling range within which any small increase in the water temperature, such as 0.5°C, was observed to have a great influence on the quench characteristics, mainly increasing the quench delay time. This subcooling range depends, but slightly, on the water flow rate and the initial surface temperature. For stainless steel the critical water temperature is in the range 74-78°C. This will be more discussed in Section 5.4.2 page 97.

8. The initial surface temperature was varied by controlling the furnace temperature, jet velocity by controlling the valve opening at the header outlet, water temperature by controlling the heating tank electric power.

9. Several tests were done under varying number of water jets. Those tests were conducted when one, two and three jets are in operation while fixing all other operating conditions.

Table 2 below shows the measurement uncertainty of the devices used. It is important to note that the uncertainty in placing the specimen beneath the water jets is mainly due to thermal expansion of the specimen and its holder. However, as will be shown in Chapter Five: Results and Discussion, this uncertainty has a negligible effect on the cooling process due to the relatively large size of the nozzle opening.

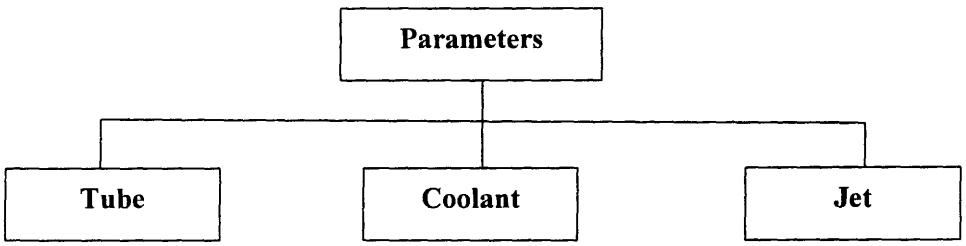

1. Material

Brass, Stainless Steel.

2. Diameter

D = 1 & 2 in.

3. Surface Temperature

T_s = 350 - 820°C.

1. Type

Water.

2. Temperature

$T_{coolant}$ = 20-85°C.

1. Velocity

0.08 - 1.5 m/s.

2. Opening

Rectangular (1×1/2 in)

3. Orientation

Parallel or in cross with tube axis.

4. Number of Jets

1, 2, 3.

Figure 20: Parameters varied to study their effect on the quench process.

Table 2: Measurement uncertainty.

Measured variable	Uncertainty
Temperature	- 0.8 °C at 650°C.
Flow rate	± 1% of reading (for single water jet). ± 6% of reading (for multiple-water jets).
Water temperature	± 0.2 °C.
Specimen dimensions and hall position	± 0.0005 mm.
Time (for high speed imaging)	± (1/fps*).
Time (for temperature measurement)	± (1/sampling rate).
Specimen location beneath the jets	± 1 mm.

* fps: frames per second.

Chapter Four

Description and Processing of the Raw Data

This chapter includes general description of the collected raw data. The data consists of temperature measurements and high speed videos. Methods and techniques used to calculate the various quantities from the raw data are also described. The extracted data, trends and correlations are left for Chapter Five: Results and Discussion.

4.1 Cooling Profiles

Examining the cooling profiles at the stagnation point for all tests indicates that each test can be classified into one of the five cooling profiles shown in Figure 21 below. The description of the five distinct profiles is shown in Table 3.

Table 3: Description of the varying cooling profiles observed in this study and shown in Figure 21.

Cooling Profile	Description and Operating Conditions
Cooling profile (a)	Rapid cooling; usually occurs for high water subcooling.
Cooling profile (b)	Initially rapid and then slow cooling followed by another rapid cooling; noticed for high water subcoolings combined with low jet velocity (brass only).
Cooling profile (c)	Initially rapid and then slow cooling; noticed for a range of "critical" water subcooling (see page 40 Section 3.3 and page 97 Section 5.4.2) with high initial surface temperature (brass only).
Cooling profile (d)	Slow cooling; usually occurs for low water subcoolings with high or moderate jet velocity.
Cooling profile (e)	Slow cooling with a "shoulder" of slow cooling in the transition boiling region; noticed for low water subcoolings combined with very low jet velocity (brass only).

For profile (a) it takes only a fraction of a second to start quenching the surface and therefore the surface temperature decreases very rapidly immediately after the jet struck the surface. This profile was noticed for both stainless steel and brass for high water subcoolings.

Profile (b) shows initially rapid and then slow cooling followed by another rapid cooling. This profile is noticed for high subcoolings combined with low jet velocity with brass material and was not obtained when testing stainless steel material.

Profile (c) shows an initial rapid decrease in surface temperature for a short time followed by a slow decrease in surface temperature indicating re-establishment of the vapor film. Again, this profile was noticed for brass specimen only with initial surface temperatures above 500°C and for a range of water subcooling, which will be called in this study a "critical subcooling range".

The behavior in profiles (b) and (c) corresponds to the high thermal conductivity of brass which allows rapid conduction of heat transfer towards the region where the vapor film starts to destabilize causing that region to re-heat. The initiated small wet patch and the vapor film will also re-heat causing the vapor film to be re-established. Profile (d) shows slow cooling which was noticed for both materials at low water subcoolings.

Profile (e) shows slow cooling with an irregularity looks like a "shoulder" in the transition boiling region similar to that of Profile (b). This profile was noticed for brass specimen only with low water subcoolings combined with very low jet velocity. Again, this irregularity corresponds to transition from transition boiling mode back to film boiling due to the rapid conduction heat transfer in the specimen causing the initial wet patch to revert to a dry patch. Brass has a high thermal conductivity which allows heat to be easily conducted to balance the heat flux demand by the jet and to maintain a high surface temperature [9] whereas the thermal conductivity of the stainless steel specimen is around one tenth that of brass.

In summary, the difference in the observed cooling profiles is most likely governed by the ability of the material to conduct heat to the region of the jet/surface interaction. Profiles (a) and (d) were reported by Mozumder [9] for carbon steel and copper; respectively.

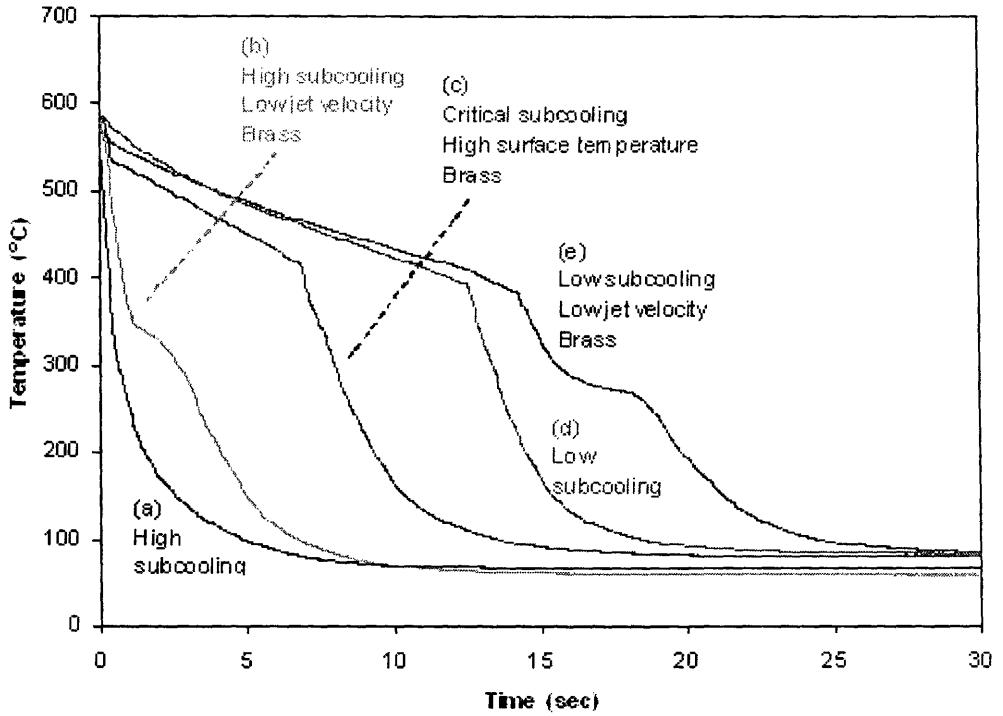

Figure 21: Types of cooling profiles at stagnation point.

4.2 Typical Cooling Profiles

Figure 22 shows a typical plot of the cooling profiles at eight locations at the 2-in OD stainless steel tube cooled by water jet at temperature 82°C and jet velocity of 0.7 m/sec. The initial tube temperature was 650°C. The eight locations are distributed at 60° intervals around the perimeter of the tube as shown in the figure and are numbered from 1 to 4 and 5 to 8 starting from the point at the top. Only eight locations are shown here as the thermocouple locations are symmetric around the tube. Such profiles, along with the high speed videos, represent the raw data from the experimental tests. Initially, and before the jet first strikes the tube, the profiles at the eight locations almost coincided but the initial temperatures at locations 5-8 are slightly higher than those at locations 1-4 due to a temperature gradient in the hot tube as it is connected to the Alumina tube holder at one end.

The process of taking the hot tube out of the furnace until the start of the cooling takes about 3 seconds using the motorized motion system. In that time the temperature of the tube drops by few degrees, less than 3°C for the high initial surface temperatures.

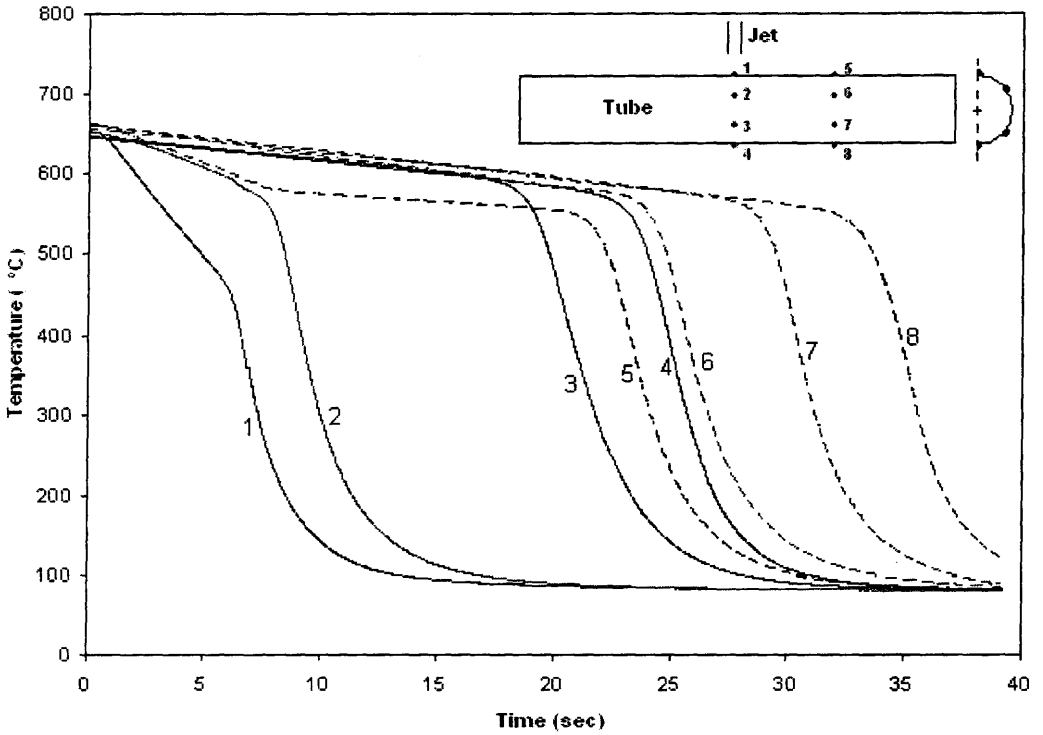

Figure 22: Typical cooling profiles at eight locations at the tube surface (Stainless steel tube, 2-in OD, T_{in} = 650°C, T_{water} = 82°C, Jet Velocity = 0.7 m/sec).

The top thermocouple and the adjacent ones (2 and 5) indicated a steeper drop in temperature in the film boiling region, which ended when the surface quenched. The cooling rates in the film boiling region at locations downstream from stagnation are lower than those at stagnation. The reason for that is a thinner water sheet thickness presents downstream from stagnation point and the water temperature increases as it moves along the surface.

The following section discusses the temperature measurement response time.

4.3 Measurement Response Time

The quench temperature at all thermocouple locations are found from the cooling profiles using the tangent line intersection method described in Figure 3 in Chapter One: Introduction. The thermocouples used in this study are a new thermocouple product released by OMEGA called OMEGA XL. This type of thermocouple provides the advantage of having the minimum deviation for a wide range of high temperatures among all other thermocouples. The deviation of this type of thermocouples as a function of the environment temperature is shown in Figure 23 (the red line) as well as the deviations of other types of thermocouples. For almost all OMEGA XL thermocouples used in this study the same amount of

deviation was noticed. However, a more important specification is the measurement response time.

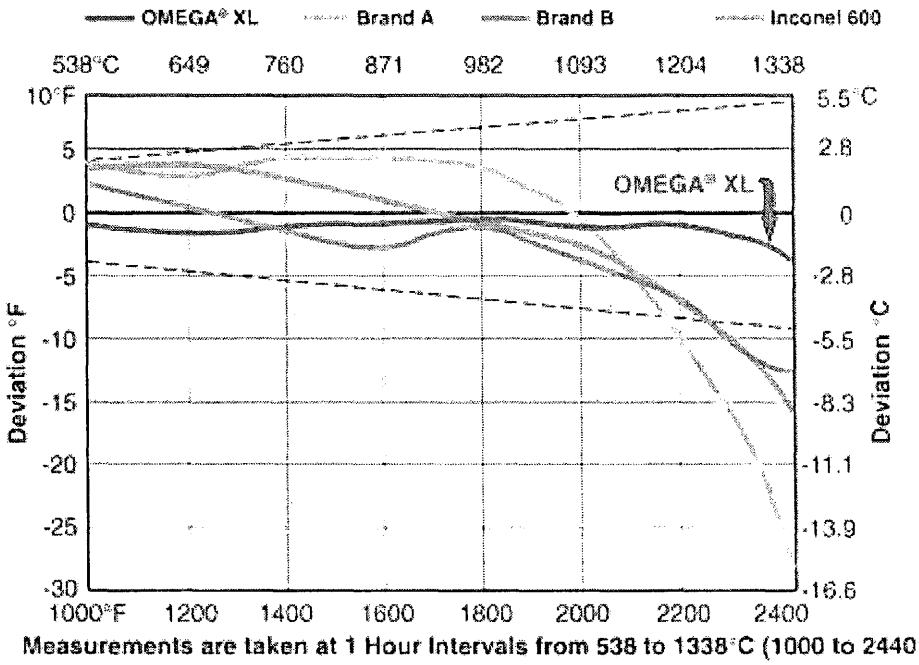

Figure 23: Deviation of OMEGA XL thermocouple as compared to other known thermocouples [39].

The measurement response time of the thermocouples was estimated by the tools used in this study: the data acquisition system and the high speed camera. The thermocouple was inserted in water in the range 0-100°C and in molten metals (Lead, Aluminum and Brass) in the range 327-940°C and the insertion process was recorded by the high speed camera. It was found that the thermocouple response time was between 0.16-0.21 sec, decreasing with increasing environment temperature, with an average of 0.185 sec. However, the response time of the thermocouple alone is insufficient. The response time of heat conduction between the surface and the thermocouple tip 1mm deep beneath the surface must also be known. This response time depends on the solid material, decreasing with increasing thermal conductivity. To estimate this response time, several tests were done using a test section with two similar thermocouples inserted at depths of 0.5 and 1.0 mm from the surface. The 0.5 mm depth between the two thermocouples showed a response time of about 0.43 sec for stainless steel and 0.12 sec for brass. Since in all tests the thermocouples were 1.0 mm deep from the surface, a doubling of this time is roughly expected. Thus, the total response time (thermocouple response time plus the solid material response time) is estimated to be 1.045 sec for stainless steel and 0.425 for brass. However, this does not include some response delay expected in the gap between the thermocouple tip and the

solid material which is filled by the silver solder material. A better estimate to the total response time including that of the gap could be estimated from the duration of the initial constant temperature region in the cooling profiles like those in Figure 28 page 53. At time zero of the plot, the jet was observed in the recorded videos to first strike the surface. However, the thermocouples start to respond after a time of about 1.13 sec for stainless steel and about 0.49 sec for brass. These final estimates are adopted for the rest of this study and the cooling curves were shifted by these delay times. Table 4 summarizes the above estimates. The cells in gray are the adopted values.

Table 4: Estimation of thermocouple and material response times.

Response time (sec) / Material	Insertion in liquid	First thermocouple: 0.5 mm in depth	Second thermocouple: 1.0 mm in depth	Cooling curves
Thermocouple	0.185	--	--	--
Stainless steel	--	0.43	1.045	1.13
Brass	--	0.12	0.425	0.49

The following section shows typical visual observations captured along with the temperature measurements shown in Figure 22.

It is worth to mention that the temperature measured by the thermocouples at a depth of 1-mm from the surface is higher than that at the surface. To estimate the temperature at the surface three thermocouples at depths of 0.5, 1.0 and 1.5 mm were instrumented at a location in the brass and the steel tubes. The temperatures measured at these locations were extrapolated to estimate the temperature at the surface. It was found that the maximum deviation between the estimated surface temperature and that measured at 1-mm depth is 12°C for brass and 18°C for steel. This is the maximum deviation as the deviation was found to depend on the water temperature: as the water temperature decreases the deviation was found to increase. As the majority of the experimental tests of this study were conducted for relatively high water temperatures the deviation is lower than the maximum deviation and could be lower than the maximum deviation by the half. However, the maximum deviation was used to set the lower limit of the error bar in the temperature measurement figures. The upper limit of the error bar was set to 3°C as estimated from Figure23.

4.4 Visual Observations

4.4.1 Film Collapse and Motion of the Re-wetting Front

Figure 25 shows the process of wet patch development for the conditions identified in Figure 22. The high speed videos captured were used to observe the film collapse, propagation and rebound of the re-wetting front and to measure the size of the boiling region. The times at which the images in Figure 25 were captured are shown on the temperature profiles in Figure 24.
All videos were captured using the PFV Ver.3 software which was also used to extract image frames from the videos. ImageJ software was used to analyze the digital images.

When the hot tubes were moved out of the furnace they were bright red in color when heated to elevated temperatures; 600°C and above, as shown in image (a) of Figure 25. After the jet strikes the tube, the area surrounding the stagnation point starts to darken as shown in image (b) where the tube was still red outside the darkened zone. After a time, the vapor film collapses, as indicated by observing a rapid growing white layer in the stagnation zone followed by a rapid rupture of the liquid sheet in that zone, as shown in image (c) of Figure 25. A darker zone immediately starts to develop and grow in size after the film collapse as shown in image (d). This zone is the wet patch zone and represents the zone were the water fully wets the cooled surface. Image (e) shows the wet patch at a later time when it has grown in both, axial and circumferential directions. In image (f), the two re-wetting fronts moving in the circumferential direction meet at the tube bottom point and wet it. In the axial direction, the re-wetting front continues to move until the tube becomes fully wetted and the surface is cooled to the jet temperature.

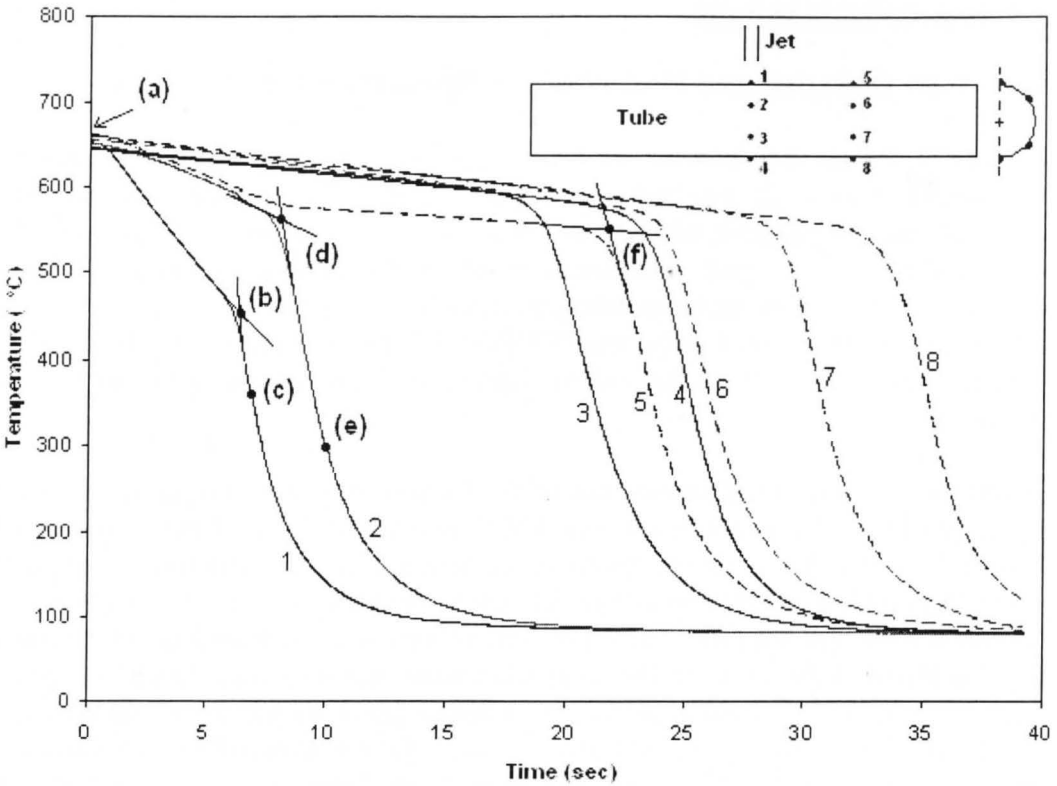

Figure 24: Typical cooling profiles at eight locations at the tube surface (Stainless steel tube, 2-in OD, $T_{in} = 650^{\circ}C$, $T_{water} = 82^{\circ}C$, Jet Velocity = 0.7 m/sec) with observations shown in Figure 25.

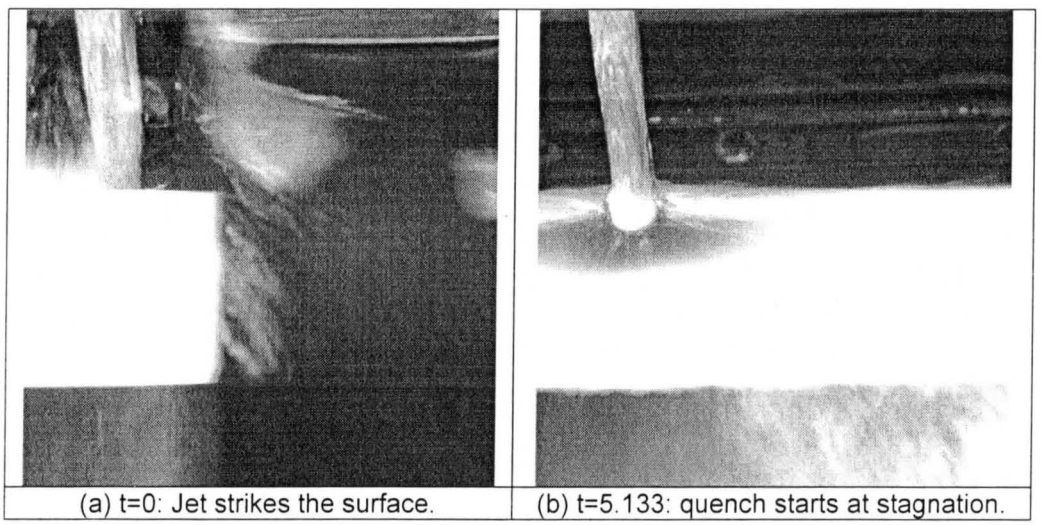

(a) t=0: Jet strikes the surface. (b) t=5.133: quench starts at stagnation.

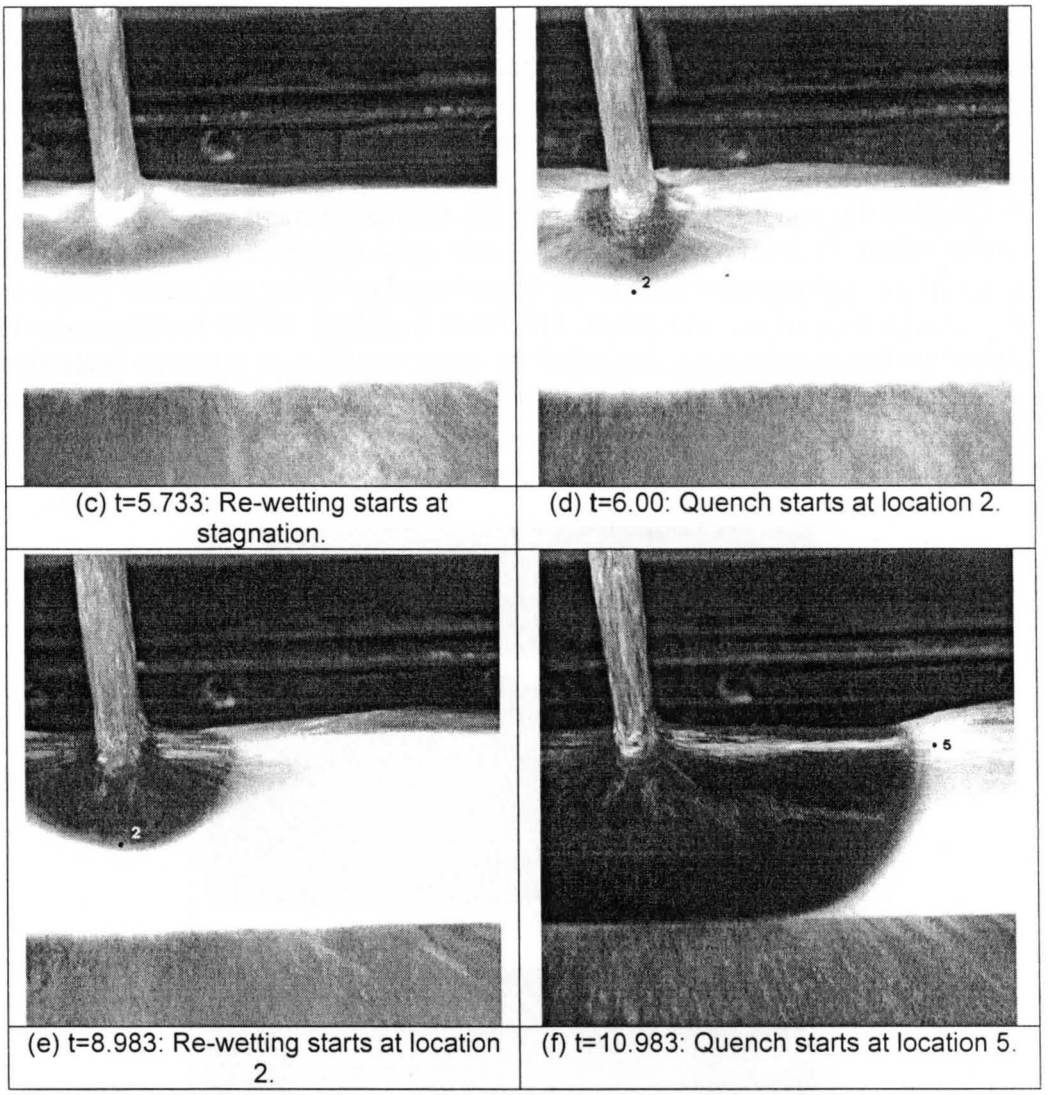

(c) t=5.733: Re-wetting starts at stagnation.

(d) t=6.00: Quench starts at location 2.

(e) t=8.983: Re-wetting starts at location 2.

(f) t=10.983: Quench starts at location 5.

Figure 25: Typical growing process of the wet patch for Stainless steel tube, 2-in OD, T_{in} = 650°C, T_{water} = 82°C, Jet Velocity = 0.7 m/sec.

4.4.2 Boiling Width and Re-wetting Front Location

As discussed in Section 1.5.3 of Chapter One page 9 when the re-wetting front propagates, the wetted area is observed to be divided into two regions: fully wetted central region with no apparent boiling and an outer thin annular region with vigorous nucleate (and transition) boiling. The inner edge of this region represents the boundary between the single-phase liquid convection region and the combined nucleate and transition boiling region. The outer edge represents the re-wetting front line where actual surface-liquid contact starts to take place. Film boiling prevails after this line. The width of this annular region is of interest in this section and identified by the boiling width.

The boiling width and the re-wetting front location were measured from the digital frames. For better vision of the boiling region boundaries most of the images were processed by the ImageJ software using the "edge finder" tool. A typical image before and after processing is shown in Figure 26. A scale factor was determined by equating the actual known tube diameter to the diameter as observed in the images. The scale factor for each experiment was then multiplied by the radius of the re-wetting front in the axial direction measured from the center of the impingement zone to the inner boundary of the wet patch. This gives the actual radius of the wet patch. The inner boundary of the boiling zone was chosen for the measurement instead of the outer boundary as it can be determined more clearly. A typical curve of the re-wetting location and the boiling region size is shown in Figure 27.

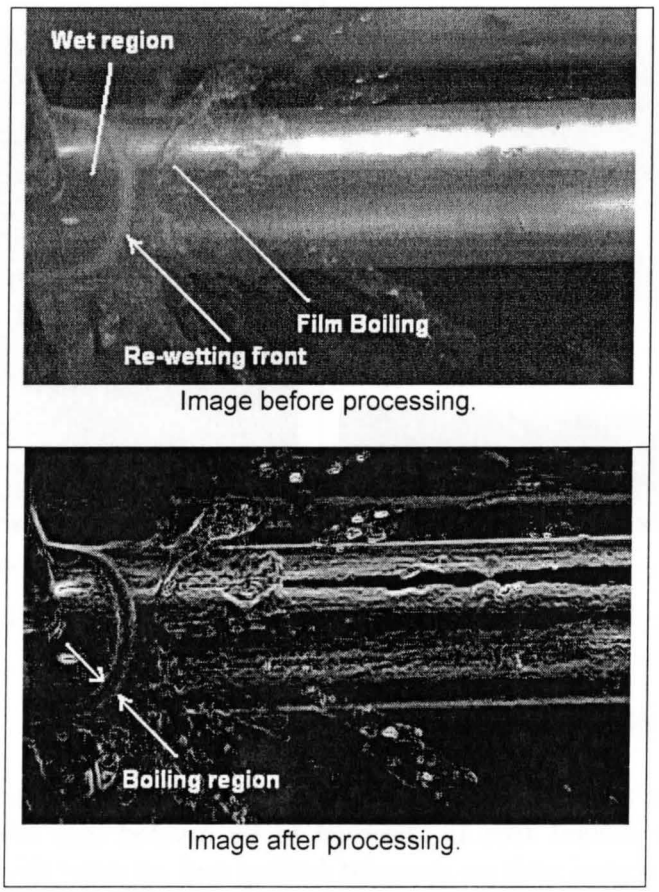

Figure 26: Typical Image processed by the "edge finder" to better locate the boundaries of the boiling region.

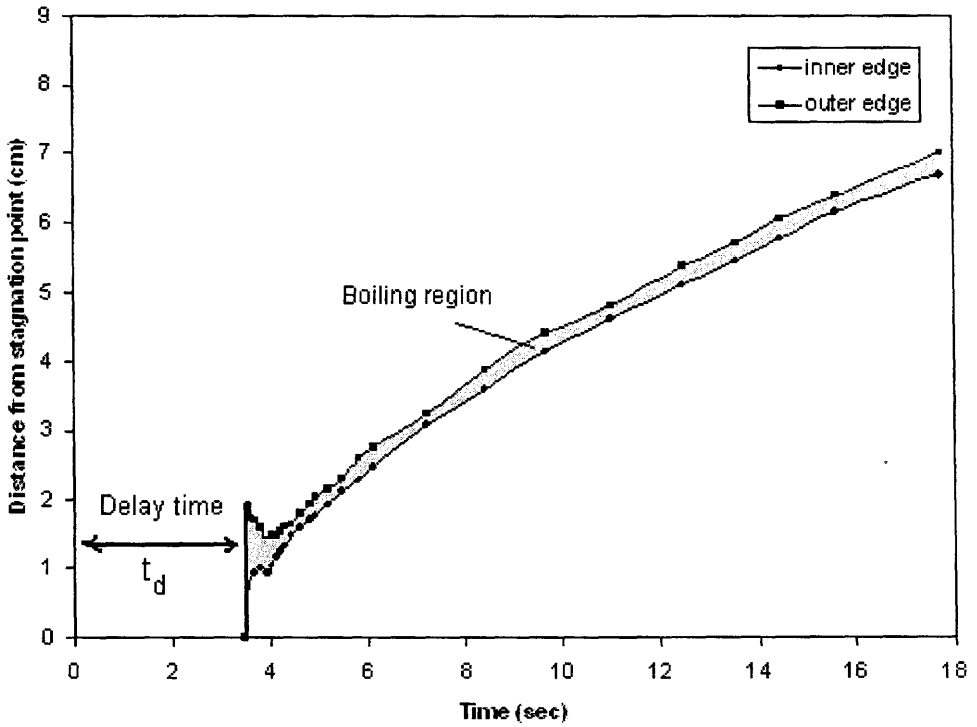

Figure 27: Re-wetting front location and boiling region size versus time during cooling of a 2-in diameter stainless steel tube, T_{in} = 500°C, T_{water} = 83°C and V_{jet} = 0.37 m/sec.

4.4.3 Re-wetting Delay Time

As defined in Chapter One: Introduction, the delay time is defined as the time interval from when the jet first strikes the hot surface and the spreading of the wet patch. This delay time will be referred to as t_d and represents the period shown in Figure 27. Another delay time that was looked at in this study is the delay time from when the jet first strikes the hot surface to the moment just after the vapor film collapse when re-wetting starts. This is characterized by a strong rupture of the liquid sheet around the stagnation point. Before the collapse, balance between the jet momentum at the stagnation point and the pressure developed in the vapor film occurs. It was found in this study that the two delay times are very close to each other and are almost equal.

4.5 Effect of Several Operating Conditions

This section includes general description of the cooling profiles under various operating conditions. The following sub-sections show plots of the cooling profiles as recorded at the stagnation point and other locations. The effects of initial surface temperature, water temperature and jet velocity are shown.

4.5.1 Effect of Initial Surface Temperature

Typical effects of the initial surface temperature on the cooling profile at the stagnation point are shown in Figure 28. It was observed that the slope (cooling rate) in the film boiling region is almost the same for the varying initial surface temperatures. The profiles shown were obtained using the 2-in stainless steel tube, water temperature of 81.6°C and jet velocity of 1.43 m/sec. When the initial surface temperature was 500°C the surface quenched almost immediately after the cooling process started and film boiling was observed to exist for a very short period of time.

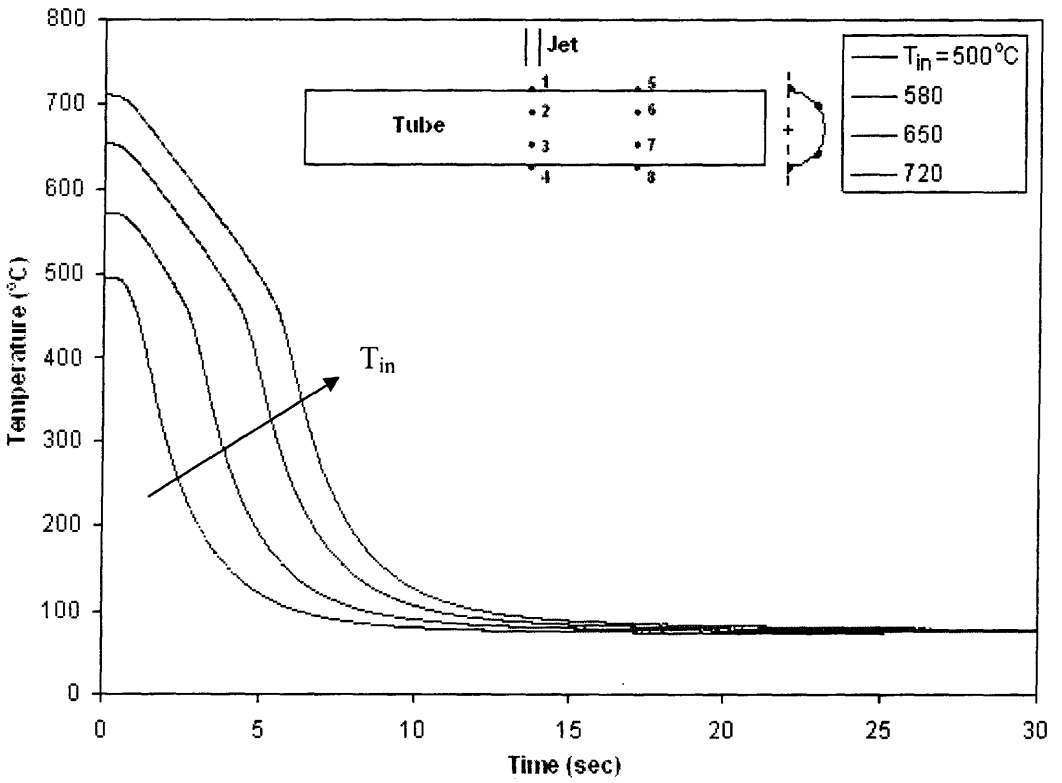

Figure 28: Effect of initial surface temperature on the cooling profile at stagnation point 1 (2-in stainless steel tube, water temperature 81.6°C and jet velocity 1.43 m/sec).

4.5.2 Effect of Water Temperature

The effect of water temperature on the cooling profile at the stagnation point for high jet velocity is shown in Figure 29.The profiles shown were obtained using the 2-in stainless steel tube for T_{in} = 550°C and a jet velocity of 0.93 m/sec. It was observed that, for this jet velocity, the slope (cooling rate) in the film boiling region is almost the same for the varying water temperatures. However, a great dependence of the quench temperature on the water temperature is observed. By

increasing water temperature from 79.0°C to 80.3°C (1.3°C increase) the quench temperature decreased by around 50°C.

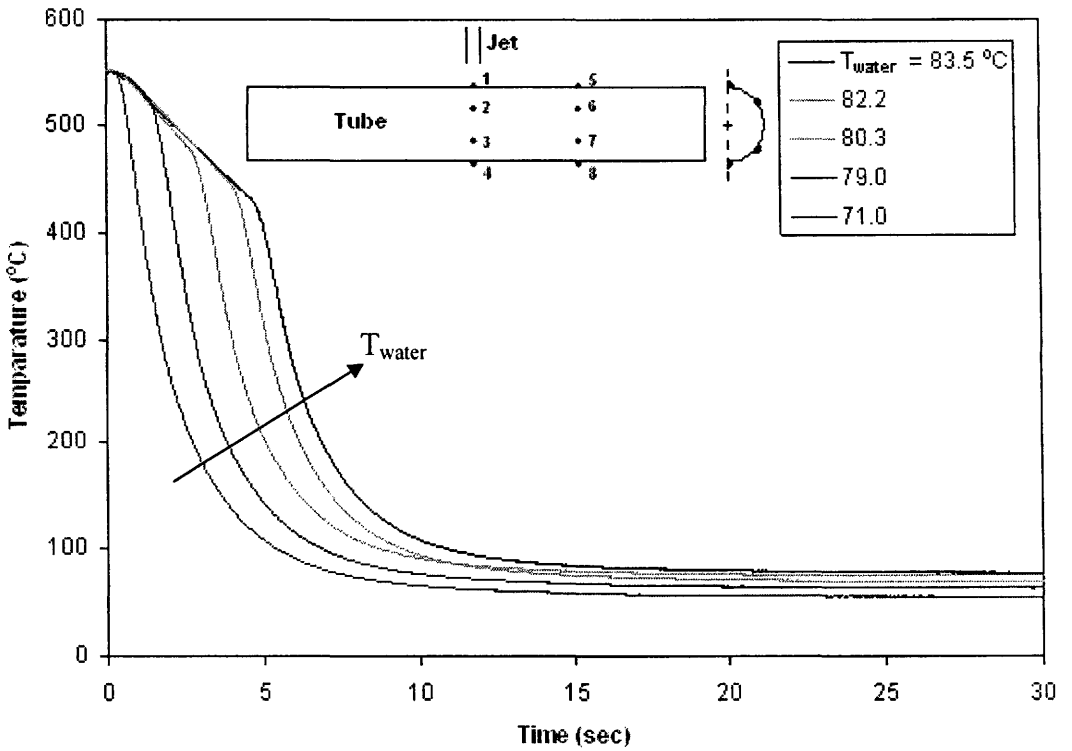

Figure 29: Effect of water temperature on the cooling profile at stagnation point 1 for high jet velocity (2-in stainless steel tube, Tin = 550°C and jet velocity 0.93 m/sec).

Under other operating conditions, water temperature was found to affect the cooling rate in the vapor film boiling region. Figure 30 shows that decreasing water temperature increased the cooling rate. The profiles shown were obtained using the 2-in stainless steel tube for T_{in} = 505°C and a jet velocity of 0.37 m/sec.

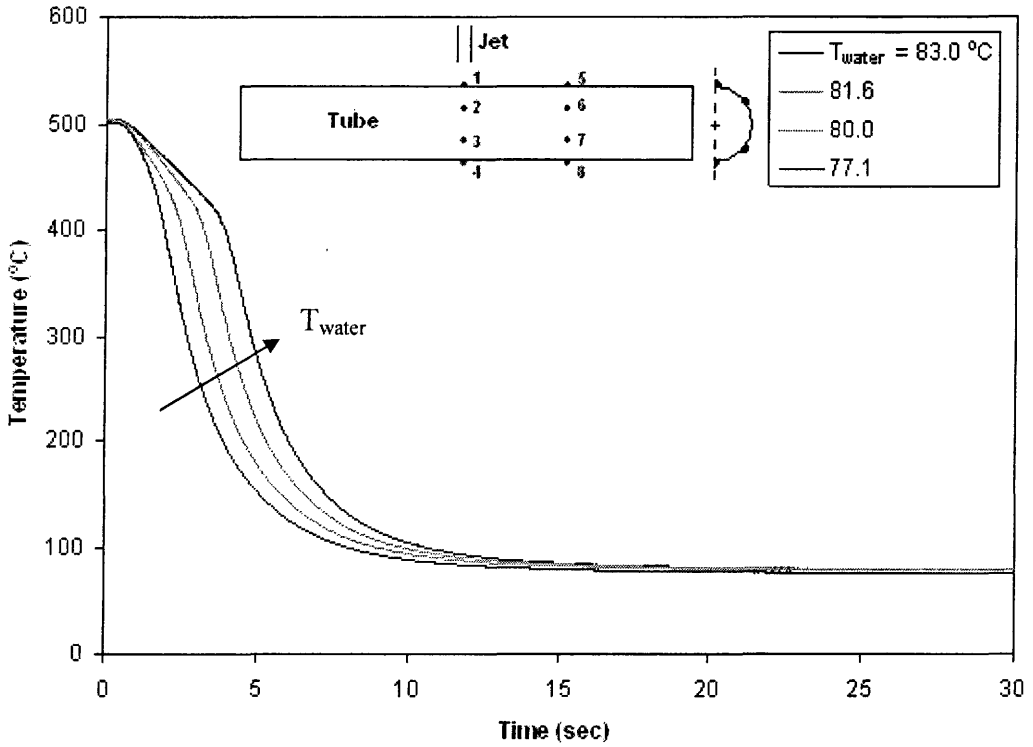

Figure 30: Effect of water temperature on the cooling profile at stagnation point 1 for low jet velocity (2-in stainless steel tube, T_{in} = 505°C and jet velocity 0.37 m/sec).

4.5.3 Effect of Jet Velocity

The effect of jet velocity on the cooling profile at the stagnation point is shown in Figure 31. The profiles shown were obtained using the 2-in stainless steel tube, T_{in} = 650°C and water temperature 83°C. It is observed that the slope (cooling rate) in the film boiling region is dependent on jet velocity: the cooling rate increases with water jet velocity.

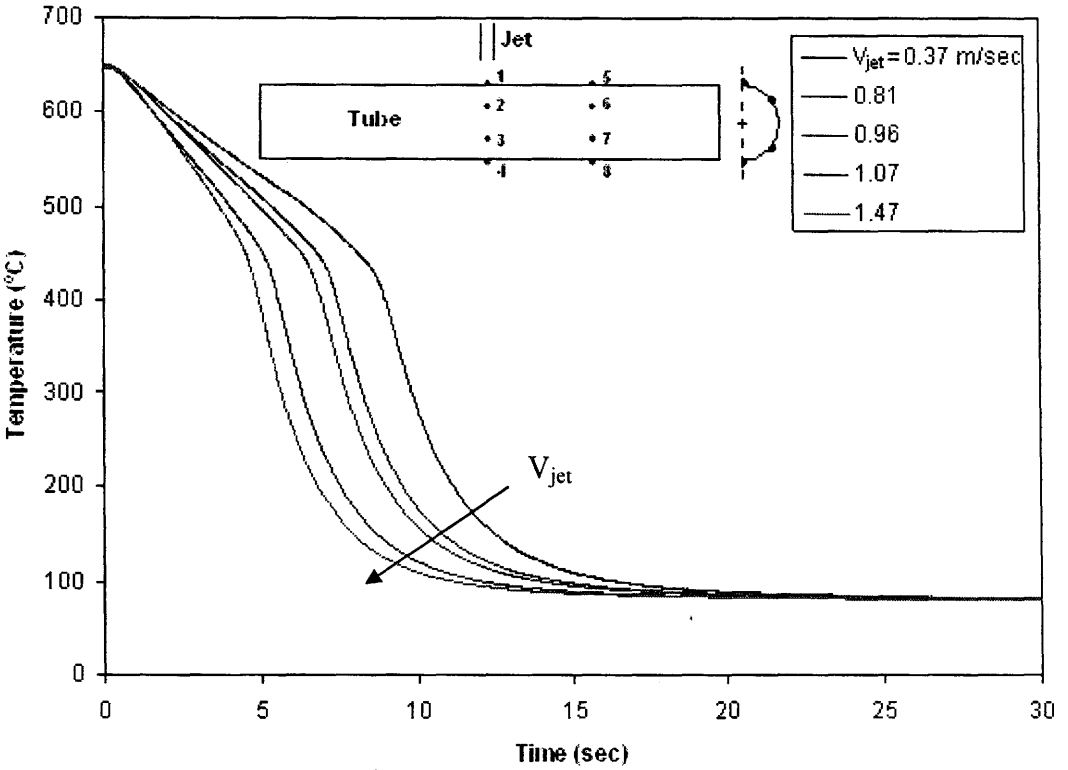

Figure 31: Effect of jet velocity on the cooling profile at stagnation point 1 (2-in stainless steel tube, T_{in} = 650°C and water temperature 83°C).

4.6 Effect of the Lifted Water Sheet

The lifted water sheet was found to have an effect on cooling, and sometimes, re-wetting the surface ahead to the re-wetting front especially when the jet velocity is high enough. Figure 32 shows the phenomena, where a 1-in brass tube initially at 800°C was cooled by water jet at 23°C and jet velocity of 0.50 m/sec. The cooling profiles at location 5 (3-in away from the stagnation point) for varying jet velocities are shown in Figure 33 where a 1-in brass tube initially at 630°C was cooled by water jet at a temperature of 23°C. For low jet velocities of 0.28 and 0.5 m/sec, point 5 was cooled by conduction as the jet hydrodynamics can not let the re-wetting front to reach that point. For jet velocity of 0.6 m/sec, point 5 quenches by the re-wetting front as it approaches the point. For higher jet velocities, and thus higher water flow rates, water splash starts to quench point 5 like when the jet velocity was 0.9 and 1.3 m/sec. As the re-wetting front moves ahead, the location where the splash strikes the surface also moves ahead which causes the temperature at point 5 to increase due to heat conduction. However, point 5 quenches again as the re-wetting front approaches the point. It is interesting to point out here that for higher jet velocities, like 1.5 m/sec, the second quench (the quench by the re-wetting front) occurs at a higher temperature as the re-wetting

front moves faster (comparison between the cooling profiles for jet velocities of 1.3 and 1.5 m/sec; respectively).

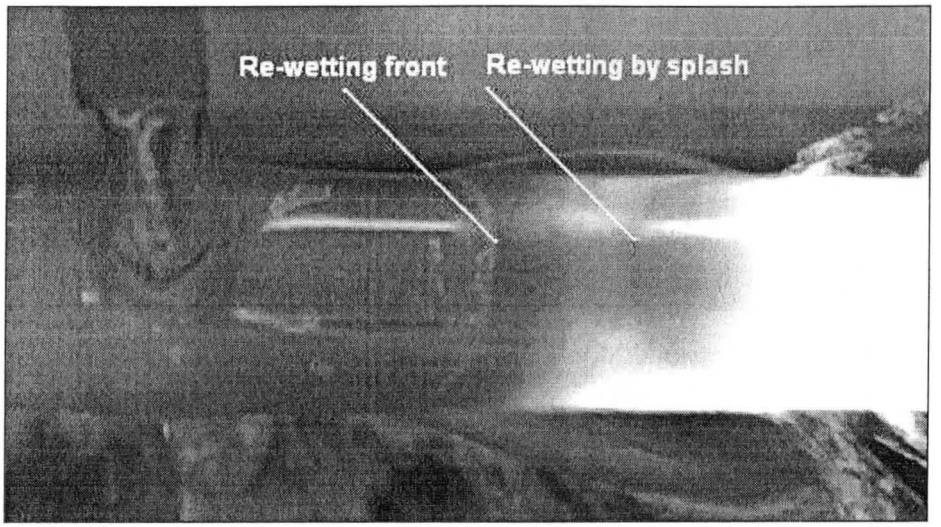

Figure 32: Re-wetting of the surface by water splash ahead of the re-wetting front (1-in brass tube, T_{in} = 800°C, T_{water} = 23°C and V_{jet} = 0.50 m/sec).

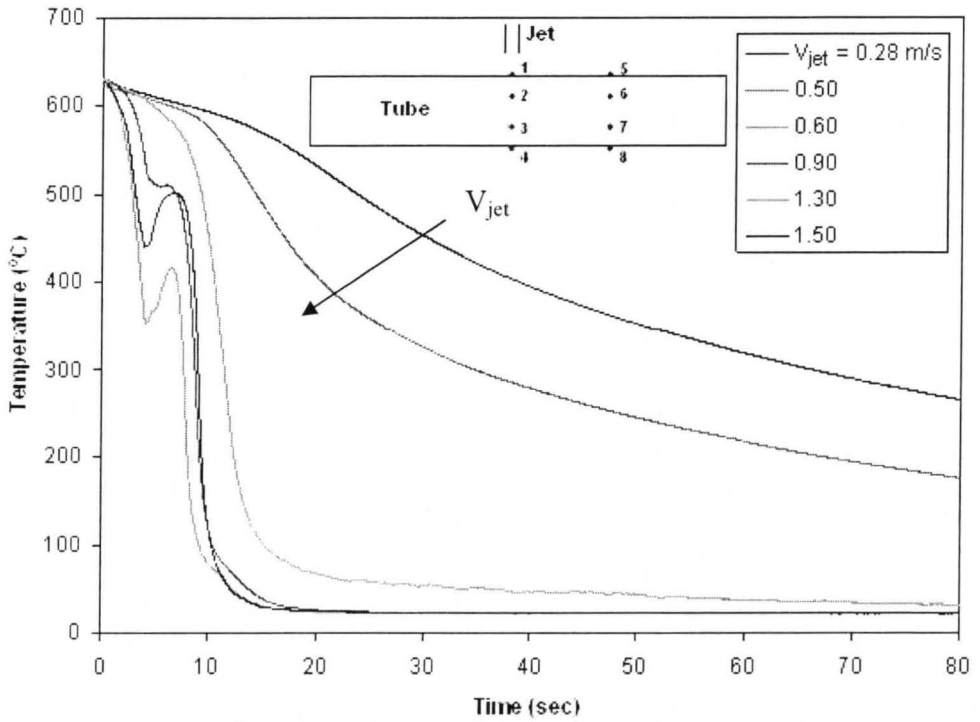

Figure 33: Effect of jet velocity on the cooling profile at point 5 (1-in brass tube, T_{in} = 630°C and water temperature 23°C).

Chapter Five

Results and Discussion

This chapter includes the results and discussion of this study. The chapter is divided into the following sections: (5.1) Re-Wetting Delay Time, (5.2) Re-Wetting Front Location and Velocity, (5.3) Boiling Region Size. Then the temperature analysis which includes: (5.4) Quench Temperature, (5.5) Re-wetting Temperature and (5.6) Vapor Film and Nucleate Boiling Cooling Rates. For high water subcoolings, the surface was found to quench in fraction of a second. Therefore, most of the data included in this chapter was obtained for relatively low water subcoolings (40°C and lower) where the operating conditions, like initial surface temperature and jet velocity were found to have a noticeable effect on the quench characteristics such as the delay time. Comparison, where possible, was held with results available in literature.

5.1 Re-Wetting Delay Time

The main objective of this section is to discuss the re-wetting delay time and to analyze the effects of initial surface temperature, jet velocity and water subcooling on this parameter. Additional experiments were done to investigate the effects of surface curvature, solid material, tube wall thickness, number of jets and jet orientation. A correlation for predicting the delay time on curved surfaces has been developed.

As indicated in Chapter One: Introduction, before the re-wetting front starts to move on a hot dry surface, an initial wet patch is formed after a time in jet impingement cooling. The size of the initial wet patch stays almost constant for a while and then starts to increase as the re-wetting front moves. Mozumder also [9] reported this phenomenon during cooling of flat surfaces.

At high water subcooling the delay time is very small but tends to high values at low subcooling. The delay time was found to go very steeply to high values within a narrow band of few degrees of water temperature. The results of delay time are presented as curves of delay time versus water temperature. All results were found to be characterized by the same shape of curve as will be shown in the following sub-sections.

5.1.1 Correlation for Delay Time

The delay time was found to be dependent on water temperature, jet velocity, initial surface temperature, solid material and tube diameter. The aim of this sub-section is to correlate the delay time to these parameters. It is assumed that the

water does not initially wet the surface due to a balance of heat transfer within the solid material by conduction, q_{solid}, with heat transfer from the surface to the liquid, q_{liquid}. The heat flux transferred by conduction within the solid is generally proportional to $\sqrt{\frac{\rho Ck}{t}}$ [9, 13]. Therefore:

$$q_{solid} = -k\frac{\Delta T}{\Delta x} = -k\frac{(T_{in} - T(t))}{\Delta x} = \gamma\sqrt{\frac{\rho Ck}{t}}(T_{in} - T(t))$$

Where γ is a constant, T_{in} is the initial surface temperature and $(T_{in}\text{-}T(t))$ is the temperature driving force for heat conduction in the solid. The heat transfer to the liquid just after initiating the wet patch can be given as:

$$q_{liquid} = h(T(t) - T_{water})$$

Where h is the heat transfer coefficient. At the moment of re-wetting initiation, it is assumed that:

$$q_{solid} = q_{liquid} = \gamma\sqrt{\frac{\rho Ck}{t}}(T_{in} - T(t)) = h(T(t) - T_{water})$$

The heat transfer coefficient is generally a function of jet velocity. The temperature difference $(T(t) - T_{water})$ can be related to $(T_{in} - T_{water})$ and $(T_{sat} - T_{water})$ [13]. Finally, according to the observations of this study, the delay time is related to tube diameter (as will be shown in sub-section 5.1.7 page 66). Therefore, at the balance:

$$\sqrt{\frac{\rho Ck}{t_d}} = f(V_{jet}, (T_{in} - T_{water}), (T_{sat} - T_{water}), d)$$

Where d is the tube diameter. Using the data collected, the following correlation was determined by the least mean square method:

$$\sqrt{\frac{\rho Ck}{t_d}} = 4.12\times10^3 V_{jet}^{\ 0.44}(T_{in} - T_{water})^{2.53}(\Delta T_{sub})^{-2.04}d^{-2.53} \qquad (1)$$

The correlation is presented in Figure 34 where the delay time for steel, brass and Mullite (Silica) tubes with different tube diameters could be predicted. The ranges of the operating conditions used to develop the correlation are as follows:

V_{jet} = 0.22-1.43 m/sec, ΔT_{sub} = 15-80°C, T_{in} = 400-740°C, d = 2.54 and 5.08 cm (1 and 2 in) and solid material: steel, brass and Mullite.

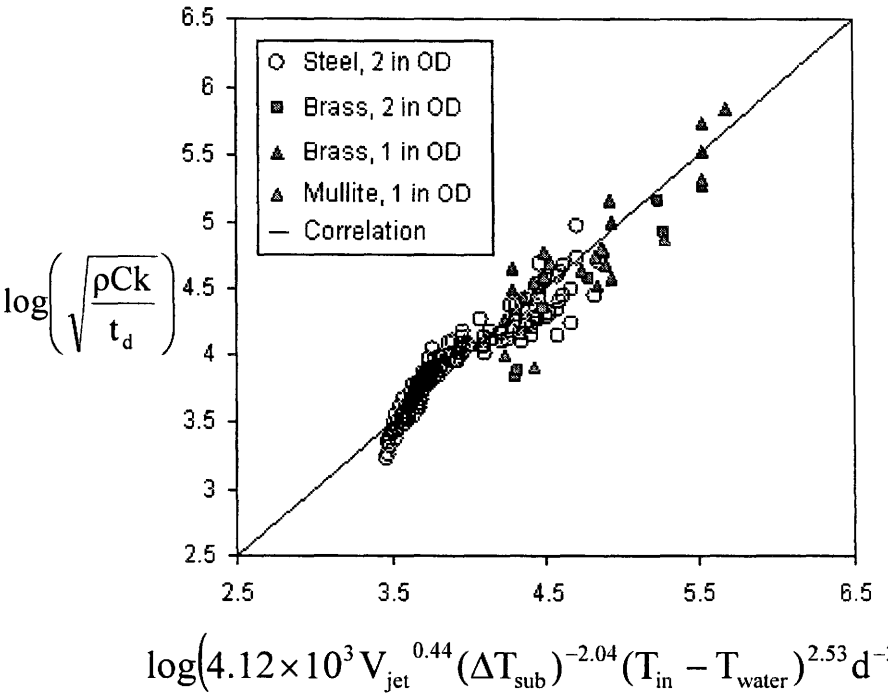

Figure 34: Data of delay time with prediction of Equation 1.

5.1.2 Comparison with Data in Literature

Figure 35 shows a comparison between the delay time measured by Piggott [7] for cooling a hot horizontal Inconel tube by a water jet and the delay time predicted by Equation 1. The operating conditions in Piggott's experiments were: mass flow rate = 15 g/sec (jet velocity = 2.12 m/sec), jet diameter = 3.0 mm, initial surface temperatures = 600, 800°C, and tube diameter = 2.54 cm. The comparison shows that the correlation under-predicts the experimental data but shows the same trend. The under-prediction is mainly due to the definition of the delay time. Piggott defined the delay time as the time from when the jet first strikes the surface to the moment when the wet patch starts to move. Here, the delay time is defined as the time from when the jet first strikes the surface to the moment of initiation of the wet patch. In Piggott's experiments, there was a delay between the two times. One another reason for the under-prediction could be using the correlation beyond the operating conditions under which it was developed (surface temperature of 800°C and 2.12 m/sec jet velocity in Piggott's experiment). However, the correlation prediction is still good.

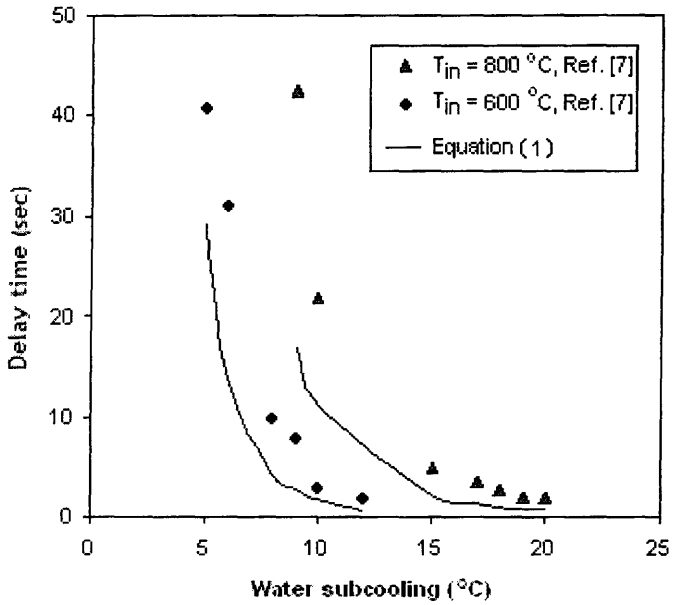

Figure 35: Comparison between delay time predicted by Equation 1 and data collected by Piggott [7] for cooling of Inconel tube with mass flow rate = 15 g/sec, jet diameter = 3.0 mm, initial surface temperatures = 600, 800°C, and tube diameter = 25.4 mm.

5.1.3 Effect of Initial Surface Temperature

Figures 36 and 37 illustrate the effect of initial surface temperature on the re-wetting delay time for a 2-in diameter stainless steel tube. As the initial surface temperature increases the delay time strongly increases for a given jet velocity and water temperature.

The reason of this behavior is that at high initial surface temperature, the vapor film boiling is preferable and most of the liquid evaporates until the surface temperature is reduced to a suitable temperature for re-wetting to start.

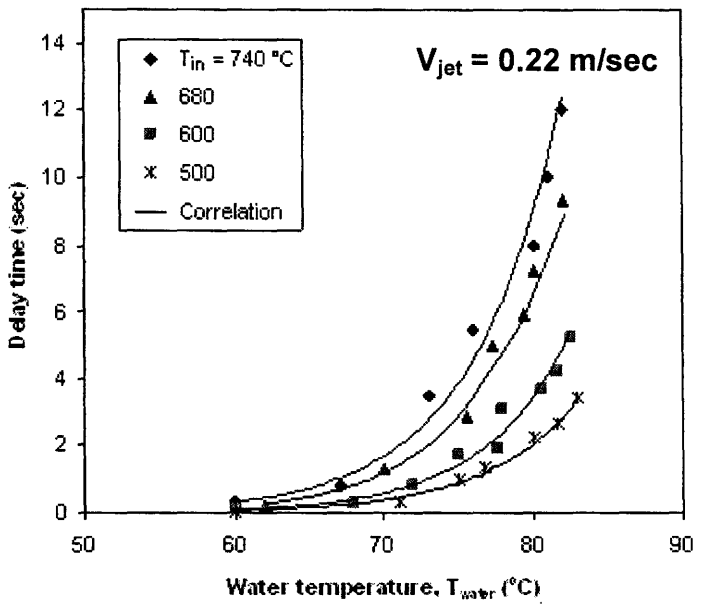

Figure 36: Effect of initial surface temperature on re-wetting delay time, V_{jet} = 0.22 m/sec.

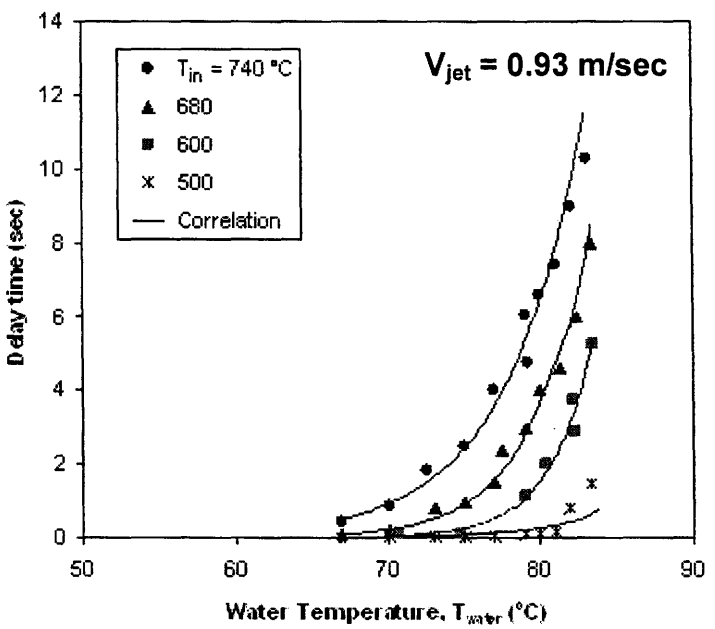

Figure 37: Effect of initial surface temperature on re-wetting delay time, V_{jet} = 0.93 m/sec.

Figure 38 shows the delay time versus the initial surface temperature for different water temperatures and jet velocity of 1.43 m/sec. For the long delay times, or high water temperatures, linear relationship is noticed between the delay time and the initial surface temperature for surface temperatures above 600°C.

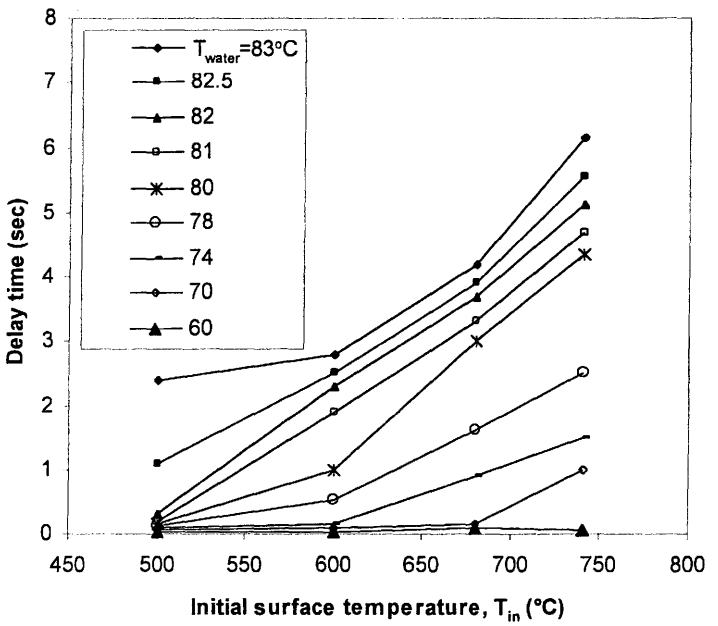

Figure 38: Effect of initial surface temperature and water temperature on re-wetting delay time, V_{jet} = 1.43 m/sec.

5.1.4 Effect of Water Subcooling

As was shown in Figures 36, 37 and 38 the delay time increases with decreasing water subcooling. This is due to the higher thickness of the vapor film in the stagnation zone for low subcoolings where it takes longer time to collapse. For high water subcoolings, the vapor film was found to destabilize very rapidly. Figure 39 shows the delay times during cooling of brass tube initially at 600°C by water jet at 21°C. The data shows the same trend as shown in the previous figures, but with very short delay times; around 0.20 sec for low jet velocities and less than 0.05 sec for high jet velocities.

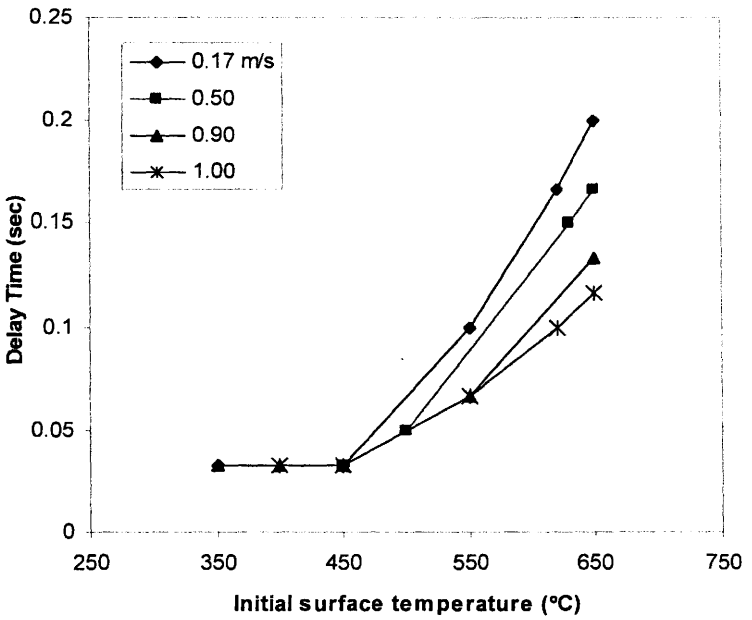

Figure 39: Effect of initial surface temperature on re-wetting delay time during cooling of 1-in brass tube for several jet velocities, $T_{water} = 21°C$.

5.1.5 Effect of Jet Velocity

Figures 40 and 41 show that the delay time increases with decreasing jet velocity for two initial surface temperatures: 600°C and 740°C; respectively.

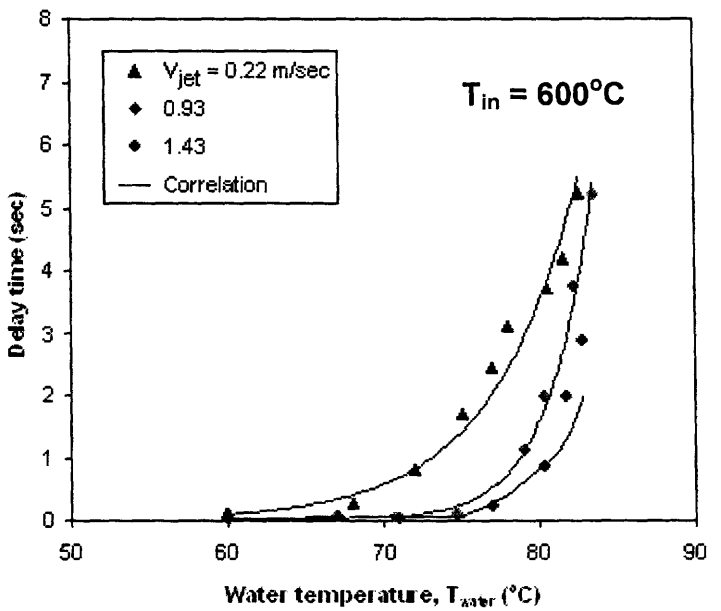

Figure 40: Effect of jet velocity on re-wetting delay time, $T_{in} = 600°C$.

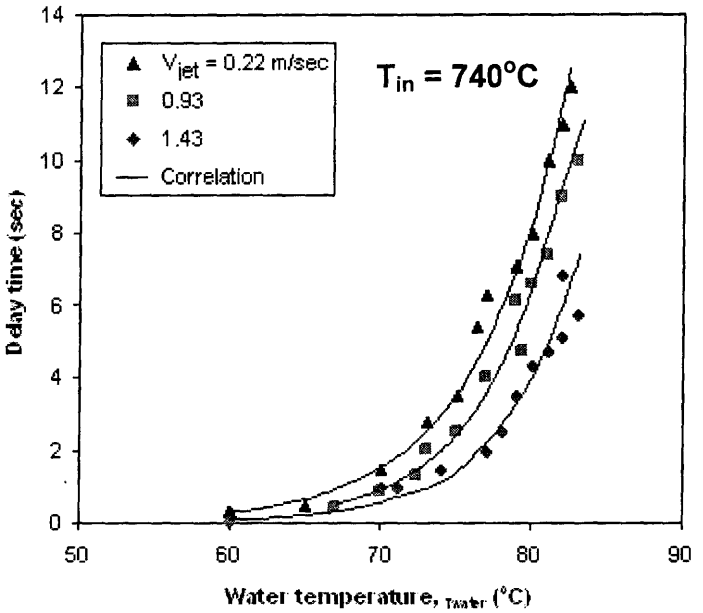

Figure 41: Effect of jet velocity on re-wetting delay time, T_{in} = 740°C.

5.1.6 Effect of Solid Material

Figure 42 shows the delay time for three materials: brass, steel and Mullite for water temperature of 83°C and initial surface temperature of 600°C. The surface material has a strong influence on the delay time as shown in the figure for a range of thermal conductivity of about 100 W/m.K. As the surface thermal conductivity increases the delay time increases for a given operating conditions. The thermal conductivity represents the ability of the material to supply heat to the region where the water jet interacts with the surface. In the case of brass the thermal conductivity is high so it is easier to supply heat and maintain a high surface temperature. The thermal conductivity of Mullite (6 W/m.K) and steel (21 W/m.K) are much lower than that of brass (109 W/m.K) so the surface cools more quickly; in fraction of a second for Mullite.

Also, the heat capacity of brass is higher than that of the other two materials which means that brass contains higher total stored heat. This results in a slow cooling rate which leads to a longer delay time.

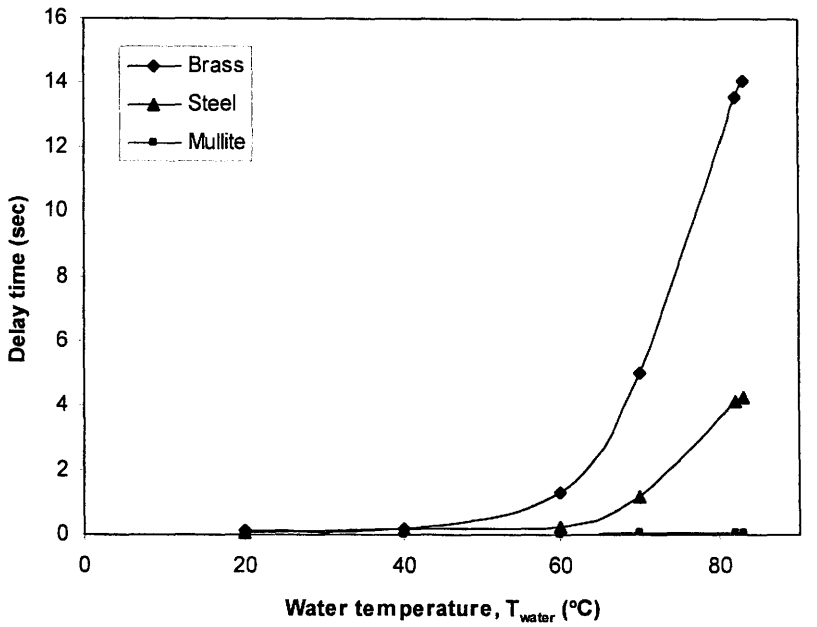

Figure 42: Effect of solid material on re-wetting delay time, 1-in tubes, T_{in} = 600°C, T_{water} = 83°C, V_{jet} = 0.6 m/sec.

5.1.7 Effect of Surface Curvature

Figure 43 shows the delay times for four brass surfaces with the same amount of solid material. Three of the surfaces (1-in tube, 2-in tube and a flat plate) have the same thickness of 3.2 mm. The flat plate is a rectangular sheet with the same length of that of the 2-in tube (12-in) and with a width equivalent to the 2-in tube perimeter (6.28-in). The lengh of the 1-in tube is 25.7-in. The fourth surface is a 2-in tube with 1.5 mm thickness. All pieces have the same amount of material and therefore their total stored heat capacity is the same.

The delay time was found to increase by increasing the surface curvature (decreasing the diameter). This behavior could be due to the ability of the curved surface to supply heat from the bottom part (where there is no liquid around the surface) to the upper part of the surface where the jet interacts with the surface. As the surface curvature decreases and approaches a flat plate, the liquid sheet covers larger area of the surface which increases the heat portion that is transferred to boil the liquid and decreases the heat conducted to the region of jet/surface interaction. The effect of tube wall thickness is discussed in the following section 5.1.8.

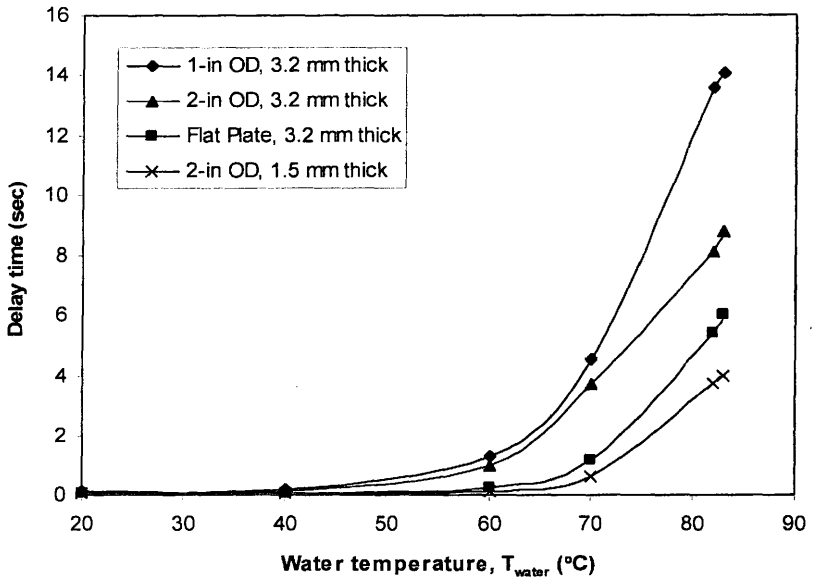

Figure 43: Effect of surface curvature on re-wetting delay time, brass surfaces, T_{in} = 600°C, T_{water} = 83°C, V_{jet} = 0.6 m/sec.

5.1.8 Effect of Material Thickness

As mentioned in the previus section 5.1.7, two 2-in tubes with different wall thicknesses were used: 3.2 mm and 1.5 mm thick. Since the two tubes have the same amount of material, their total bulk stored heat capacity is the same.

However, due to the higher wall heat capacity for the thicker tube in the stagnation region, the vapor generation rate is higher, and the duration of the film boiling is longer. As a result, for the thicker tube, the delay time is longer than that for the thin wall tube under the same operating conditions. As the material thickness decreases, the amount of heat conducted to the jet/surface interaction region decreases which decreases the delay time. This result is shown in Figure 44.

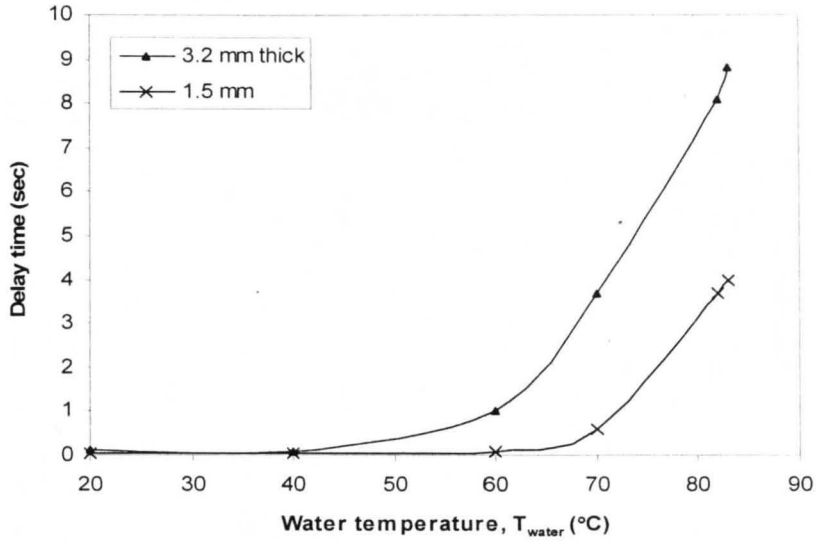

Figure 44: Effect of wall thickness on re-wetting delay time, 2-in brass tubes, T_{in} = 600°C, T_{water} = 83°C, V_{jet} = 0.6 m/sec.

5.1.9 Effect of Jet Orientation

Two jet orientations were tested: Orientation 1 and Orientation 2. In Orientation 1 the axis of the slot jet is perpendicular to the tube axis. In Orientation 2 the jet axis and the tube axis are parallel. These jet orientations are shown in Figure 45.

As shown in Figure 46, jet orientation has a small effect on the delay time. However, in Orientation 2 slightly lower delay times are observed. This could be due to the fact that in Orientation 2 more water goes in the axial direction which enhances the cooling process and therefore accelerating initiating the wet patch.

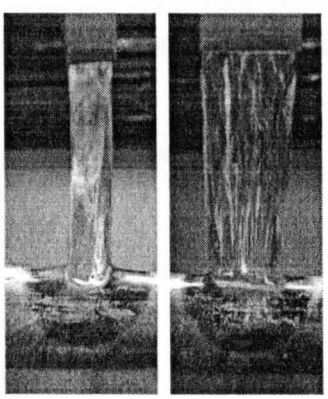

Figure 45: Jet orientations tested in this study, Orientation 1 (left) and Orientation 2 (right) during cooling of 1-in brass tube, T_{in} = 500°C, T_{water} = 82°C and V_{jet} = 0.6 m/sec.

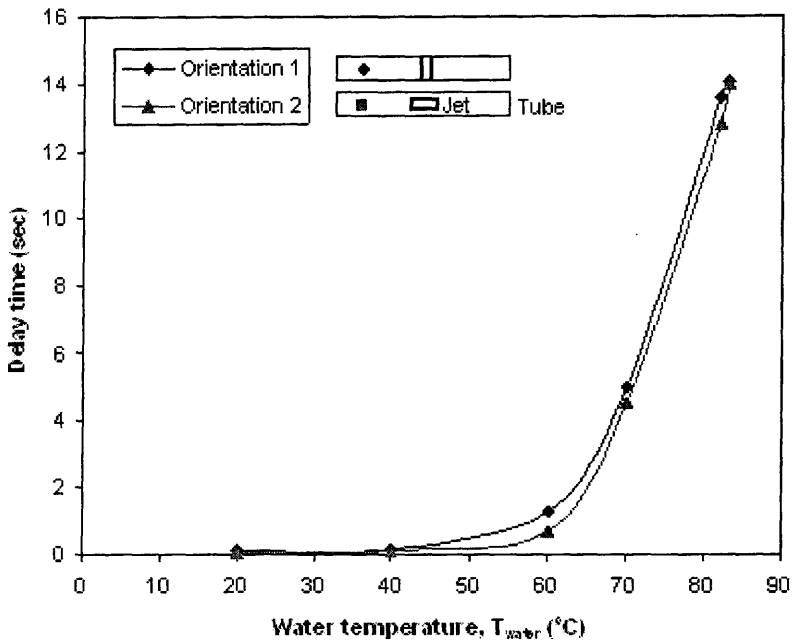

Figure 46: Effect of jet orientation on re-wetting delay time, 1-in brass tube, T_{in} = 500°C, T_{water} = 82°C, V_{jet} = 0.6 m/sec.

5.1.10 Summary and Comments

Emphasis has been given here to find out the parameters that govern the re-wetting delay time. The effect of several operating conditions on the delay time has been analyzed. The delay time is a strong function of water subcooling and initial surface temperature. Also, jet velocity affects the delay time. The delay time increases with increasing water temperature, initial surface temperature and decreasing jet velocity. Other parameters that can increase the delay time were found to be: increasing surface curvature and wall thickness. Surface material greatly affects the delay time; it increases with increasing thermal conductivity. The delay time increases in order of Mullite, steel and brass for the same operating conditions. A correlation was developed for estimating the delay time and found to provide good prediction of the experimental data collected in this study and data found in literature.

5.2 Re-Wetting Front Location and Velocity

The re-wetting front location and re-wetting velocity are very important parameters in quench studies as they indicate how quickly the fluid cools the hot surface. In this study, the captured high speed videos were used to measure the re-wetting front location from the center of the stagnation region to the inner side of the boiling region.

The re-wetting front velocity was then calculated from the measured front location as will be shown in the following paragraphs.

In typical images, the re-wetting front in circumferential direction during the cooling process is shown Figure 47 where the images were captured at a rate of 500 frames/sec and a resolution of 512×512 pixels. The perimeter was fully wetted after 4.656 sec. The corresponding re-wetting front in the axial direction is shown in Figure 48.

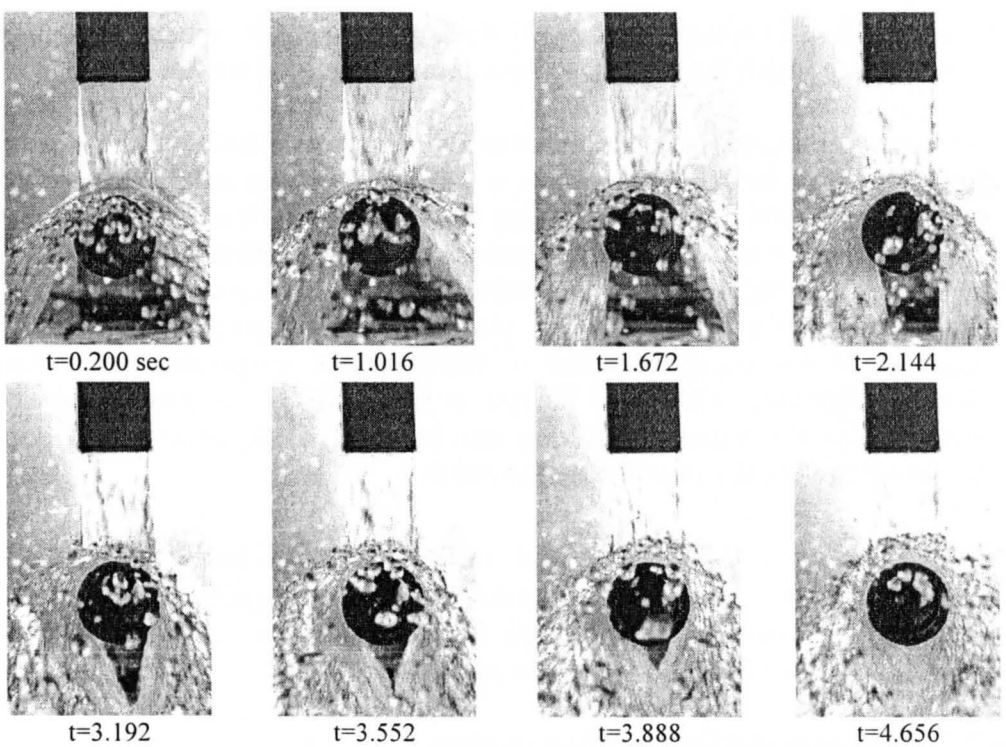

Figure 47: Re-wetting front in circumferential direction during cooling of 1-in diameter brass tube, $T_{in} = 700^{\circ}C$ and $T_{water} = 21^{\circ}C$.

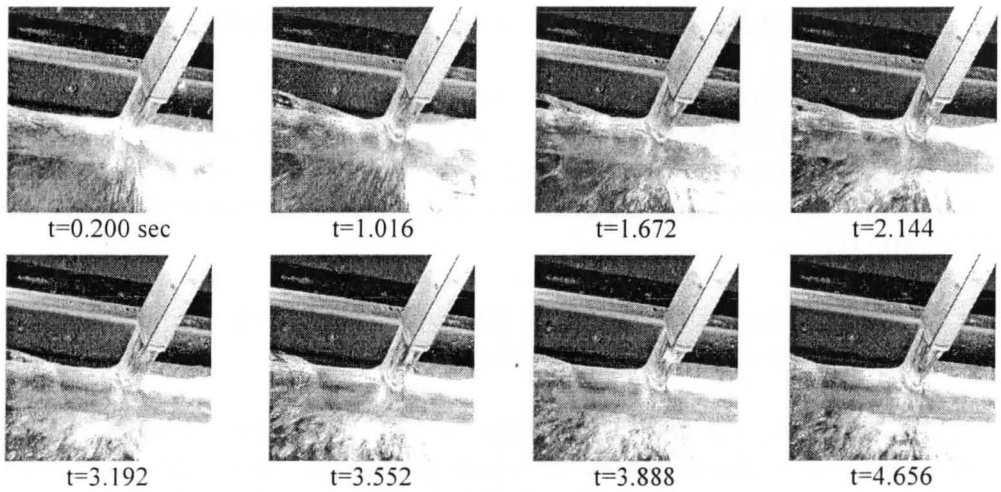

Figure 48: Re-wetting front in axial direction during cooling of 1-in diameter brass tube, $T_{in} = 700^{\circ}C$ and $T_{water} = 21^{\circ}C$.

As indicated in Chapter One: Introduction, the re-wetting velocity is defined as the velocity at which the re-wetting front propagates along the hot dry surface.

The re-wetting front velocity in the axial direction was calculated by dividing the location distance between two points at the surface in the axial direction by the time interval required for the re-wetting front to move between the two locations. This was done for several location points at the surface. Almost all of the tests of this study show that the re-wetting velocity tends to be constant after the rapid initiation of the wet patch. A typical plot is shown in Figure 49 in the next sub-section when discussing the effect of initial surface temperature on re-wetting velocity. Therefore, what is of interest in this study is the average re-wetting velocity, u_{rw}, determined by taking the average of the re-wetting velocities calculated between the several location points.

Many researchers have found that the re-wetting velocity decreases with increasing initial surface temperature, increasing liquid temperature and decreasing jet velocity. The findings of this study are consistent with these findings as will be shown in the following sub-sections.

5.2.1 Effect of Initial Surface Temperature

Figure 49 shows the effect of initial surface temperature on the re-wetting front location during cooling of a 2-in diameter stainless steel tube for $T_{water} = 83^{\circ}C$ and $V_{jet} = 0.93$ m/sec. For comparison, the figure also shows the wetting front location on an unheated tube. As shown in the figure, longer time is required to reach a certain point on the surface as the initial surface temperature increases. The figure

also shows that the delay time to initiate the wet patch on the surface increases by increasing initial surface temperature.

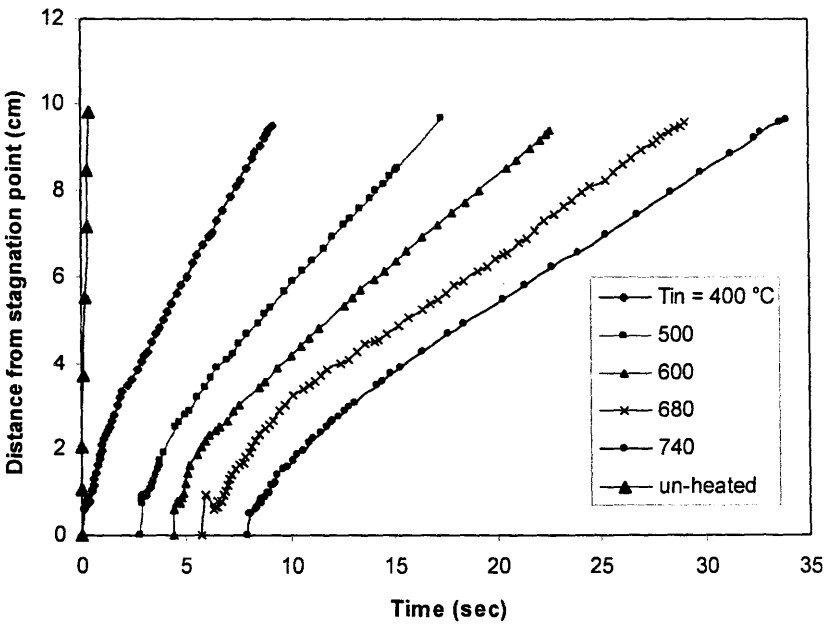

Figure 49: Re-wetting front location versus time during cooling of a 2-in diameter stainless steel tube for varying initial surface temperatures, T_{water} = 83°C and V_{jet} = 0.93 m/sec.

Figures 50, 51 and 52 show the effect of initial surface temperature on the re-wetting front velocity for several water temperatures and for three jet velocities: 0.22, 0.93 and 1.43 m/sec; respectively. The figures show that the average re-wetting velocity decreases with increasing initial surface temperature. As the difference in temperature between the solid and the water increases the heat transferred to the water increases for a constant T_{water}. Therefore large number of droplets is generated at the leading edge of the re-wetting front. These droplets slow down the forward movement of the re-wetting front. Also, increasing the initial surface temperature causes the water temperature to more increase as it moves on the surface decreasing its cooling capability.

The initial surface temperature and the re-wetting velocity were found to be best correlated by a power law function as shown in Equation 2. The constants appearing in the equation are shown in Table 5 for several operating conditions. Ueda [30] also found that the re-wetting front velocity decreases by increasing initial surface temperature and although they did their experiments with vertical tubes the re-wetting velocity and the initial surface temperature were correlated by a power law function.

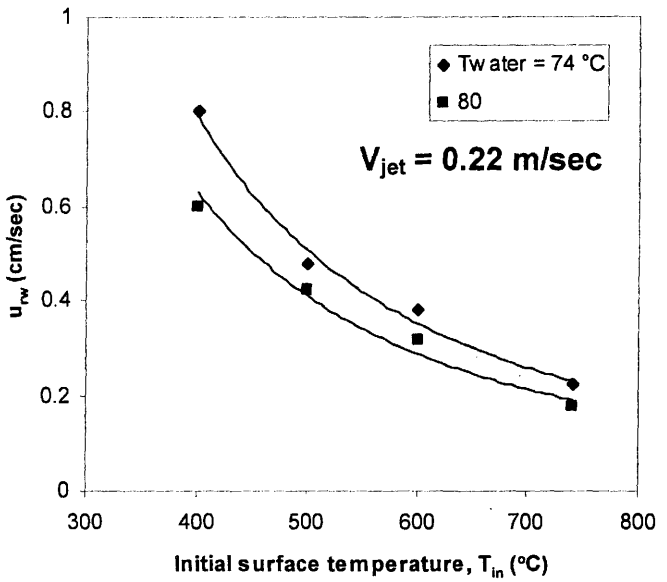

Figure 50: Re-wetting front velocity versus initial surface temperature during cooling of a 2-in diameter stainless steel tube for various water temperatures, V_{jet} = 0.22 m/sec.

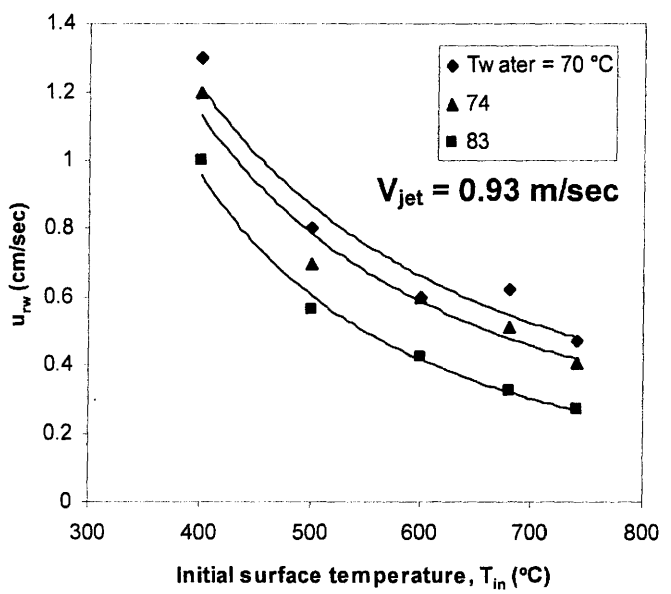

Figure 51: Re-wetting front velocity versus initial surface temperature during cooling of a 2-in diameter stainless steel tube for various water temperatures, V_{jet} = 0.93 m/sec.

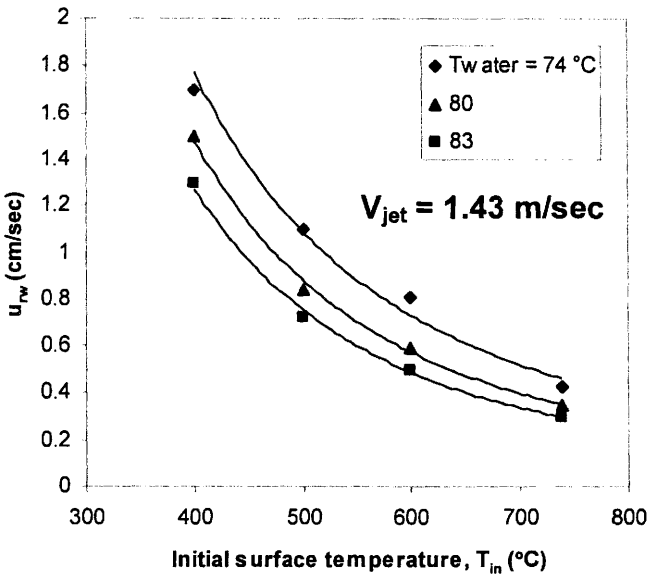

Figure 52: Re-wetting front velocity versus initial surface temperature during cooling of a 2-in diameter stainless steel tube for various water temperatures, V_{jet}= 1.43 m/sec.

$$u_{rw}(\text{cm/sec}) = a.T_{in}^{\ b} \qquad (2)$$

Table 5: Constants of Equation 2 for several operating conditions.

Conditions	a (cm/sec.$^{o}C^{b}$)	b
V_{jet} = 0.22 m/sec		
T_{water}=74°C	1.30×10^{5}	-2.01
T_{water}=80 °C	7.06×10^{4}	-1.94
V_{jet} = 0.93 m/sec		
T_{water}=70 °C	8.04×10^{3}	-1.47
T_{water}=74 °C	2.02×10^{4}	-1.63
T_{water}=83 °C	2.48×10^{5}	-2.08
V_{jet} = 1.43 m/sec		
T_{water}=74 °C	8.65×10^{5}	-2.18
T_{water}=80 °C	2.00×10^{6}	-2.33
T_{water}=83 °C	2.00×10^{6}	-2.35

5.2.2 Effect of Jet Velocity

Figure 53 shows the re-wetting front location versus time for several jet velocities during cooling of a 2-in diameter stainless steel tube for T_{water} = 70°C and T_{in} = 600°C.

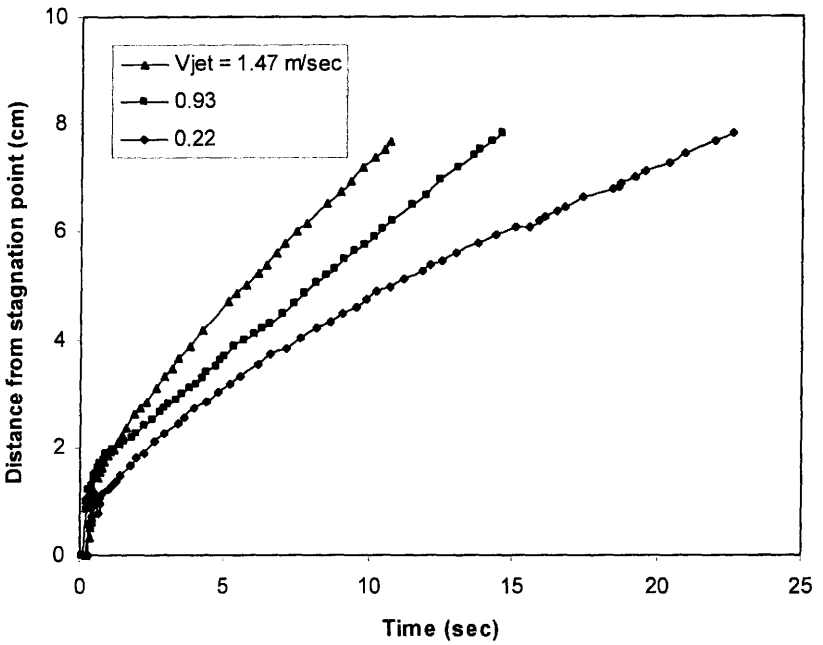

Figure 53: Re-wetting front location versus time during cooling of a 2-in diameter stainless steel tube for various jet velocities, T_{water} = 70°C and T_{in} = 600°C.

Figures 54 and 55 show the effect of jet velocity on the re-wetting velocity for several initial surface temperatures and for two water temperatures: 70 and 80°C; respectively. The re-wetting velocity increases with increasing jet velocity especially for low surface temperatures and low water temperatures. The increase in jet velocity induces more liquid downstream of the re-wetting front which enhances the heat transfer to the vapor film. This results in faster cooling of the surface ahead of the re-wetting front which leads to a higher re-wetting velocity [40].

Figure 56 shows the re-wetting velocity versus jet velocity for varying water temperatures. Same conclusions could be drawn from this figure as from Figures 54 and 56. Moreover, linear relationship is observed between re-wetting velocity and jet velocity.

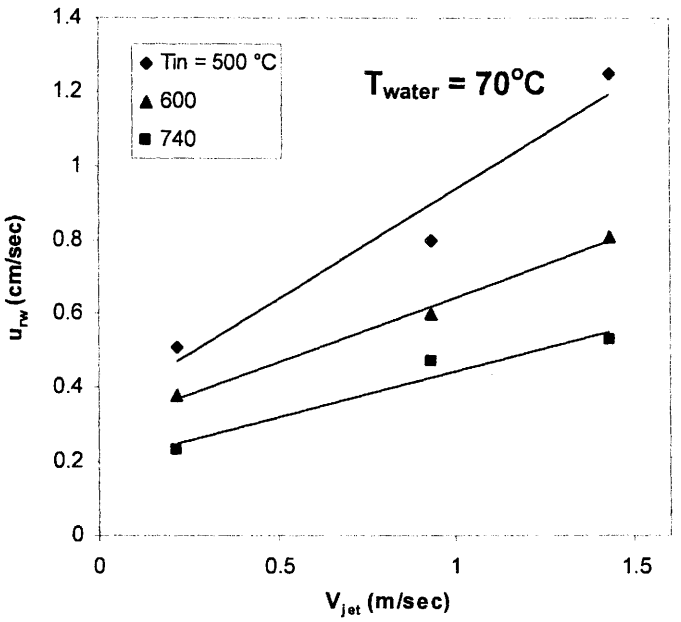

Figure 54: Re-wetting front velocity versus jet velocity during cooling of a 2-in diameter stainless steel tube for several initial surface temperatures, $T_{water} = 70^{o}C$.

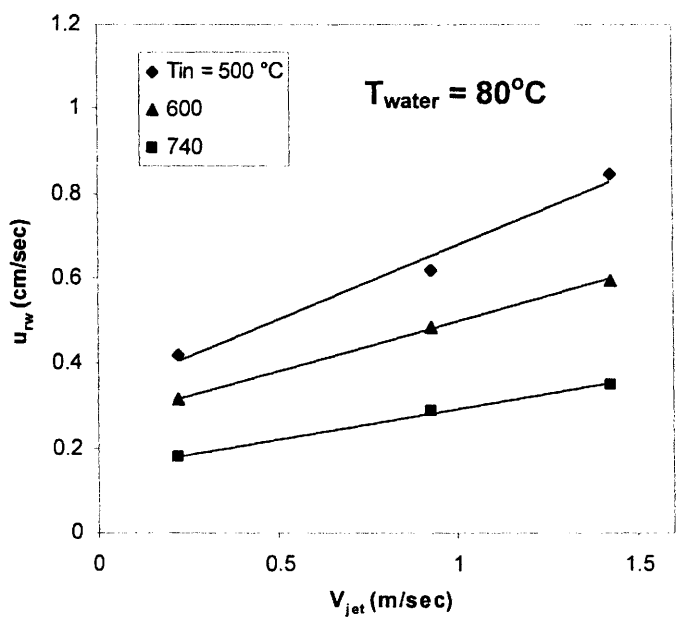

Figure 55: Re-wetting front velocity versus jet velocity during cooling of a 2-in diameter stainless steel tube for several initial surface temperatures, $T_{water} = 80^{o}C$.

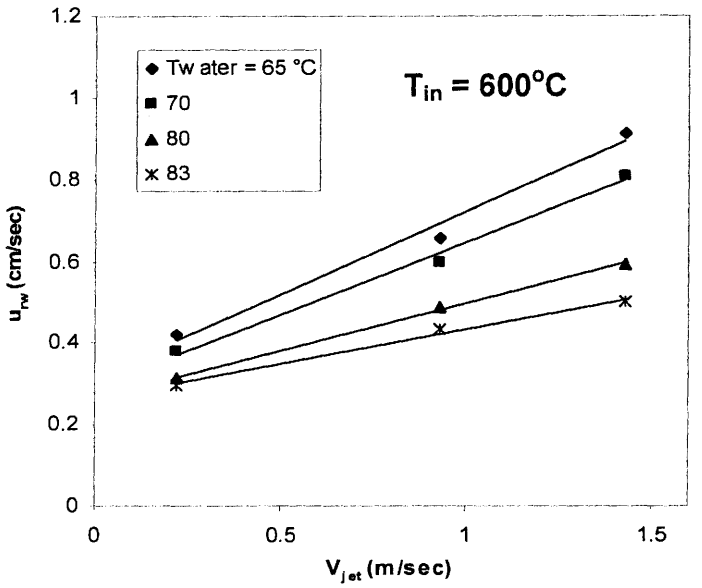

Figure 56: Re-wetting front velocity versus jet velocity during cooling of a 2-in diameter stainless steel tube for various water temperatures, T_{in} = 600°C.

5.2.3 Effect of Water Subcooling

Figure 57 shows a typical plot of the re-wetting front location versus time for several water temperatures.

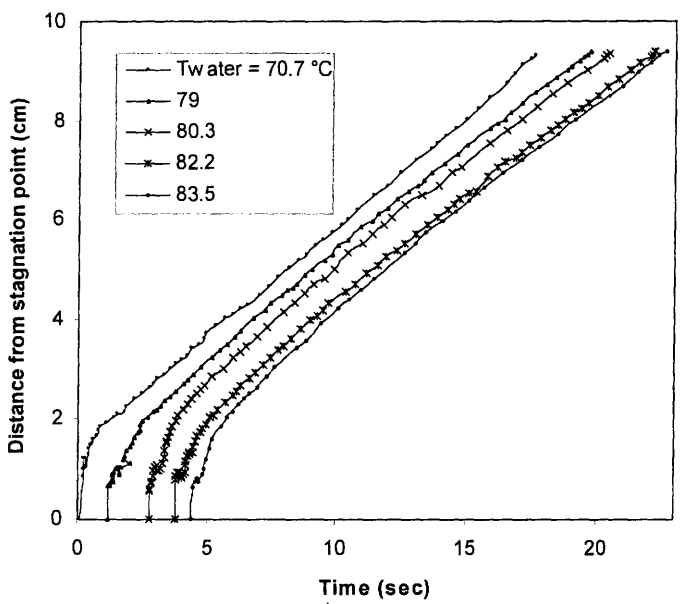

Figure 57: Re-wetting front location versus time during cooling of a 2-in diameter stainless steel tube for various water temperatures, T_{in} = 600°C and V_{jet} = 0.93 m/sec.

Figures 58 to 61 show the effect of water temperature on the re-wetting velocity for several jet velocities and for four initial surface temperatures: 500, 600, 680 and 740°C; respectively. It is shown that as the water temperature decreases the re-wetting velocity increases and the effect being more marked at high jet velocities. This could be explained by the increase in the heat transfer coefficient by increasing the jet velocity. This result is in agreement with Piggott and Porthouse [16] for falling film cooling of vertical surfaces.

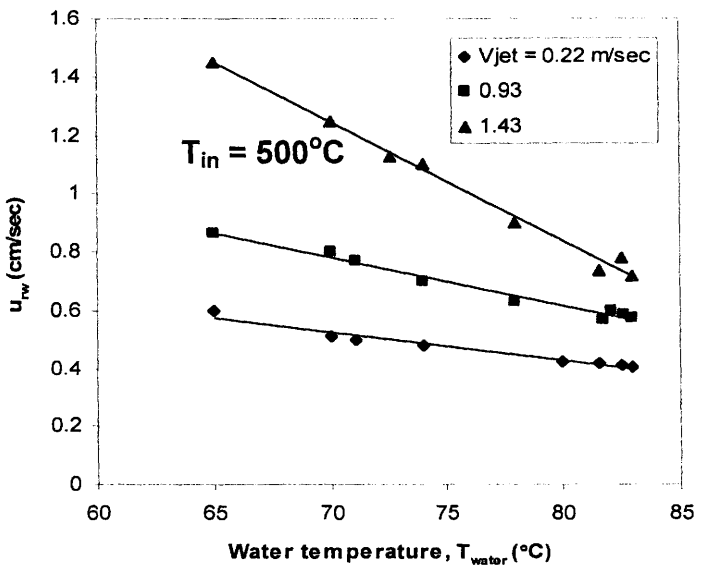

Figure 58: Re-wetting front velocity versus water temperature during cooling of a 2-in diameter stainless steel tube for various jet velocities, T_{in} = 500°C.

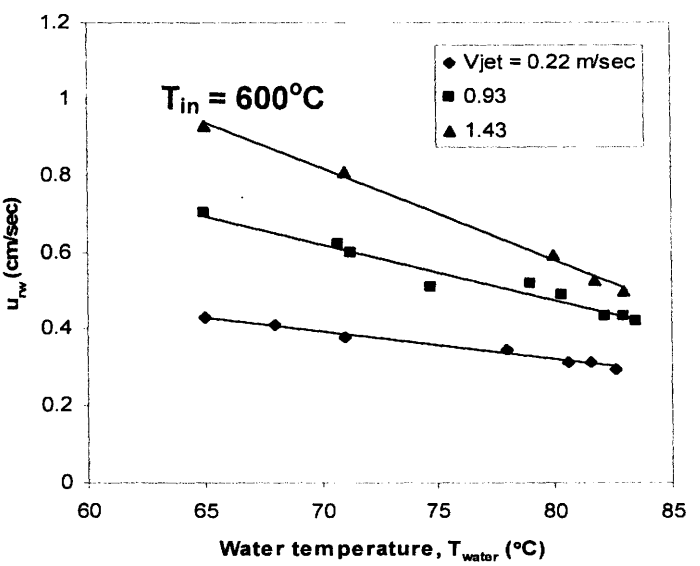

Figure 59: Re-wetting front velocity versus water temperature during cooling of a 2-in diameter stainless steel tube for various jet velocities, T_{in} = 600°C.

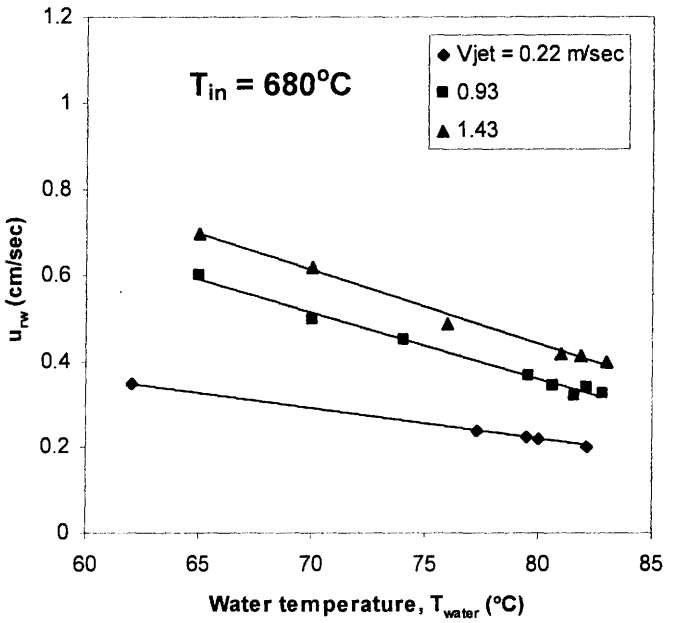

Figure 60: Re-wetting front velocity versus water temperature during cooling of a 2-in diameter stainless steel tube for various jet velocities, T_{in} = 680°C.

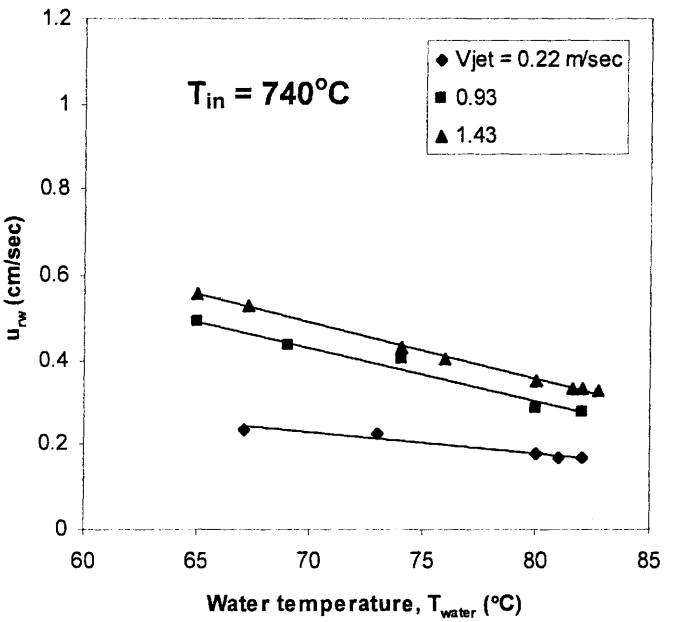

Figure 61: Re-wetting front velocity versus water temperature during cooling of a 2-in diameter stainless steel tube for various jet velocities, T_{in} = 740°C.

Figures 62, 63 and 64 show the effect of water temperature on the re-wetting velocity for several initial surface temperatures and for three jet velocities: 0.22, 0.93 and 1.43 m/sec; respectively. Linear relationship is noticed between the re-wetting velocity and water temperature for the three jet velocities.

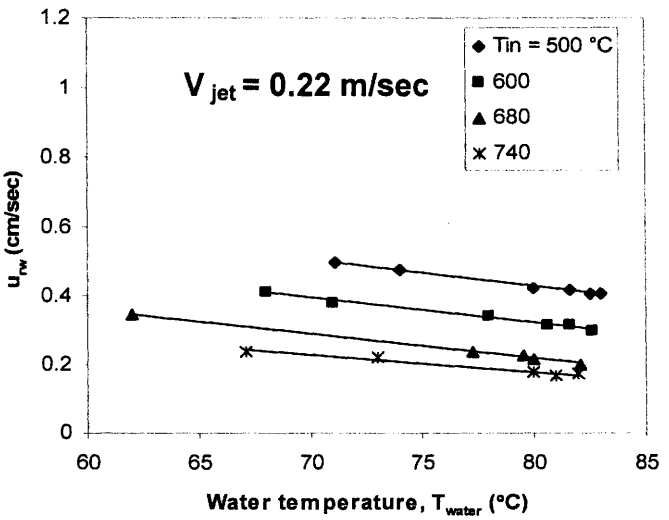

Figure 62: Re-wetting front velocity versus water temperature during cooling of a 2-in diameter stainless steel tube for various initial surface temperatures, V_{jet} = 0.22 m/sec.

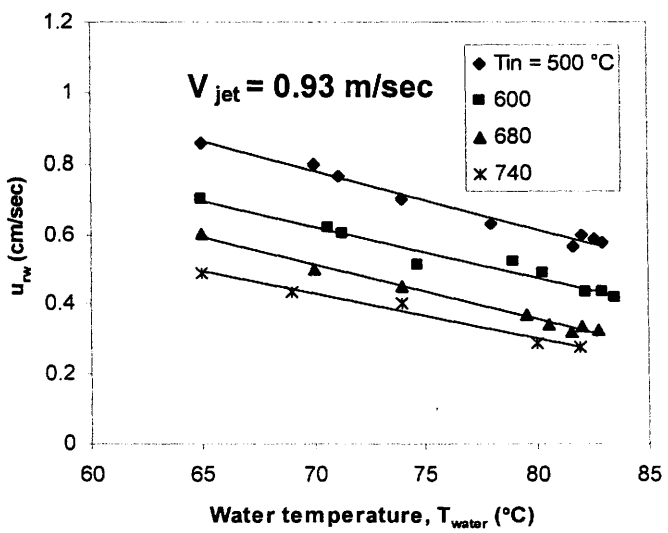

Figure 63: Re-wetting front velocity versus water temperature during cooling of a 2-in diameter stainless steel tube for various initial surface temperatures, V_{jet} = 0.93 m/sec.

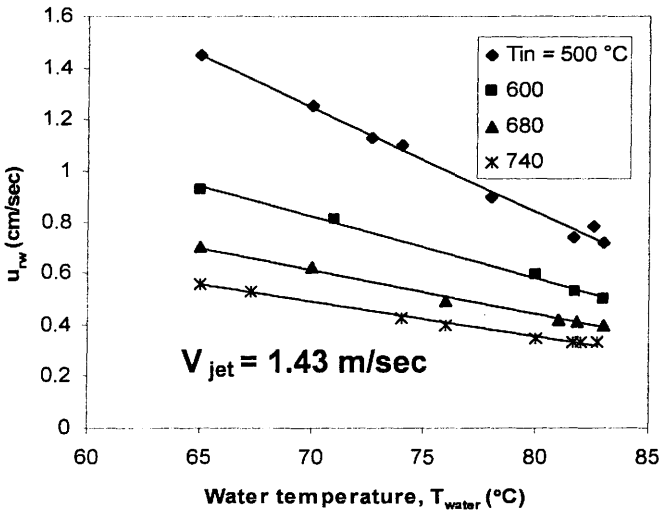

Figure 64: Re-wetting front velocity versus water temperature during cooling of a 2-in diameter stainless steel tube for various initial surface temperatures, V_{jet} = 1.43 m/sec.

It is common in literature to correlate the inverse of the re-wetting front velocity to the product of jet velocity and water subcooling [18, 30, 16]. This product describes parameters from the liquid side only and it gives indication of the ability of the liquid to cool the surface. In this study, the relation between these parameters was found to be as follows:

$$e^{1/u_{rw}} = B.(V_{jet}.\Delta T_{sub})^{n} \qquad (3)$$

Where B and n are constants. Figure 65 shows the relation for four initial surface temperatures and the constant values are shown in Table 6.

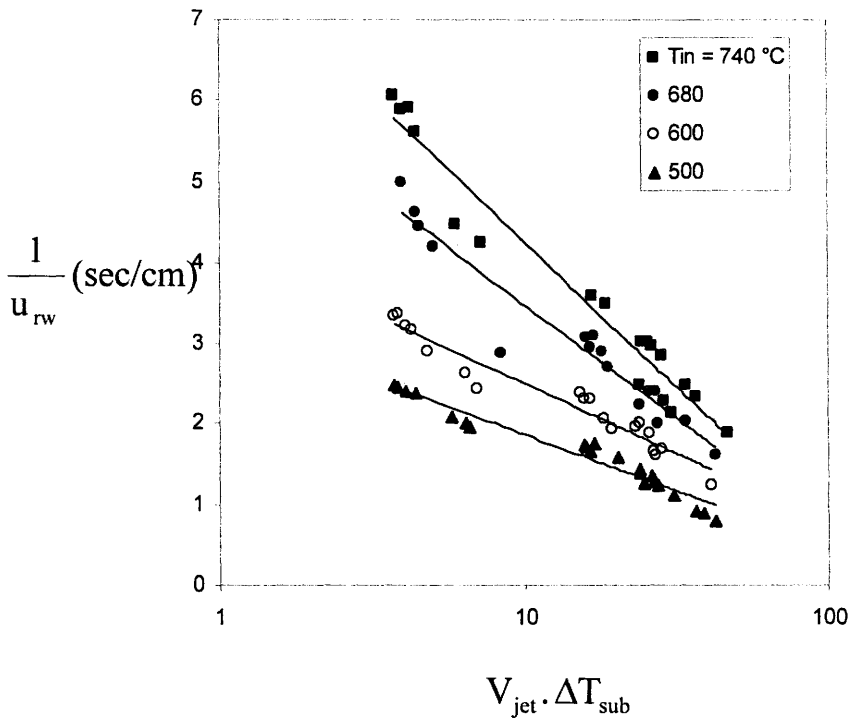

Figure 65: Data of re-wetting front velocity with correlation prediction, 2-in steel tube.

Table 6: Constants of Equation 3 for several initial surface temperatures.

Condition	*ln*B	n (sec/cm)
T_{in}=500°C	3.26	-0.60
T_{in}=600°C	4.24	-0.75
T_{in}=680°C	6.29	-1.22
T_{in}=740°C	7.85	-1.55

5.2.4 Effect of Surface Curvature

It is advantageous to explore wetting of unheated curved surfaces before discussing re-wetting of hot dry curved surfaces. Figure 66 shows the wetting front location in axial direction on three surfaces: flat plate, 2-in tube and 1-in tube. It is noticed that the curvature of the surface has a considerable effect on the maximum distance the wetting front can reach on the surface. The maximum distance increases as the surface curvature decreases and it is maximum for a flat plate. This is due to jet hydrodynamics which provide more pressure on the liquid in axial direction on a flat plate. For a curved surface, some portion of the liquid slips down on the surface and flows beneath the tube.

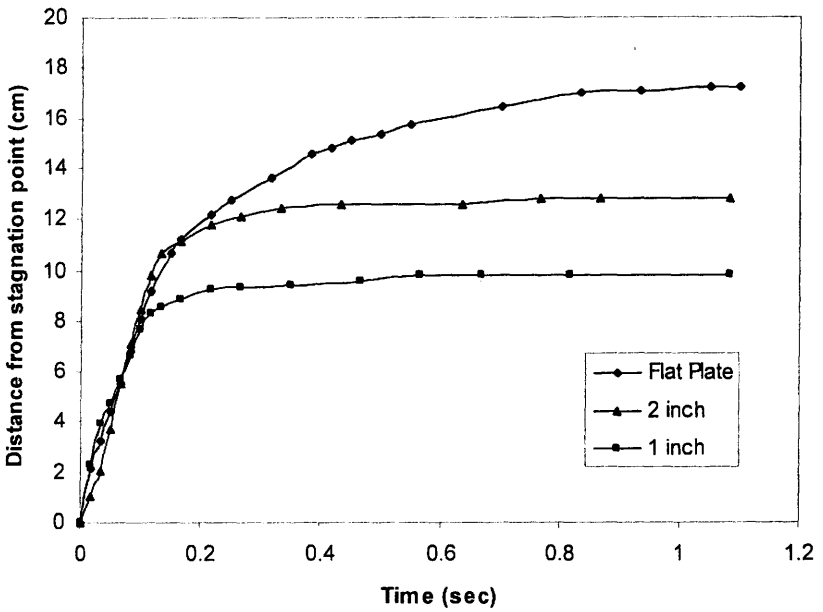

Figure 66: Effect of surface curvature on wetting front location in axial direction for three surfaces with different curvatures at room temperature.

Figure 67 shows the re-wetting front location for three hot brass surfaces initially at 600°C but with different curvatures. In this figure it can be seen that re-wetting of the flat plate starts before that of the 2-in tube which also starts before the 1-in tube. Again, as discussed in sub-section 5.1.7 page 66, this is caused by the fact that as the surface curvature decreases the surface quenches faster due to surface geometry which enhances heat transfer to the liquid. Also, the figure shows that as the surface curvature decreases, the liquid can spread to a higher distance as discussed in the previous paragraph.

Figure 68 shows the re-wetting velocity for the three surfaces for several water temperatures.

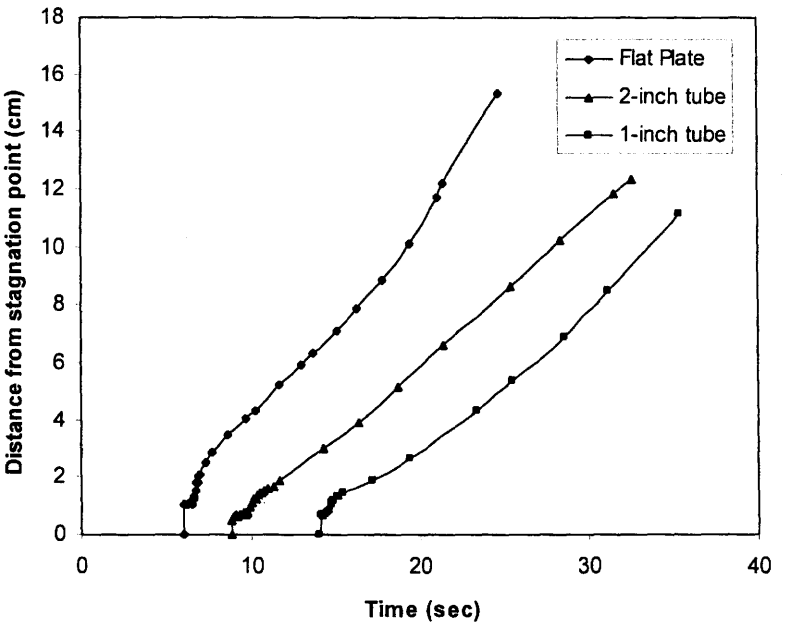

Figure 67: Effect of surface curvature on re-wetting front location in axial direction for three brass surfaces initially at 600°C, T_{water} = 83°C and V_{jet} = 0.6 m/sec.

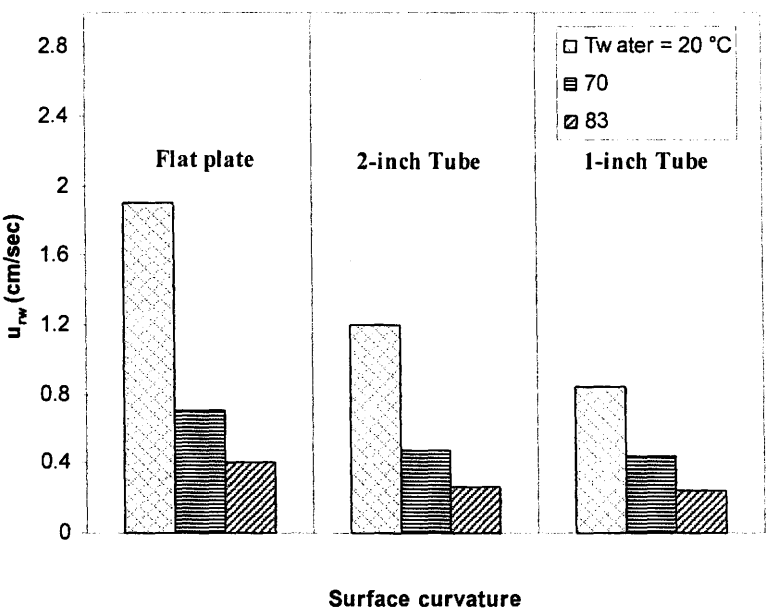

Figure 68: Effect of surface curvature on re-wetting front velocity in axial direction for three brass surfaces initially at 600°C, V_{jet} = 0.6 m/sec and several water temperatures.

5.2.5 Effect of Solid Material

Figure 69 shows the re-wetting front location for different types of materials (Mullite, Steel and Brass). It can be seen that the material type has a considerable effect on the delay time as well as on the re-wetting front velocity. This is due to the difference in thermal conductivity between the materials tested. The re-wetting velocity on Mullite is higher than that at the other tubes as its thermal conductivity is much lower. The effect of solid material was also discussed in section 5.1.6 page 65.

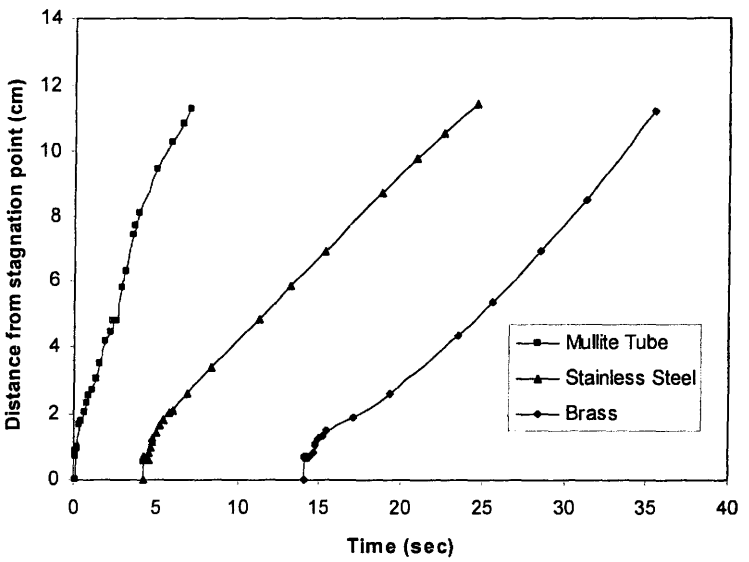

Figure 69: Effect of solid material on the re-wetting front location in axial direction for three 1-tubes with different material types initially at 600°C, T_{water} = 83°C and V_{jet} = 0.6 m/sec.

5.2.6 Effect of Number of Jets

In this study, most of the tests were done with a single jet directed towards the center point of a horizontal tube. The effect of the number of jets on the motion of the re-wetting front was studied by fixing the operating conditions but increasing the number of jets in operation from a single jet to two and then to three jets. Figure 70 shows an image of cooling of a 1-in brass tube by two jets. The nozzles are 3-in apart and of same dimensions and surface-to-nozzle spacing. The effect of number of jets on the re-wetting front location is shown in Figure 71 where the re-wetting front measured from the stagnation point beneath jet 1 towards that of jet 2 is shown. The figure shows that the number of jets has some effect on the re-wetting delay time, which decreased by increasing the number of the jets. This trend is expected because the rate of cooling increases when the number of jets cooling the surface increases. The re-wetting front location for the three cases (1,

2 or 3 jets in operation) is initially almost the same but it is larger when 2 and 3 jets are in operation. Jet 3 is 6 inches away from jet 1 and thus seems to have a small effect on re-wetting the region beneath jet 1.

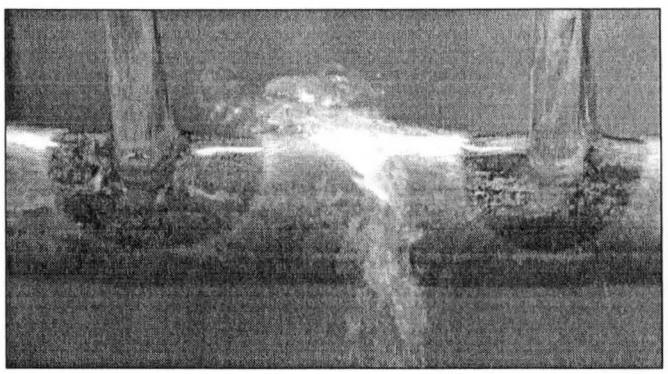

Figure 70: Cooling of 1-in brass tube by two jets, T_{in} = 500°C, T_{water} = 82°C and V_{jet} = 0.6 m/sec.

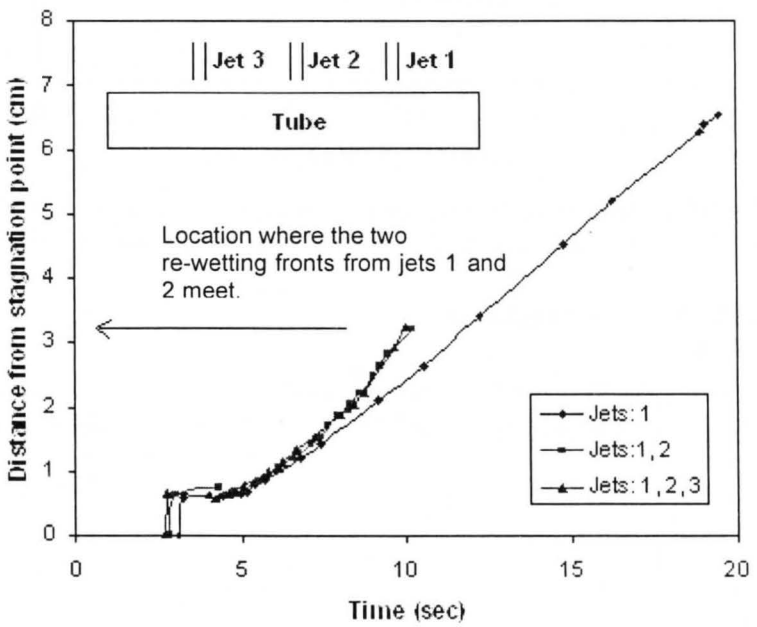

Figure 71: Effect of number of jets on the re-wetting front location in axial direction during cooling of 1-in brass tube, T_{in} = 500°C, T_{water} = 82°C and V_{jet} = 0.6 m/sec.

5.2.7 Effect of Jet Orientation

Figure 72 shows the effect of jet orientation on the re-wetting front velocity as a function of water temperature. Two jet orientations were tested; Orientation 1 and Orientation 2 as described in sub-section 5.1.9 page 68. Jet orientation was found to have a small effect on the re-wetting front velocity in the axial direction but

with a slight increase for Orientation 2. This slight increase might be due to the fact that in Orientation 2 more liquid flows in the axial direction than in Orientation 1 where more liquid slips down on the curved surface and flows beneath the tube.

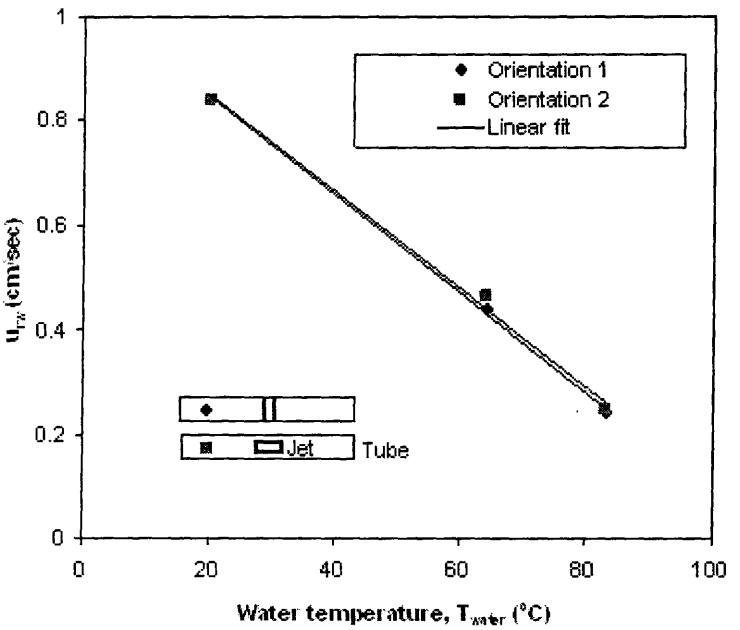

Figure 72: Effect of jet orientation on the re-wetting front velocity in axial direction during cooling of 1-in brass tube, T_{in} = 500°C, T_{water} = 82°C and V_{jet} = 0.6 m/sec.

5.2.8 Effect of Material Thickness

Figure 73 shows the effect of tube wall thickness on the re-wetting location during cooling of 2-in brass tubes initially at 600°C, T_{water} = 83°C and V_{jet} = 0.6 m/sec.

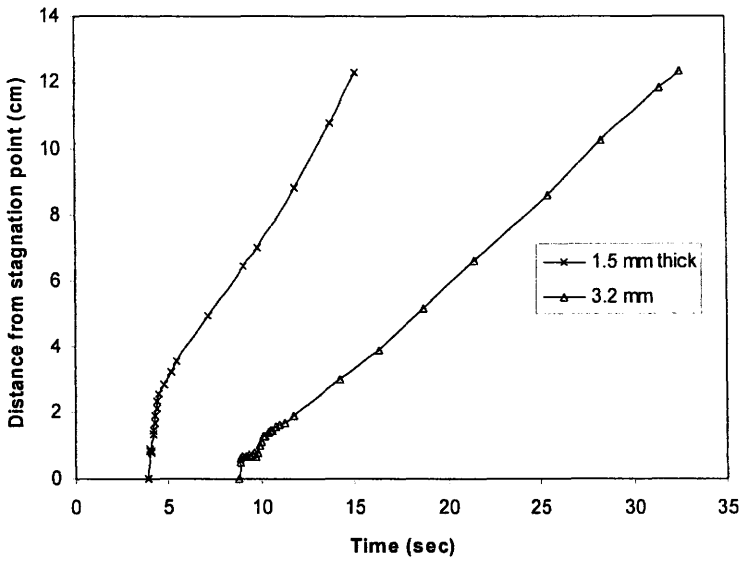

Figure 73: Effect of material thickness on the re-wetting front location in axial direction during cooling of 2-in brass tubes, T_{in} = 600°C, T_{water} = 83°C and V_{jet} = 0.6 m/sec.

The figure shows that the wall thickness has a considerable effect on the delay time as well as the re-wetting velocity. The average re-wetting velocity for the two different thicknesses are shown in Figure 74 for several water temperatures. The effect of the tube wall thickness has already been discussed in section 5.1.8 page 67.

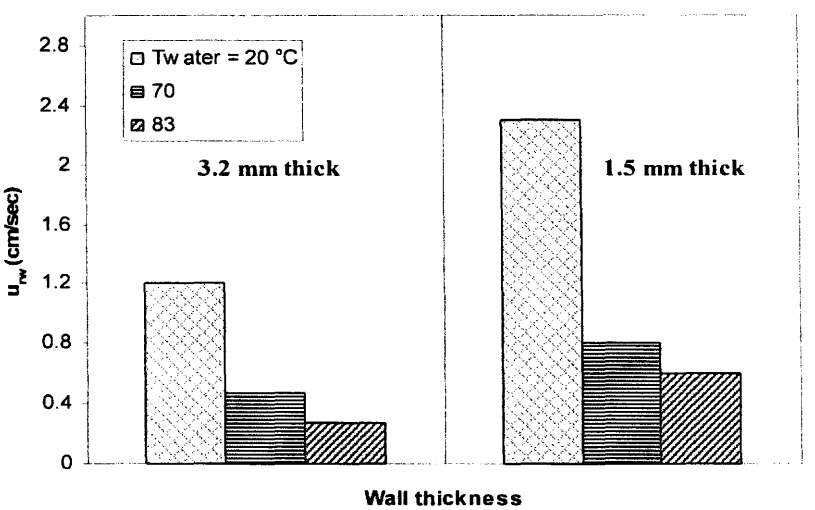

Figure 74: Effect of material thickness on the re-wetting front velocity in axial direction during cooling of 2-in brass tubes for several water temperatures, T_{in} = 600°C, and V_{jet} = 0.6 m/sec.

5.2.9 Rebound of the Re-Wetting Front

As mentioned in Chapter One: Introduction, the re-wetting front was found to rebound a small distance after the initiation of the wet patch. Figure 75 shows this behavior during cooling of 1-in brass tube initially at 800°C with jet velocity of 0.22 m/sec and jet temperature of 21°C. This behavior is due to rapid heat conduction in the solid tube towards the region where the wet patch is initiated on the surface. The initiation of the wet patch creates a high temperature gradient in the solid and forms a deriving force for rapid heat conduction towards the wet patch. The rapid heat conduction causes the region of the surface surrounding the wet patch to re-dry which causes the re-wetting front to rebound. This behavior was not found in literature and it is believed to be first reported in this study.

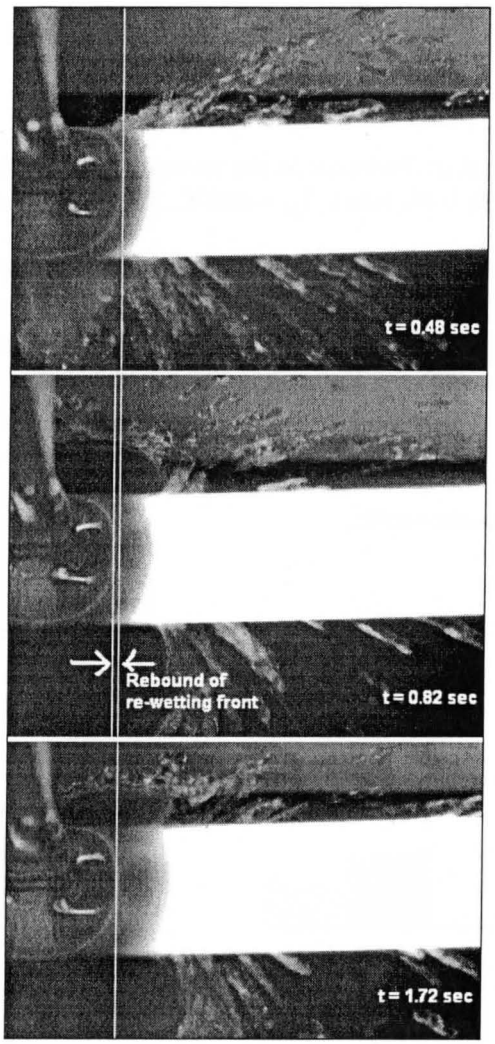

Figure 75: Rebound of the re-wetting front during cooling of a 1-in diameter brass tube, $T_{in} = 800°C$, $V_{jet} = 0.22$ m/sec and $T_{water} = 21°C$.

Figure 76 shows the rebound distance during cooling of a 2-in steel tube initially at 600°C versus water temperature for different jet velocities. As can be seen in the figure, the rebound distance increases by decreasing jet velocity and by decreasing water temperature. As jet velocity increases, the jet hydrodynamics form higher resistance to the rebound of the re-wetting front. Also, as water temperature decreases, the surface cools faster and the deriving force of heat conduction within the surface increases. The effect of water temperature tends to be sharper as water temperature increases.

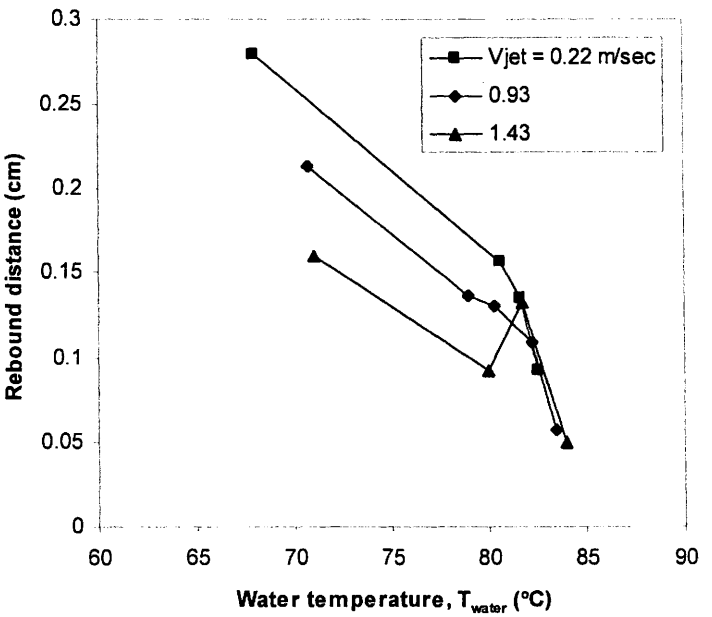

Figure 76: Effect of water temperature on the re-wetting front rebound distance in axial direction during cooling of a 2-in diameter stainless steel tube for various jet velocities, T_{in} = 600°C.

Figure 77 shows the rebound distance against jet velocity for several water temperatures where linear relation is observed. The effect of jet velocity is stronger as water temperature decreases.

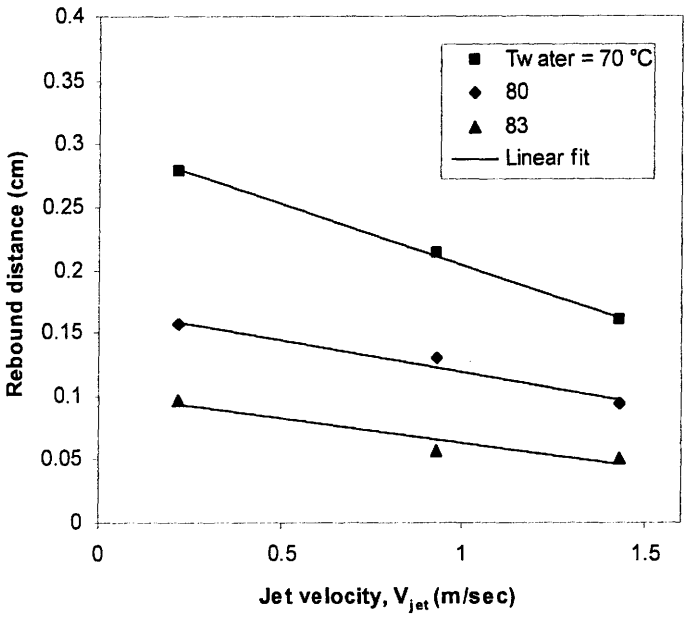

Figure 77: Effect of jet velocity on the re-wetting front rebound distance in axial direction during cooling of a 2-in diameter stainless steel tube for various water temperatures, T_{in} = 600°C.

5.2.10 Summary and Comments

The effect of several operating conditions on the re-wetting front location and re-wetting velocity has been analyzed. The re-wetting velocity is a strong function of initial surface temperature and jet velocity. Water subcooling has also a considerable effect. The re-wetting velocity increases with increasing jet velocity, decreasing surface temperature and decreasing water temperature. Other parameters that can increase the re-wetting velocity were found to be: decreasing surface curvature and decreasing wall thickness. Surface material was also found to have an effect. Correlations were developed for estimating the re-wetting velocity and found to provide good prediction of the experimental data collected in this study. The re-wetting velocity was found to be proportional to water temperature and jet velocity and related with a power function to initial surface temperature. It was also related with a logarithmic function to the product of jet velocity and water subcooling. Looking at the details of the re-wetting front itself, it was found that the front could rebound just after the formation of the wet patch. The amount of the rebound was found to increase by decreasing water temperature and jet velocity.

5.3 Boiling Region Size

Very few studies are available in literature that discusses the size of the boiling region. This area of research is relatively unexplored and it is the aim of this section to investigate this region. The leading edge (the outer edge) of the boiling region is defined as the re-wetting front. The inner edge represents the location where the vigorous boiling stops and the forced convection heat transfer mode becomes dominant at the further inside of the inner edge. The term "stop boiling position" was used by Hammad [13, 33] and Mozumder [9] to refer to the inner edge of the boiling region.

Visible observations during the quench tests show that the outer annular region of the wet region is characterized by vigorous boiling. The boiling region was observed to stay almost constant in size as the re-wetting front progresses towards the end of the tube in the axial direction.

5.3.1 Effect of Initial Surface Temperature and Water Subcooling

Figure 78 shows the effect of initial surface temperature on the boiling region size for several water temperatures. The boiling region size increases with decreasing the initial surface temperature and with increasing water temperature. Under these conditions the transition and nucleate boiling are preferable more than the film boiling and thus the boiling region size increases. Linear relationship is observed between the boiling region size and the initial surface temperature.

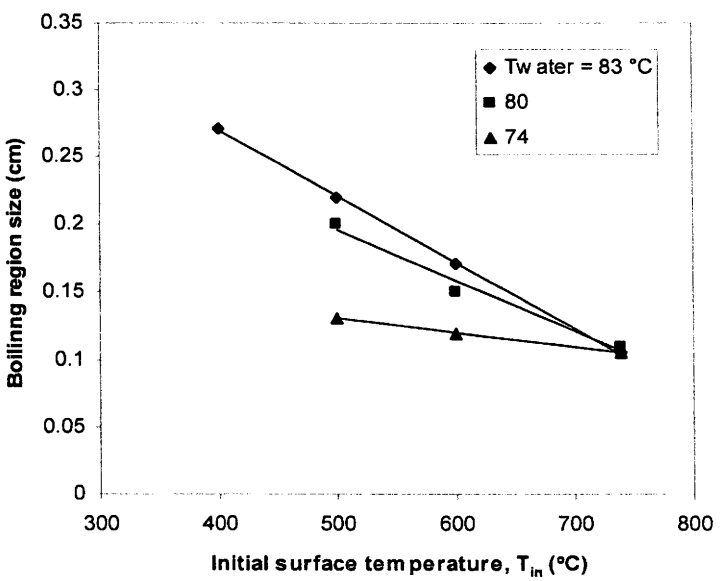

Figure 78: Effect of initial surface temperature on the boiling region size in axial direction during cooling of a 2-in diameter stainless steel tube for various water temperatures, V_{jet} = 0.93 m/sec.

5.3.2 Effect of Solid Material

Figure 79 shows the effect of solid material type on the boiling region size. As it is shown, for particular experimental conditions and for a certain location of the re-wetting front on the surface, the boiling region size on brass tube is higher than that on steel tube. Therefore, as the thermal conductivity of the material increases, the boiling region size increases. Mitsutake [21] also reported an increase in the size of the boiling region by the increase in thermal conductivity in their experiments. The material with higher thermal conductivity can supply more heat to enlarge the boiling region size.

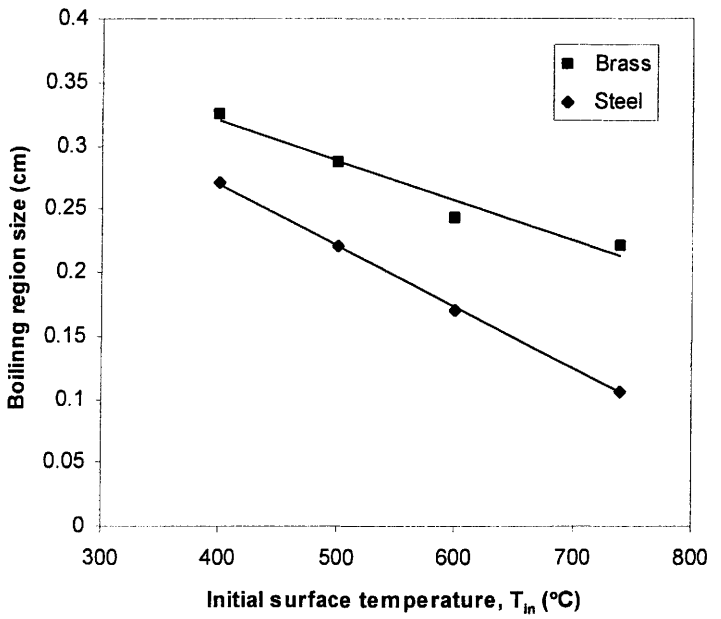

Figure 79: Effect of solid material type on the boiling region size in axial direction during cooling of 2-in diameter tubes, $T_{water} = 83°C$ and $V_{jet} = 0.6$ m/sec.

5.3.3 Effect of Number of Jets

The boiling region was noticed to slightly increase in size as the number of jets increases. This is due to the higher cooling rate provided as the number of jets increases; conditions where transition and nucleate boiling are preferable more than film boiling.

5.3.4 Summary and Comments

The boiling region size was found to increase with water temperature and with decreasing initial surface temperature. As the solid thermal conductivity increases, the boiling region size was found to increase.

5.4 Quench Temperature

As mentioned in Chapter One: Introduction, the quench temperature of a hot surface is defined as the temperature at which the onset of the rapid cooling occurs. The quench temperature can be determined by taking the intersection point between two tangent lines drawn at the temperature-time profile before and after the rapid decrease in temperature. The re-wetting temperature, however, is defined as the temperature at which actual contact between the liquid and the hot surface occurs.

All theoretical models of quench cooling require knowledge of either the quench temperature or the re-wetting temperature and incorrectly assumed values of these temperatures could lead to enormous errors in the final analysis of the problem [15]. The aim of this section is to study the quench temperature under varying operating conditions. Discussion of the re-wetting temperature is left for the next section.

5.4.1 Effect of Initial Surface Temperature

Figures 80 and 81 show the quench temperature versus the initial surface temperature for several water temperatures during cooling of a 2-in diameter stainless steel tube for jet velocity V_{jet} = 1.43 m/sec. The figures show the quench temperature at Location 1 and Location 2 at the tube surface; respectively.

A linear relationship between the quench temperature and the initial surface temperature is obtained. Figure 80 shows that the quench temperature is more dependent on the initial surface temperature for lower water temperatures. The dependence gets weaker as water temperature increases. As water temperature increases it approaches the saturation temperature where less effective heat transfer occurs. Under such condition, the quench temperature becomes less dependent on the operating conditions. This will be discussed further in section 5.4.2 page 97 when presenting the effect of water subcooling on the quench temperature.

In Figure 81 the quench temperature at Location 2 also shows a linear relationship with the initial surface temperature but with a weak dependence on water temperature. This weak dependence is due to the increase in water temperature as water moves on the hot surface towards Location 2 at the tube.

An interesting point to raise here is that the quench temperature at Location 2 shows a dependence on the initial surface temperature for the all water temperatures investigated. This is dissimilar to the case at Location 1 where the dependence on the initial surface temperature gets weaker as water temperature increases. This is because the quench process at Location 2, where the surface

temperature is still high and close to the initial surface temperature, occurs by propagation of the quench front. At Location 1, however, as the water temperature increases, the surface experiences a longer quench delay time during which the surface temperature decreases by vapor film boiling. The cooling rate of vapor film boiling at Location 1 is much higher than that at Location 2 as will be shown in section 5.6.3 page 124 when discussing the cooling rates in vapor film and nucleate boiling regimes.

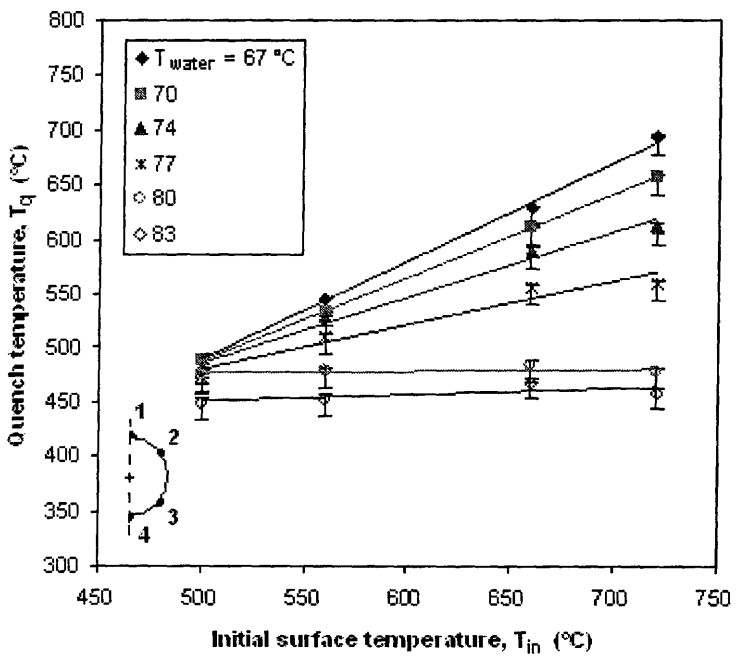

Figure 80: Quench temperature at Location 1 versus initial surface temperature during cooling of a 2-in diameter stainless steel tube for V_{jet} = 1.43 m/sec.

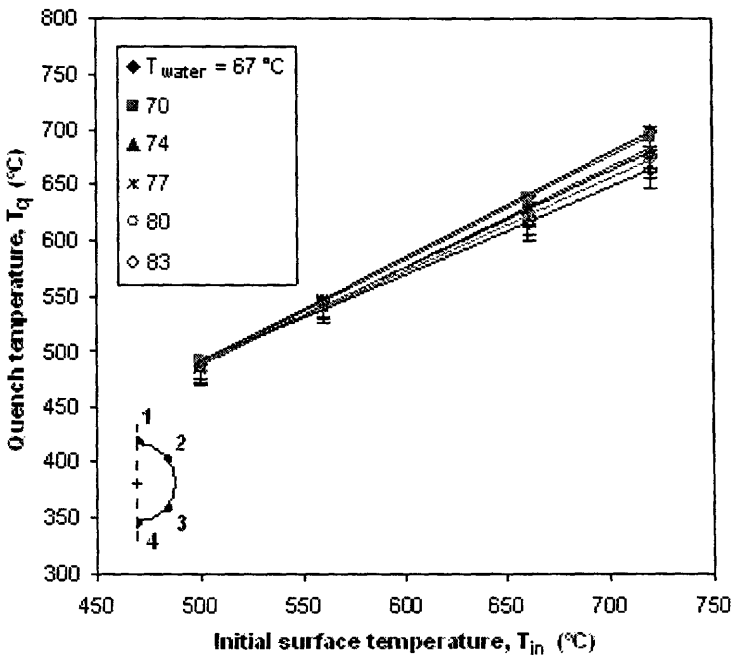

Figure 81: Quench temperature at Location 2 versus initial surface temperature during cooling of a 2-in diameter stainless steel tube for V_{jet} = 1.43 m/sec.

The quench temperature at Location 3 and Location 4 shows similar linear relationship with the initial surface temperature. For comparison, Figure 82 shows the quench temperature versus the initial surface temperature at Locations 1-4 during cooling of the 2-in diameter stainless steel tube for T_{water} = 74°C and V_{jet} = 1.43 m/sec. For higher water temperatures, Location 3 and Location 4 show similar dependency on the initial surface temperature like that at Location 2 which was shown in Figure 81.

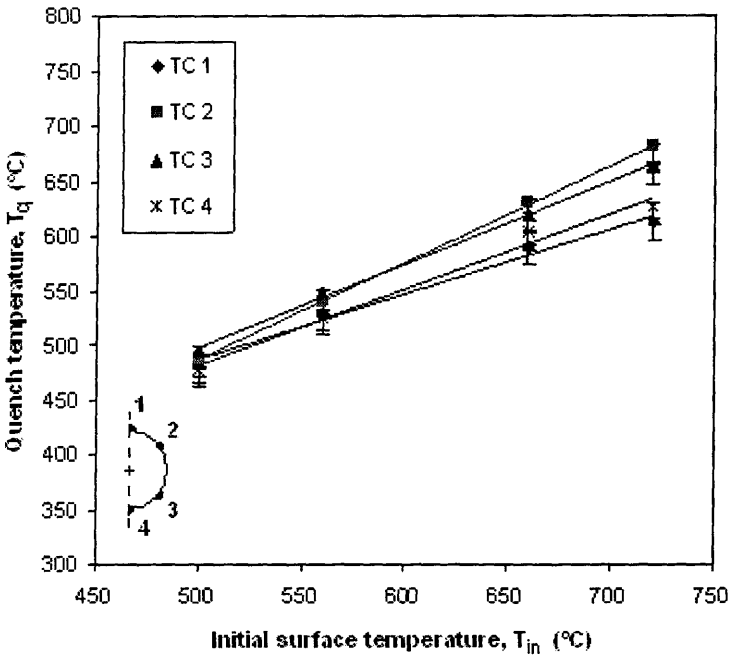

Figure 82: Quench temperature at Locations 1-4 versus initial surface temperature during cooling of a 2-in diameter stainless steel tube for T_{water} = 74°C and V_{jet} = 1.43 m/sec.

5.4.2 Effect of Water Subcooling

The quench temperature increases with increasing liquid subcooling. When the liquid gets cooler, thinner vapor film is expected which collapses faster. Therefore, the vapor film collapses at a higher temperature [10].

Figure 83 shows the quench temperature at Location 1 versus water temperature during cooling of a 2-in diameter stainless steel tube for varying initial surface temperatures and for V_{jet} = 1.43 m/sec. The quench temperature shows a strong dependence on water temperature for water temperatures higher than those of the circled points. For water temperatures less than the circled points, the quench temperature depends on the initial surface temperature and weakly depends on water temperature. Here, the quench occurs very rapidly in fractions of a second after applying the water.

For water temperatures above 81°C, the quench temperature tends to almost a constant value (ranging between 450-470°C) for the varying initial surface temperatures.

The range in which the quench temperature strongly depends on water temperature will be referred to here as the "critical water subcooling" range. For water temperatures higher than 81°C the water temperature increases as the water moves on the hot surface and quickly approaches the saturation temperature.

Therefore, for those high water temperatures the quench temperature shows weak dependence on the initial water subcooling.
For initial surface temperature of 500°C the strong dependence of the quench temperature on water temperature was observed in the range of water temperature between 81-83°C.

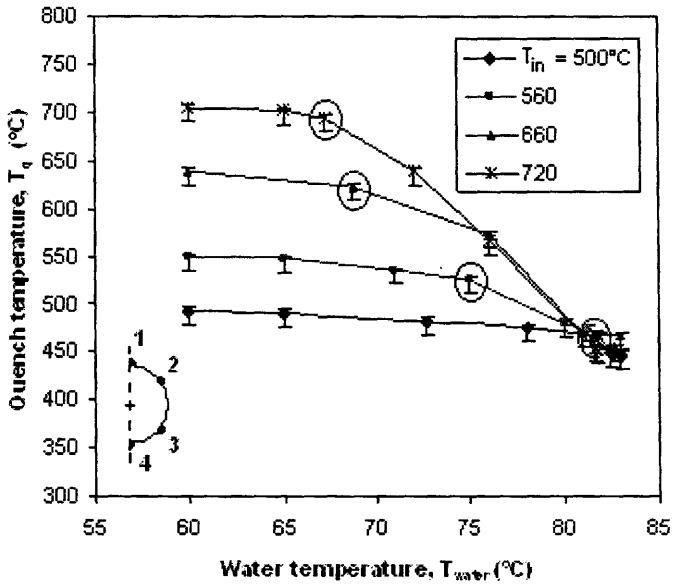

Figure 83: Quench temperature at Location 1 versus water temperature during cooling of a 2-in diameter stainless steel tube for varying initial surface temperatures and for V_{jet} = 1.43 m/sec.

The water temperatures of the circled points appearing in Figure 83 are plotted against the initial surface temperature in Figure 84. The resulting curve forms a boundary between the region of rapid quench (short delay times) and the region of delayed quench (relatively long delay times; like 2 seconds and more).

Usually, transition between the two regimes occurs suddenly by any small increase in water temperature. In the rapid quench region the conditions for vapor film destabilization are rapidly reached just after the jet interacts with the surface. If, initially, the conditions for vapor film destabilization are not reached (due to high heat conduction in the solid towards the stagnation region) then the whole solid must cool down by vapor film boiling before the film destabilizes. This results in a much longer quench delay time.

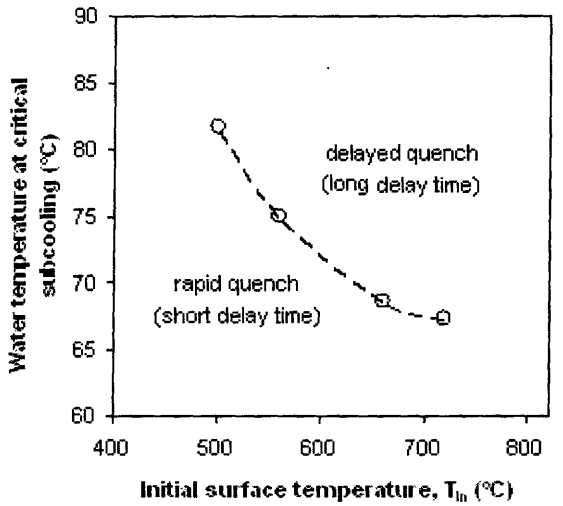

Figure 84: Water temperature at critical subcooling versus initial surface temperature during cooling of a 2-in diameter stainless steel tube for V_{jet} = 1.43 m/sec.

5.4.3 Effect of Spatial Location

At locations on the tube surface other than the stagnation point, the quench temperature shows weak dependence on water subcooling but depends on the initial surface temperature. Again, at these locations, the water temperature had already got higher as the water moved on the hot surface. Figure 85 to Figure 90 show the quench temperature versus water temperature for varying initial surface temperature at Locations 2 to Location 7; respectively. Locations 5-7 are at the same vertical axis and are located 3 inches away from the stagnation point along the tube horizontal axis. All locations are shown in the corresponding figure.

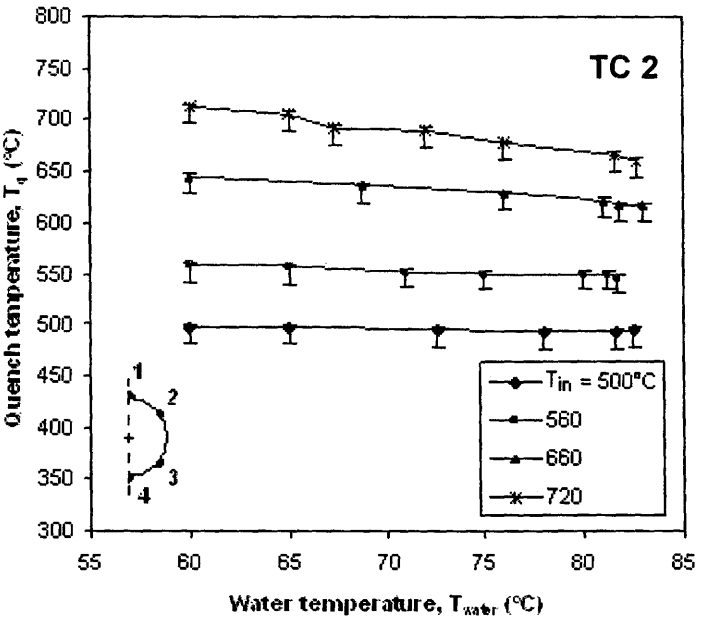

Figure 85: Quench temperature at Location 2 versus water temperature during cooling of a 2-in diameter stainless steel tube for varying initial surface temperature and for V_{jet} = 1.43 m/sec.

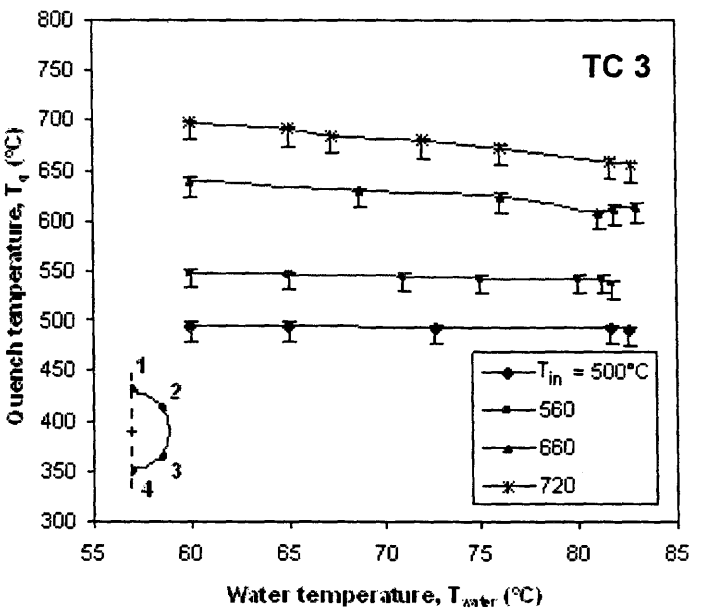

Figure 86: Quench temperature at Location 3 versus water temperature during cooling of a 2-in diameter stainless steel tube for varying initial surface temperature and for V_{jet} = 1.43 m/sec.

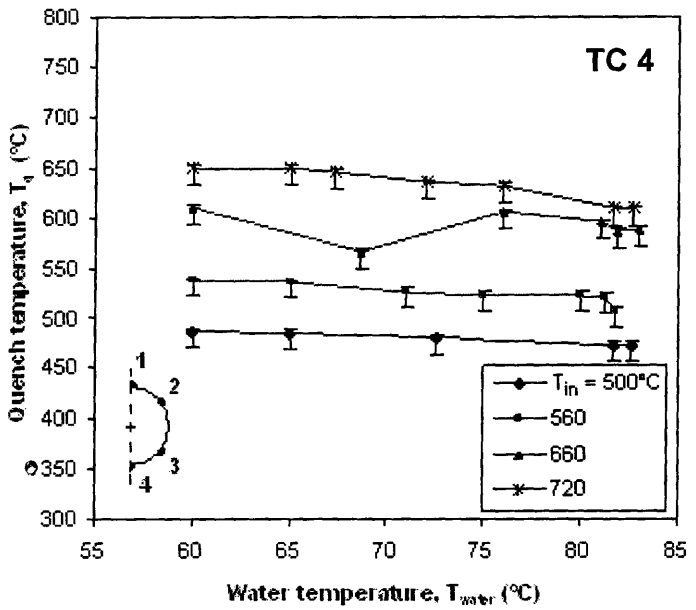

Figure 87: Quench temperature at Location 4 versus water temperature during cooling of a 2-in diameter stainless steel tube for varying initial surface temperature and for V_{jet} = 1.43 m/sec.

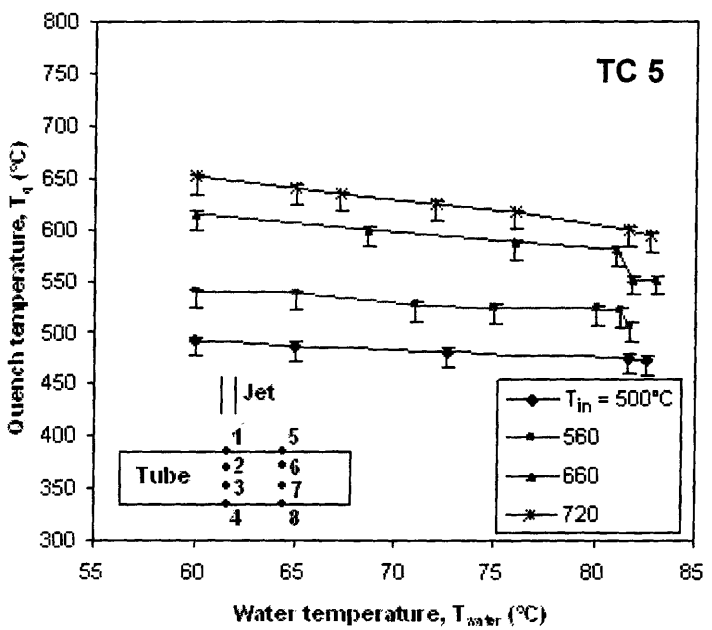

Figure 88: Quench temperature at Location 5 versus water temperature during cooling of a 2-in diameter stainless steel tube for varying initial surface temperature and for V_{jet} = 1.43 m/sec.

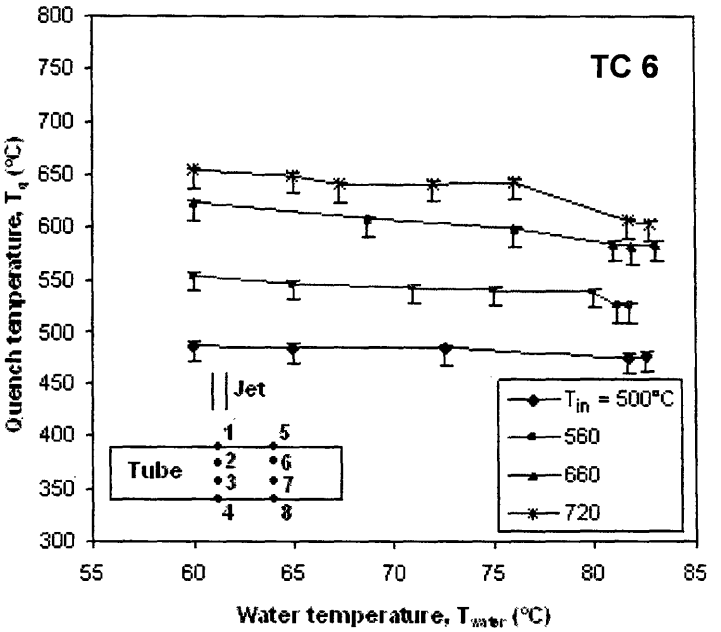

Figure 89: Quench temperature at Location 6 versus water temperature during cooling of a 2-in diameter stainless steel tube for varying initial surface temperature and for V_{jet} = 1.43 m/sec.

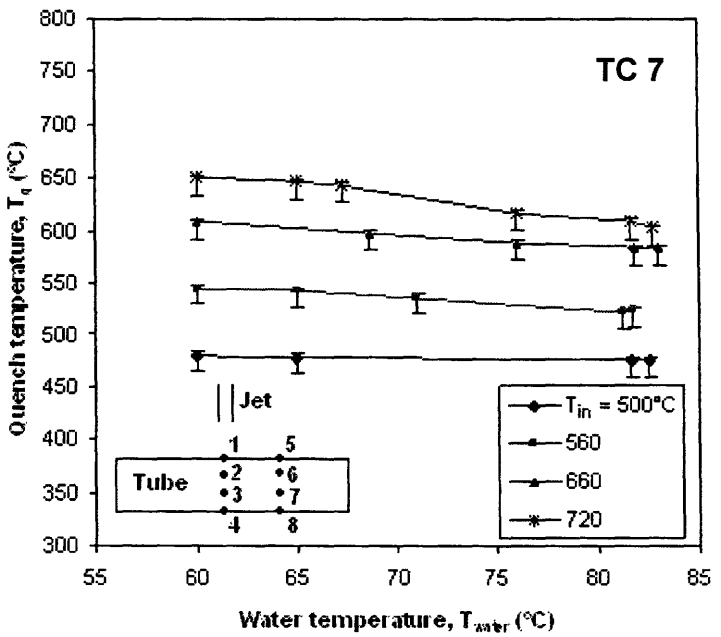

Figure 90: Quench temperature at Location 7 versus water temperature during cooling of a 2-in diameter stainless steel tube for varying initial surface temperature and for V_{jet} = 1.43 m/sec.

For ease of comparison between the spatial locations, Figure 91 shows the quench temperature at Locations 1 to Location 4 versus water temperature for initial surface temperature T_{in} = 720°C and V_{jet} = 1.43 m/sec. This figure shows that the quench temperature decreases by going towards the tube bottom point from TC 2 to TC 4. This is because the tube lower part cools by conduction to the upper part as the upper surface quenches. Figure 92 shows similar results for initial surface temperature of 500°C.

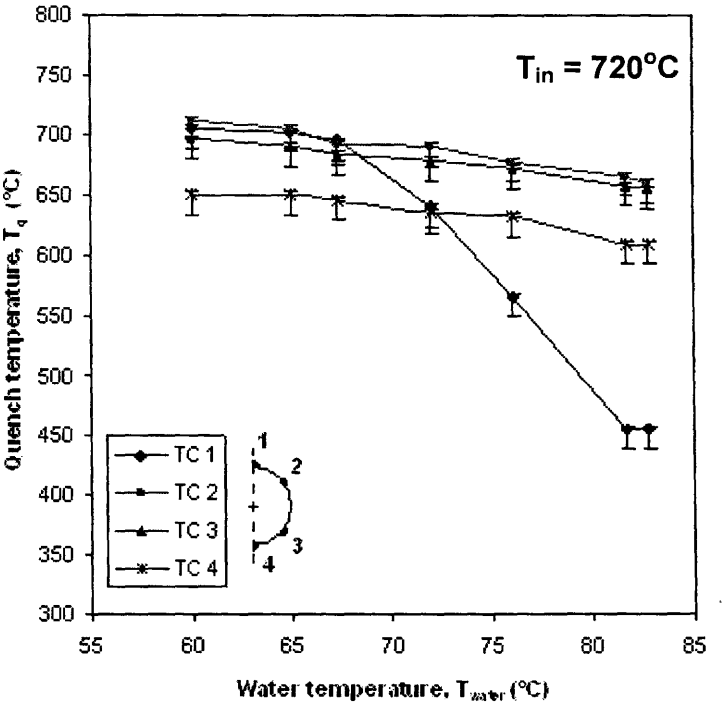

Figure 91: Quench temperature at Locations 1-4 versus water temperature during cooling of a 2-in diameter stainless steel tube for T_{in} = 720°C and V_{jet} = 1.43 m/sec.

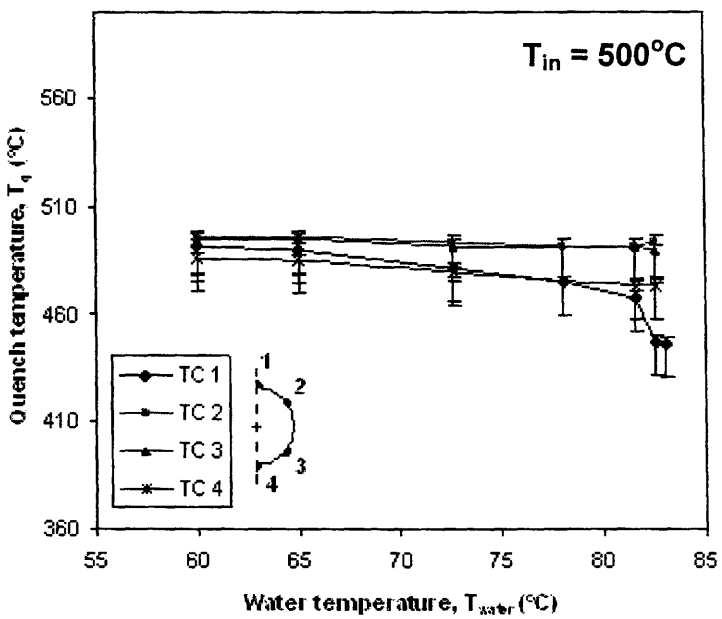

Figure 92: Quench temperature at Locations 1-4 versus water temperature during cooling of a 2-in diameter stainless steel tube for T_{in} = 500°C and V_{jet} = 1.43 m/sec.

Figure 93 shows the quench temperature at Locations 5-7 versus water temperature for initial surface temperature T_{in} = 660°C and V_{jet} = 1.43 m/sec. Location 5 shows similar behaviour to that of Location 1, as Location 5 is more affected than Location 6 and Location 7 by the vapor film boiling that occurs on the surface in the initial stage of the cooling process. This effect was also previously shown in Figure 22 in Chapter Four page 45.

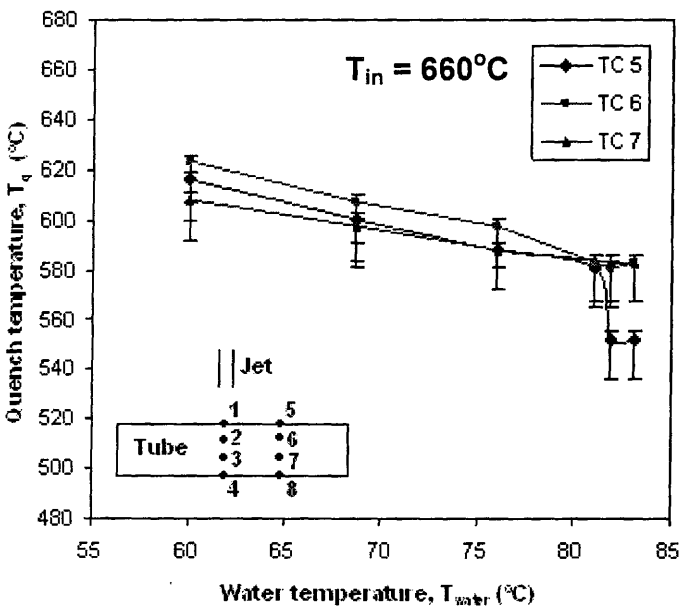

Figure 93: Quench temperature at Locations 5-7 versus water temperature during cooling of a 2-in diameter stainless steel tube for T_{in} = 660°C and V_{jet} = 1.43 m/sec.

Figure 94 shows the quench temperature for Locations 5-7 for initial surface temperature of 500°C.

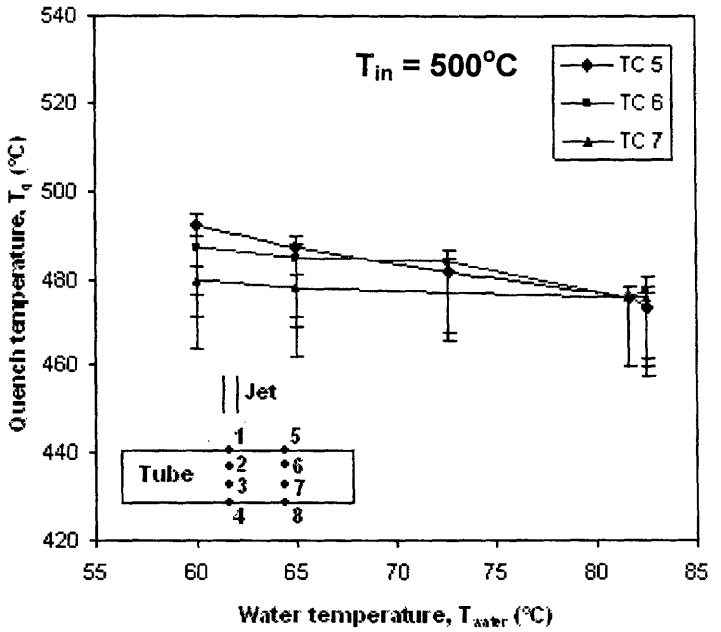

Figure 94: Quench temperature at Locations 5-7 versus water temperature during cooling of a 2-in diameter stainless steel tube for T_{in} = 500°C and V_{jet} = 1.43 m/sec.

5.4.4 Effect of Jet Velocity

The jet velocity was found to have a weak effect on the quench temperature: the quench temperature slightly increased by increasing jet velocity. As the jet velocity increases the quench delay time decreases. However, this does not lead to a higher quench temperature as increasing jet velocity also increases the cooling rate of vapor film boiling. This causes the surface to quench at almost the same temperature regardless of the jet velocity. This behavior was also shown in Figure 31 in Chapter Four page 56.

Similarly, Gadala [37] found that the quench at the stagnation point during jet impingement cooling of a hot steel surface is mainly and greatly affected by water temperature but hardly affected by water flow rate.

5.4.5 Correlation for the Quench Temperature

The quench temperature at the stagnation point was found to depend on water subcooling and initial surface temperature. However, only the tests for which the delay time exceeded 2 seconds were used to obtain a correlation for the quench temperature. This is in order to exclude the tests where rapid quenches occurred immediately after applying the coolant. For example, for the tests shown in Figure 29 in Chapter Four page 54, the test with water temperature 71°C was excluded.

These tests show weak dependence on the initial surface temperature as was shown in Figure 83 page 98.
The correlation was obtained using the least mean square method and found to take the form:

$$T_q(^\circ C) = 12.18(\Delta T_{sub}) + 246.4 \qquad (4)$$

The above correlation was obtained using the following ranges of operating conditions: V_{jet} = 0.22-1.43 m/sec, T_{in} = 500-720°C and T_{water} = 72-84°C using the 2-in diameter stainless steel tube. A plot of the correlation and the experimental data is shown in Figure 95. The figure shows that the quench temperature value is within the range 420-580°C for the above mentioned operating conditions.

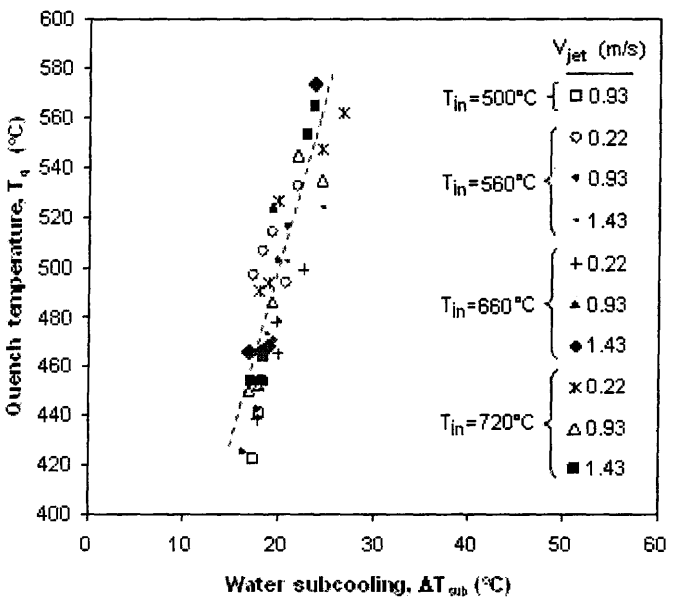

Figure 95: Correlation for the quench temperature at Location 1 during cooling of a 2-in diameter stainless steel tube for T_{in} = 500-720°C and V_{jet} = 0.22-1.43 m/sec.

5.4.6 Summary and Comments

Determining the quench temperature is important for reactor safety. Most quench theoretical models require knowledge of the quench temperature. In this section the effect of several parameters on the quench temperature during cooling a stainless steel tube was studied. It was found that the quench temperature is mainly affected by the degree of water subcooling and the location on the test tube. A major conclusion of this section is that a water subcooling range exists beyond which the dependence on water subcooling is insignificant. A correlation for the quench temperature as a function of water subcooling was developed based on the experimental data collected in this study.

5.5 Re-Wetting Temperature

The re-wetting temperature is defined as the temperature at which actual liquid-solid contact occurs. Determination of the re-wetting temperature is of great importance in reactor safety analysis. This temperature represents a limit between a high temperature region, where inefficient film boiling cooling takes place, and a lower temperature region, where much more efficient nucleate boiling occurs [41, 42]. Gunnerson [41] reported that generally the re-wetting temperature may span a wide range of values, depending on the thermo-physical nature of the hot surface and the liquid. The re-wetting temperature is always lower than the quench temperature.

This temperature is very hard to determine from the temperature-time profile and visual observation of the re-wetting process is required.

In this study the re-wetting temperature at the stagnation point was determined from the captured high speed videos at the moment when the liquid sheet is ruptured due to the rapid vaporization resulting from entering the transition and nucleate boiling region. This moment is compared with the cooling profile measured by the thermocouple at the stagnation point. For the other locations, the re-wetting temperature was determined by comparing the visual observation at the moment when the leading edge of the re-wetting front reaches that location with the temperature-time profile obtained by the thermocouple at that same location.

The effects of several parameters on the re-wetting temperature are discussed in the following sub-sections. Comparison, where possible, with other studies is presented.

Before discussing the effect of the operating conditions on the re-wetting temperature and for better understanding of the quench and the re-wetting temperatures, the two temperatures are plotted in Figure 96 versus water temperature. Also, shown in the figure are the quench delay time and the re-wetting delay time. The measurements shown in the figure were obtained at stagnation point during cooling of a 1-in diameter brass tube initially at T_{in} = 580°C and for V_{jet} = 0.93 m/sec. The quench delay time was determined from the cooling profile at the quench temperature. The re-wetting delay time, however, was determined from the visual observation when the rupture of the liquid sheet occurs. At low water temperatures, the quench and the re-wetting temperatures approach each other. In the critical water subcooling region, around 77-83°C, there was more than 100°C difference between the two temperatures.

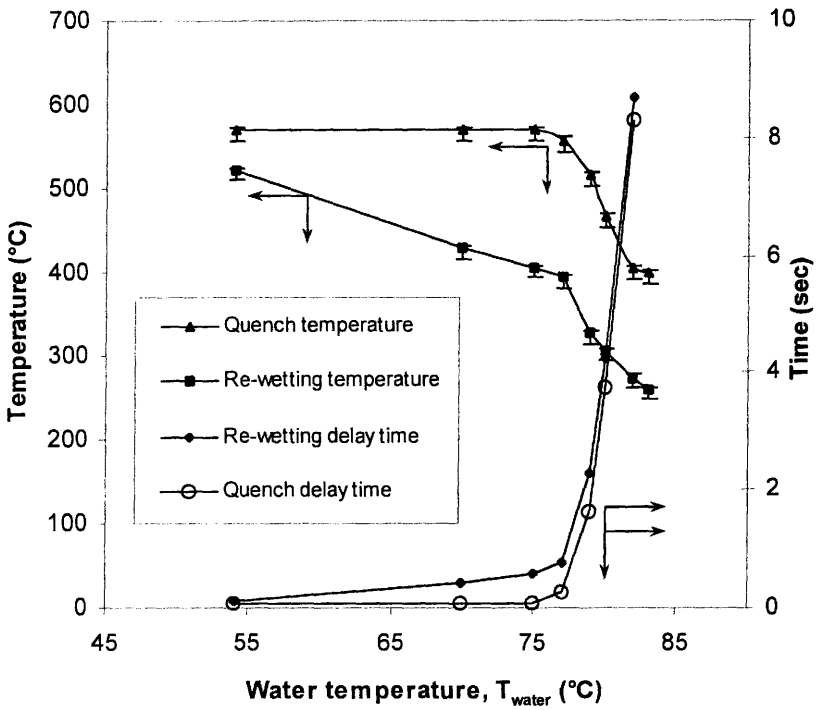

Figure 96: Quench and re-wetting temperatures at Location 1 and delay times versus water temperature during cooling of a 1-in diameter brass tube for T_{in} = 580°C and V_{jet} = 0.93 m/sec.

5.5.1 Correlation for the Re-Wetting Temperature

The re-wetting temperature at the stagnation point was found to relate linearly with water subcooling for all jet velocities and initial surface temperatures. The correlation was found to take the form:

$$T_{rw}(°C) = 7.91\Delta T_{sub} + 223.2 \qquad (5)$$

The above correlation was obtained using the following ranges of operating conditions: V_{jet} = 0.22-1.43 m/sec, T_{in} = 500-720°C and T_{water} = 68-84°C using a 2-in diameter stainless steel tube. Also, only those tests for which the delay time exceeds 2 seconds were used to obtain this correlation.

Figure 97 shows a plot of the correlation and the experimental data for the varying operating conditions. The correlation provides good fit of the data.

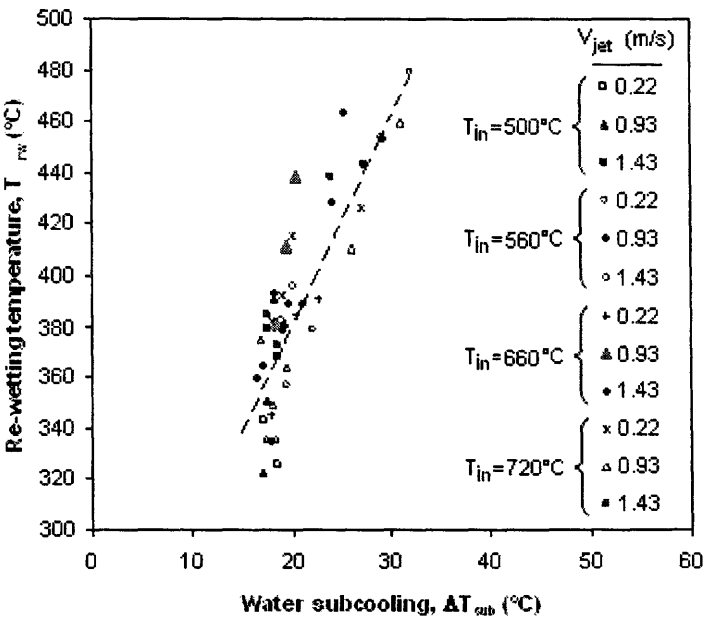

Figure 97: Correlation for the re-wetting temperature at Locations 1 during cooling of a 2-in diameter stainless steel tube for T_{in} = 500-720°C and V_{jet} = 0.22-1.43 m/sec.

5.5.2 Comparison with Correlations Available from Literature

Several correlations for the quench and minimum film boiling temperatures are available from literature and have been developed using experimental data. Many of them are correlated to coolant subcooling in a relation similar to Equation 5.

Following is a group of popular empirical correlations where T_{mfb} denotes minimum film boiling temperature. These correlations will be compared with Equation 4 and Equation 5. In some of these correlations (Ohnishi correlation) the minimum film boiling temperature was defined the same way as the quench temperature was defined here. The correlations are:

Lauer and Hufschmidt (L-H) correlation (water with stainless steel cylinder and sphere) [10]:

$$\Delta T_{mfb} = 5.893\ \Delta T_{sub} + 228.6$$

Adler correlations [10]:

$$\Delta T_{mfb} = 6\ \Delta T_{sub} + 130 \text{ (distilled water with stainless steel sphere)}$$

$$\Delta T_{mfb} = 7\ \Delta T_{sub} + 175 \text{ (de-ionized water with stainless steel sphere)}$$

Bradfield correlation (water with copper sphere) [3, 10]:

$$\Delta T_{mfb} = 6.15\ \Delta T_{sub} + 200$$

Groneveld and Stewart (G-S) correlation at atmospheric pressure (water with Inconel tube) [43]:

$$T_{mfb} = 6.3\ \Delta T_{sub} + 289$$

Ohnishi correlation [3]:

$$\Delta T_{mfb} = 5.1\ \Delta T_{sub} + 350$$

Figure 98 shows a plot of Equation 4 and Equation 5 and the above empirical correlations.

As can be seen from the figure, the equations are consistent with the other correlations.

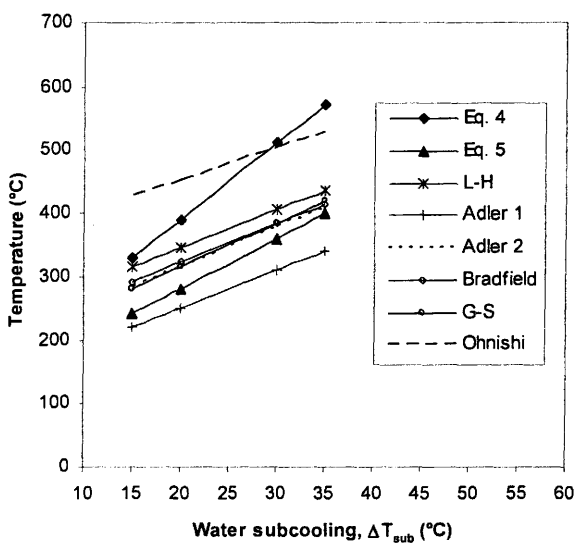

Figure 98: Comparison of Equations 4 and 5 with correlations available from literature.

5.5.3 Effect of Initial Surface Temperature

Figure 99 shows the re-wetting temperature versus water temperature for varying initial surface temperatures. The effect of the initial surface temperature is not significant especially for the higher water temperatures; the conditions which are of interest in this study. However, it can be seen that the re-wetting temperature increases slightly with increasing initial surface temperature.

As was mentioned in Chapter Two: Literature Review, it was experimentally found that the re-wetting temperature increases as a linear function of the initial surface temperature in the experiments done by Stevens [38]. They studied film and transition boiling on 1.9 cm diameter copper sphere moving through subcooled water. It was reported by J. Carbajo [10] that this linear relation was not confirmed by other experiments. In this study, a linear relationship between both the quench and the re-wetting temperatures was noticed (as was shown in Figures 80-82, pages 95-97). However, the linear relationship between the quench temperature and the initial surface temperature is clearer than that of the re-wetting temperature.

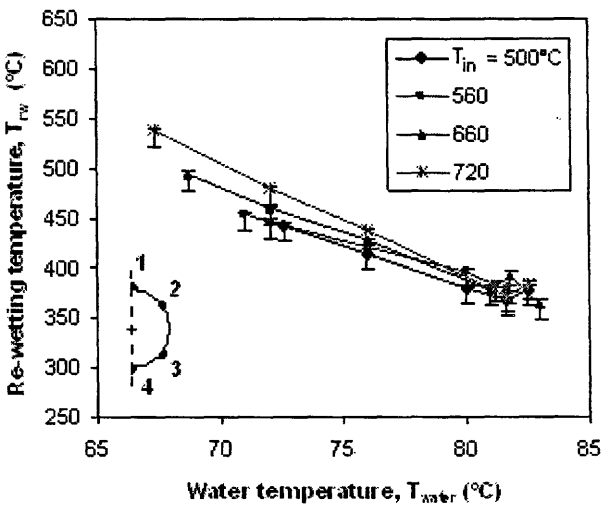

Figure 99: Re-wetting temperature at Location 1 versus water temperature for varying initial surface temperatures during cooling of a 2-in diameter stainless steel tube and for V_{jet} = 1.43 m/sec.

5.5.4 Effect of Jet Velocity

In this study, weak dependence was observed of the re-wetting temperature on the jet velocity in the range 0.22-1.43 m/sec. The re-wetting temperature was found to only slightly increase with increasing jet velocity. Stevens [38] in his study of film and transition boiling on the copper spheres moving through subcooled water found that the velocity of the sphere had no effect on the minimum film boiling temperature. Other researchers reported that for subcooled conditions with low flow rates the mass flux effect is small or non-existent [42]. Gadala [37] found that the stagnation point during jet impingement on a flat steel plate is hardly affected by water flow rate.

5.5.5 Quench and Re-wetting Temperatures in Axial Direction

In this study, a test section was prepared to study the quench and the re-wetting temperatures in the axial direction upon quenching by jet impingement. The test section was a 1-in brass tube prepared as discussed in Chapter Three. The tube was instrumented with five thermocouples located at: 0.0, 1.3, 3.5, 5.08 and 6.7 cm from the stagnation point.

Figure 100 shows an image of the tube upon cooling with water jet at velocity of V_{jet} = 0.93 m/sec for initial surface temperature T_{in} = 580°C. The thermocouple locations are shown in the figure. The figure also shows the corresponding surface temperature at the five locations at time t = 9.1 sec from starting the cooling process. At this time, Location 1 has already wet while Location 2 is around the re-wetting temperature. Locations 3, 4 and 5 are still at a high temperature.

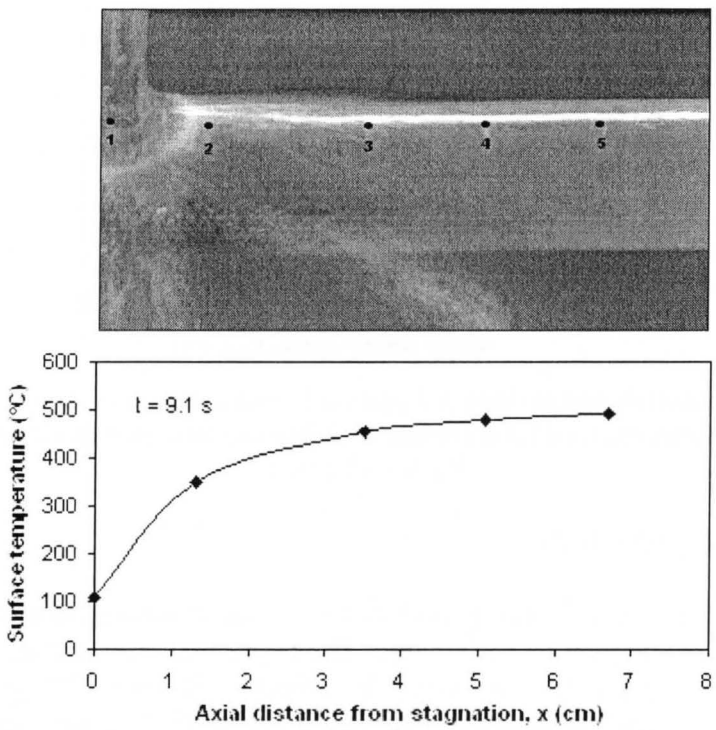

Figure 100: Surface temperature and the corresponding image during cooling of a 1-in diameter brass tube for V_{jet} = 0.93 m/sec and T_{in} = 580°C after t = 9.1 sec. The five locations are at: 0.0, 1.3, 3.5, 5.08 and 6.7 cm from the stagnation point.

For other points in the time domain, a plot of the surface temperature versus the relative axial distance is shown in Figure 101. The relative axial distance is the axial distance divided by the width of the jet. The figure shows the temperature at each location from t = 0.0 until the whole tube has cooled to the jet temperature.

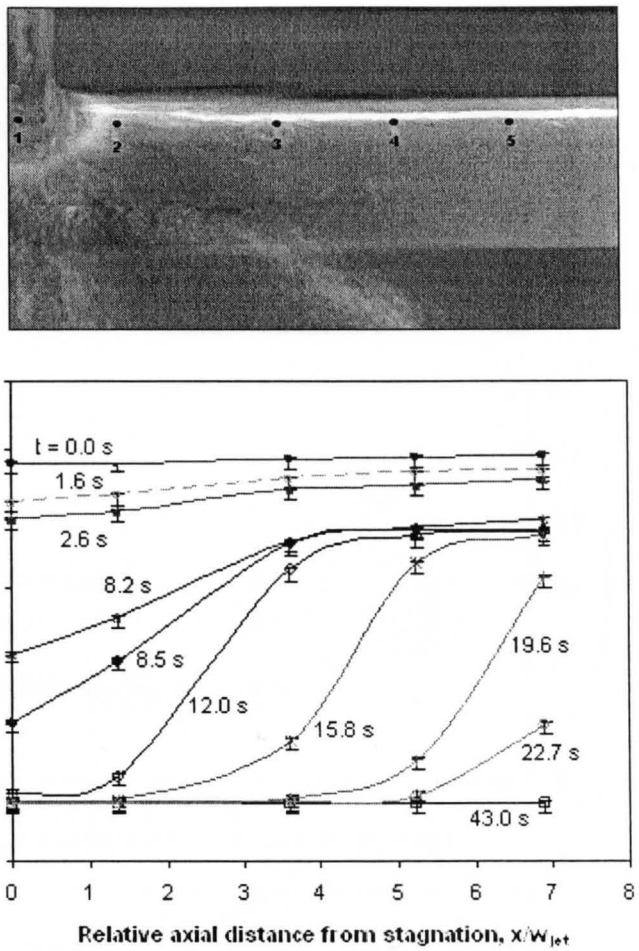

Figure 101: Surface temperature versus the relative axial location during cooling of a 1-in diameter brass tube for V_{jet} = 0.93 m/sec and T_{in} = 580°C. The five locations are at: 0.0, 1.3, 3.5, 5.08 and 6.7 cm from the stagnation point.

To investigate the effect of water subcooling, Figure 102 shows the quench and the re-wetting temperatures at the five locations for water temperatures in the range 54-82°C for initial surface temperature T_{in} = 580°C and for V_{jet} = 0.93 m/sec.

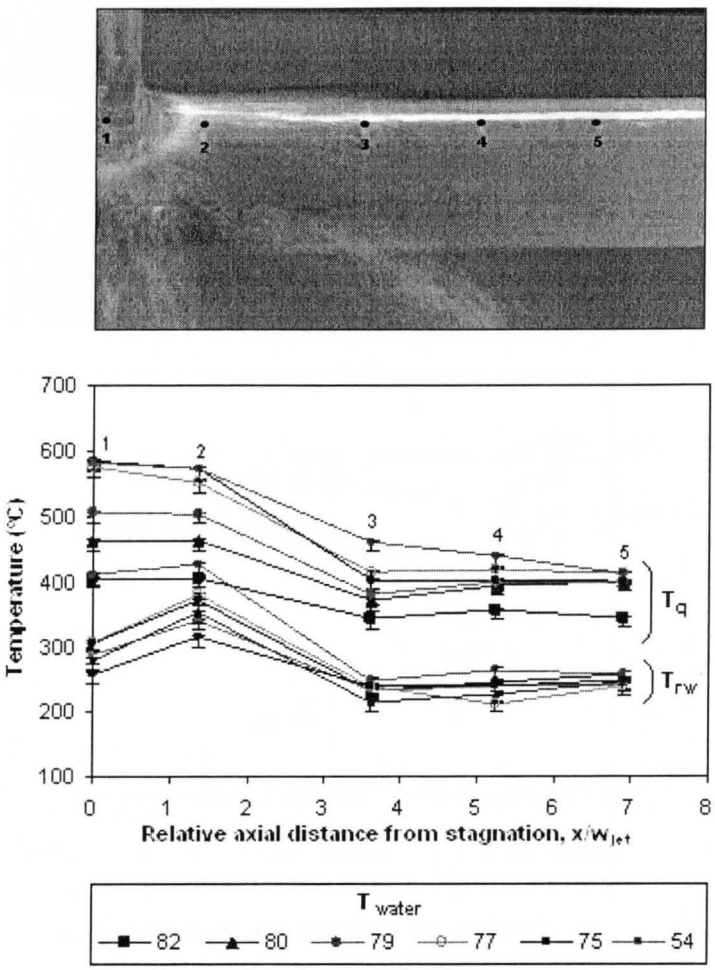

Figure 102: Quench and re-wetting temperatures versus the relative axial location for several water temperatures during cooling of a 1-in brass tube for initial surface temperature T_{in} = 580°C and V_{jet} = 0.93 m/sec.

The quench temperature at Location 1 and Location 2 are almost the same as they are located close to each other. The quench temperature starts to level off to almost a constant value at the other locations. This is because the upper surface of the tube has cooled down due to film boiling and heat conduction to the stagnation area and due to the increase in water temperature as the water moves on the surface.

It can be seen that the length on the tube axis does not have a considerable effect on both the quench and the re-wetting temperatures for high water temperatures and at Locations 3, 4 and 5.

5.5.6 Effect of Tube Size and Solid Material

The quench and the re-wetting temperatures versus water subcooling during cooling of a 1-in brass tube are shown in Figure 103. These correlations were found to take the form:

$$T_q = 20.91\ \Delta T_{sub} + 36.7 \quad (6)$$

$$T_{rw} = 6.04\ \Delta T_{sub} + 256.3 \quad (7)$$

Figure 104 shows these correlations as well as the correlations obtained for the 2-in stainless steel tube as was shown previously in Equation 4 and Equation 5.

The figure shows that the quench temperature of the brass tube is lower than that of the stainless steel tube and it is more sensitive to the water subcooling (steeper slope for brass). The lower quench temperatures of brass compared to those of steel are due to the effect of the two factors: the solid material and the surface curvature. As was shown in sub-section 5.1.6 page 65 the delay time increases by increasing the solid thermal conductivity. This causes the surface to cool to a lower temperature before it starts to quench. Also, as was shown in sub-section 5.1.7 page 66 the delay time increases by decreasing tube diameter. This again causes the surface to cool to a lower temperature before it reaches the quench temperature.

Jet impingement cooling results in localized cooling near the stagnation region for steel in contrast to brass where the entire heated tube quickly feels the effect of the jet on the surface. Brass can easily supply heat to the region of the jet-surface interaction which increases the quench delay time. Therefore, brass shows lower quench temperatures.

From the above discussion, it is concluded that by using the brass tube the combined effects of both increasing the thermal conductivity and decreasing the tube size worked to decrease the quench temperature compared to that of the steel tube. The maximum decrease in the quench temperature was around 70°C. The quench temperatures for the two tubes approach each other as water subcooling increases.

The two tubes show almost the same re-wetting temperature as shown in Figure 104. The re-wetting temperature is concluded to be less dependent on the solid material. This result is consistent with findings of other researchers. A. Mozumder et al. [44] experimentally found that the re-wetting temperature of droplets impinged on four hot surfaces (Aluminum, copper, brass and steel) was independent of the solid material for the four tested surfaces. Also, as was mentioned in Chapter Two: Literature Review, J. Hammad [13] studied the effect

of solid material during jet quenching of three high temperature cylindrical blocks using a circular water jet directed upwards towards the flat bottom of the cylinders. The three blocks were made of copper, brass and steel. It was found that the re-wetting temperature was not affected by the block material especially near the stagnation region.

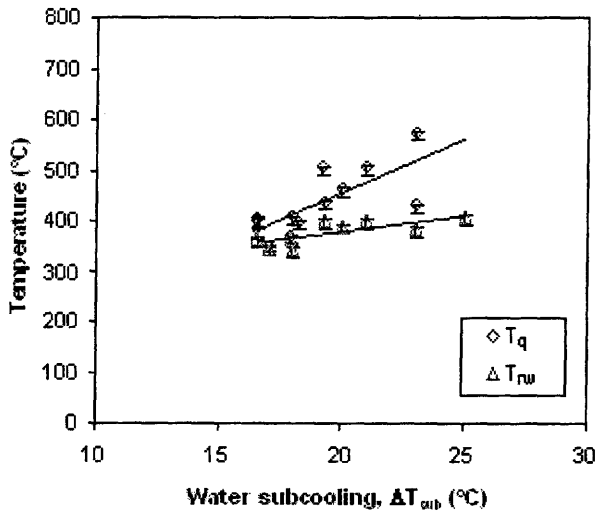

Figure 103: Correlations for quench and re-wetting temperatures at Locations 1 during cooling of a 1-in diameter brass tube.

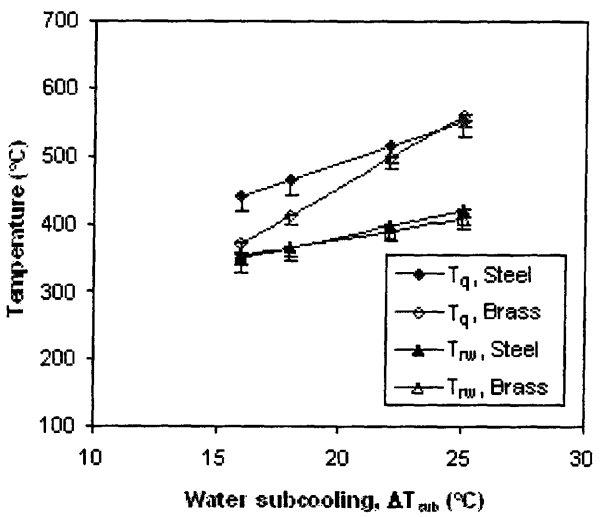

Figure 104: Comparison of quench and re-wetting correlations obtained for Steel and Brass tubes.

5.5.7 Effect of Number of Tubes

A Few tests were conducted in this study to investigate quenching of two horizontal tubes. The tubes were aligned with vertical spacing of 16 mm in between and the lower tube was instrumented with thermocouples. The thermocouples are located axially at: 0.0, 1.3, 3.5, 5.08 and 6.7 cm from the stagnation point and one sixth thermocouple is located 60^{o} at the same axis with thermocouple 1. The lower tube was quenched twice: once alone and once with the existence of the upper tube and the resulting temperature-time profiles were compared. Figure 105 shows an image of the two tubes being cooled. The wet patch on the lower tube was found to spread from the tube sides towards the tube upper and lower parts. Figure 106 shows the cooling profiles obtained for quenching the single tube and Figure 107 shows those obtained for the lower tube upon cooling the two tubes. The figures also show the thermocouple locations. The top point at the lower tube shows a lower quench temperature than that when the upper tube was not existent. Figure 107 shows a considerable delay in quenching Location 1 and Location 2 as they quench only after quenching Location 6 which is located at the side of the tube. Also, liquid sheet lifting at the upper tube causes the temperature at Location 6 to increase before it re-quenches again.

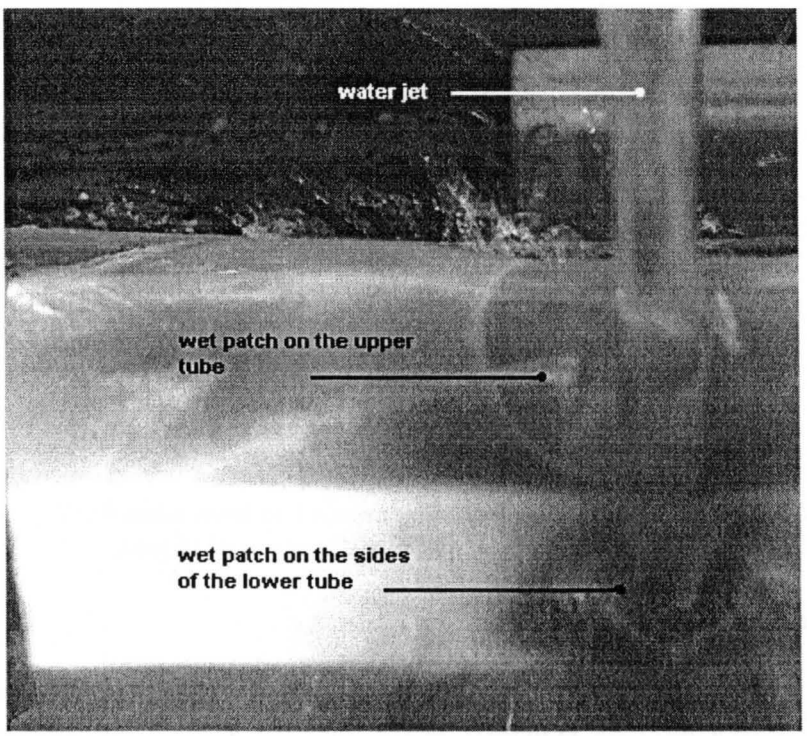

Figure 105: Cooling of two 1-in brass tubes for V_{jet} = 0.93 /sec, T_{water} = 54°C and T_{in} = 600°C. The wet patch on the lower tube spreads from the sides towards the tube upper and lower parts.

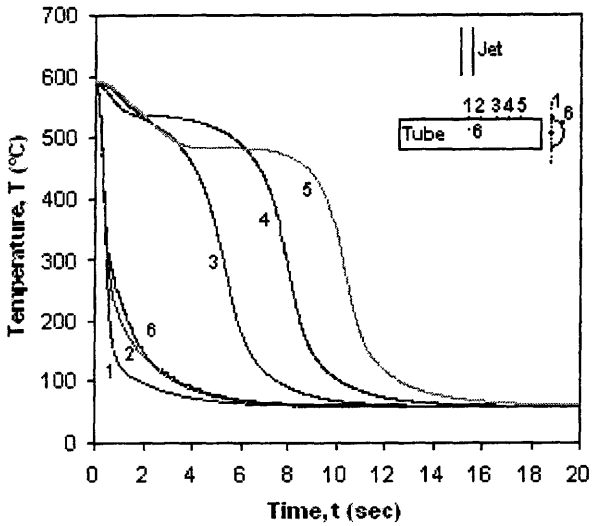

Figure 106: Cooling profiles during cooling of single 1-in brass tube for V_{jet} = 0.93 /sec, T_{water} = 54°C and T_{in} = 600°C.

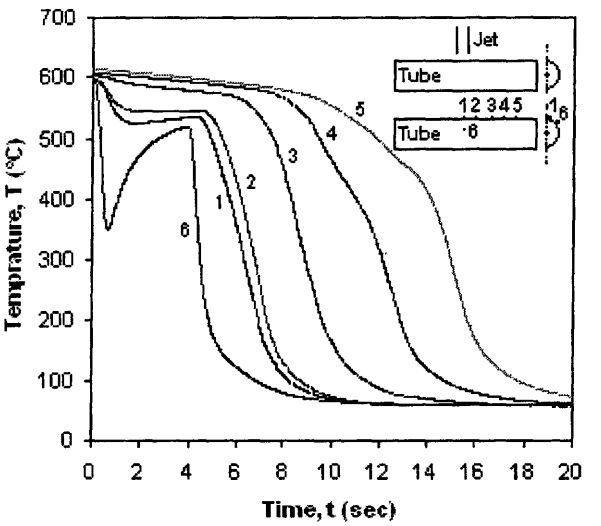

Figure 107: Cooling profiles during cooling of two 1-in brass tubes for V_{jet} = 0.93 /sec, T_{water} = 54°C, T_{in} = 600°C and spacing of 16 mm.

5.5.8 Summary and Comments

The effects of various parameters on the re-wetting temperature were studied. The re-wetting temperature is generally lower than the quench temperature. It was found that the re-wetting temperature is mainly affected by water subcooling and a correlation of the re-wetting temperature as a function of water subcooling has been developed. The correlations developed for the quench and re-wetting

temperatures agree with empirical correlations available from literature. The re-wetting temperature was found to depend on the axial direction on the tube surface for locations close to the stagnation point. However, weak dependence was observed as the distance from the stagnation point increases. In cooling two horizontal tubes aligned with vertical spacing in between, the lower tube showed generally lower quench temperatures than those when it was cooled alone.

5.6 Vapor Film and Nucleate Boiling Cooling Rates

Cooling of a hot surface experiencing vapor film boiling causes the vapor film to collapse, resulting in nucleate boiling where very rapid heat transfer starts to take place. As the surface cools further the nucleate boiling is followed by single phase convection. Therefore, in determining the cooling rate (°C/sec) upon quench cooling, one should look at the cooling rates in three distinct stages: vapor film boiling, nucleate boiling and single phase convection.

In vapor film boiling, heat is transferred to the liquid by conduction through the vapor film and by radiation and convection. The transferred heat works on heating the liquid and evaporating part of it.

In nucleate boiling, as the surface temperature is higher than the saturation temperature of the liquid, steam bubbles are formed within the liquid in small cavities at the hot surface. The bubbles grow in size and at a critical size they detach from the wall and are transferred to the bulk of the liquid. As the temperature of the bulk liquid is lower than that at the hot surface, the bubbles collapse. Therefore, heat is carried away quickly and efficiently from the hot surface. If the surface temperature continues to decrease to a value less than the saturation temperature, nucleate boiling stops and single phase convective cooling starts to take place.

In this section the effect of several parameters on the cooling rates of vapor film and nucleate boiling are discussed. The cooling rates in the vapor film and nucleate boiling regimes were determined from the slope of the cooling profile before and after the rapid decrease in temperature; respectively. This was done for several locations at the tube where thermocouples are instrumented.

Investigating the cooling rates is important as they give an indication of the heat flux which is usually related to the cooling rate.

5.6.1 Effect of Initial Surface Temperature and Degree of Subcooling

Figure 108 shows the cooling rates of vapor film boiling and nucleate boiling at the stagnation point versus water temperature during cooling of a 2-in stainless steel tube for V_{jet} = 1.43 /sec and for varying initial surface temperatures. R_{vapor} represents the cooling rate of vapor film boiling and $R_{nucleate}$ represents the cooling rate of nucleate boiling, both measured in °C/sec.

The figure shows that, for the current jet velocity, the cooling rates show some increase with decreasing water temperature and slightly depend on the initial surface temperature. As water temperature decreases the heat, conducted from the

surface through the vapor film increases. This increases the efficiency of the cooling by vapor film boiling.

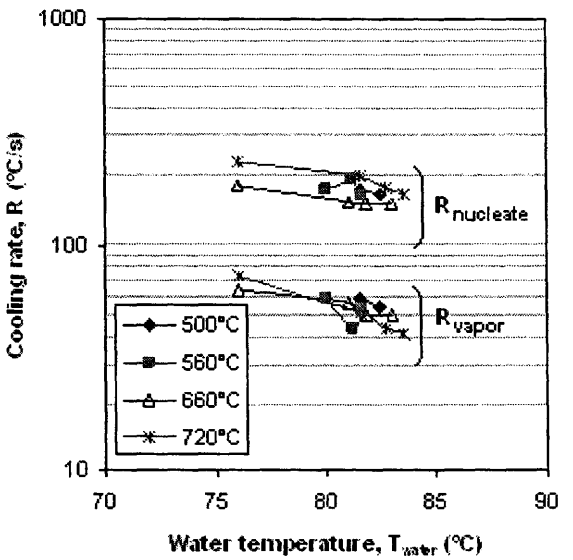

Figure 108: Cooling rates of vapor film boiling and nucleate boiling at stagnation point versus water temperature during cooling of a 2-in stainless steel tube for V_{jet} = 1.43 /sec and for varying initial surface temperatures. R_{vapor}: cooling rate of vapor film boiling, $R_{nucleate}$: cooling rate of nucleate boiling.

5.6.2 Effect of Jet Velocity

Figure 109 shows the cooling rates at the stagnation point versus water temperature during cooling of a 2-in stainless steel tube for T_{in} = 720°C and for varying jet velocities. As the jet velocity increases, both cooling rates increase. The vapor film boiling cooling rate is more dependent on the water temperature for the high jet velocity V_{jet} = 1.43 /sec. Highly increasing the jet velocity increases the pressure on the vapor film and makes it thinner which increases the cooling rate.

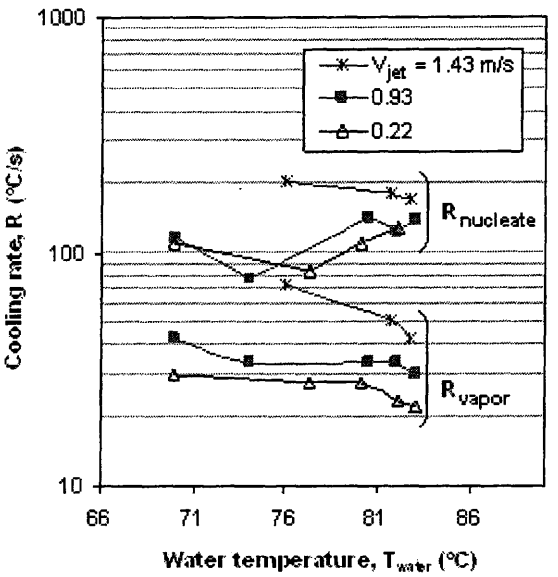

Figure 109: Cooling rates of vapor film boiling and nucleate boiling at stagnation point versus water temperature during cooling of a 2-in stainless steel tube for T_{in} = 720°C and for varying jet velocities. R_{vapor}: cooling rate of vapor film boiling, $R_{nucleate}$: cooling rate of nucleate boiling.

In nucleate boiling, for jet velocities of 0.22 and 0.93 m/sec, the figure shows a decrease in the cooling rate followed by an increase. The unexpected increase can be explained as follows: for these low and moderate jet velocities, as the water temperature increases the quench delay time increases. During this delay time, the whole surface cools down by vapor film boiling. When the conditions for vapor film destabilization are achieved, the vapor film destabilizes on a wide area on the surface and transition and nucleate boiling start to take place on this area. As this area increases in size, the nucleate boiling cooling rate increases.

However, for lower water temperatures, the delay time is relatively short which means that film boiling exists for a shorter time on the whole surface. Therefore, when the vapor film destabilizes, it destabilizes on a localized area surrounding the stagnation point. Under such conditions, the resulting nucleate boiling rate will be lower than that for higher water temperatures. This behavior again, was observed for the low and moderate jet velocities of 0.22 and 0.93 m/sec as shown in Figure 109. One another factor is that decreasing water temperature increases the quench temperature. Increasing the quench temperature increases the nucleate cooling rate due to the change in water viscosity. As the viscosity decreases with the increased temperature, better wetting of the surface occurs and consequently better heat transfer. This explains why the cooling rate decreases by the initial increase in water temperature (in the range 70-76°C).

5.6.3 Effect of Spatial Location

Figure 110 shows the vapor film boiling cooling rate at Locations 1-4 versus water temperature during cooling of a 2-in stainless steel tube for T_{in} = 660°C and for V_{jet} = 1.43 m/sec. The cooling rate depends on the azimuthal location on the tube surface and it is maximum at the stagnation point and decreases by moving down towards the tube bottom point. This is because the stagnation region is located directly beneath the jet where the water is at a lower temperature than what it becomes at the other locations. Figure 111 shows the nucleate boiling cooling rate at the same locations. The nucleate boiling cooling rate also depends on the spatial location but at stagnation its value is closer to that at Location 2.

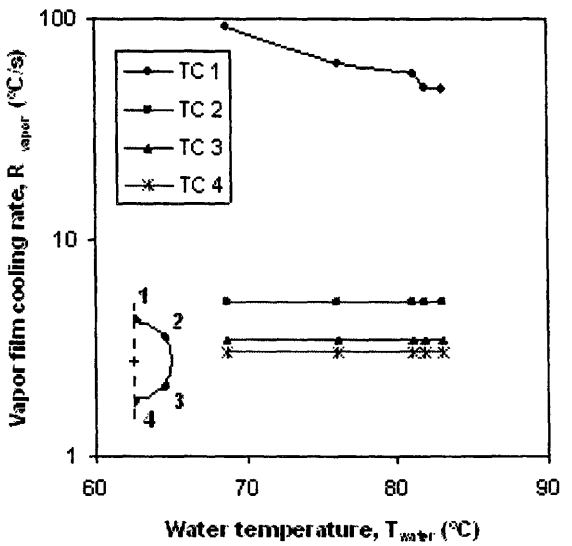

Figure 110: Cooling rate of vapor film boiling at Locations 1-4 versus water temperature during cooling of a 2-in stainless steel tube for T_{in} = 660°C and V_{jet} = 1.43 m/sec.

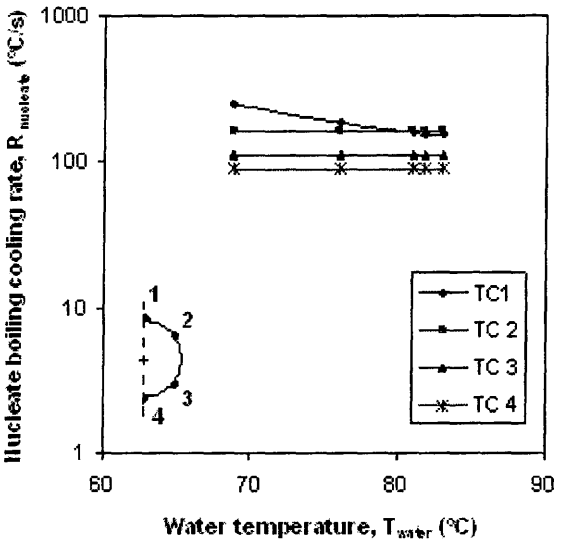

Figure 111: Cooling rate of nucleate boiling at Locations 1-4 versus water temperature during cooling of a 2-in stainless steel tube for T_{in} = 660°C and V_{jet} = 1.43 m/sec.

5.6.4 Summary and Comments

In this section the effects of several parameters on the cooling rates of vapor film boiling and nucleate boiling were studied. Determination of the cooling rates is important as the heat flux is usually related to the cooling rate. It was found that, generally, increasing water temperature slightly decreases the cooling rates and increasing jet velocity increases the cooling rates. The cooling rates also depend on the spatial location: the cooling rates decrease by moving towards the tube bottom point. The stagnations point shows the maximum cooling rates.

There exists a combination of jet velocities and water temperatures for which the nucleate boiling cooling rate unexpectedly increases by increasing water temperature and the cooling rate does not always show a decrease by increasing water temperature.

Chapter Six

Conclusions

Quench cooling of a hot dry surface involves the rapid decrease in surface temperature resulting from bringing the hot surface into sudden contact with a coolant at a lower temperature prior to re-wetting the surface. Situations involving quench heat transfer are encountered in a number of postulated accidents in the CANDU reactors, such as quenching of hot fuel elements experiencing post – dryout conditions during a loss of flow accident or quenching of a hot calandria tube in certain loss of coolant accidents in which a pressure tube deforms into contact with its calandria tube.

The quench cooling is a very complex heat transfer process and involves several sub-processes which are complicated themselves. Any theoretical modeling of the process should take into consideration a large number of affecting variables, such as initial surface temperature, coolant temperature, flow velocity, surface geometry and solid material. In literature, there is a considerable confusion in defining the different terms usually used in quench studies.

In this study the quench temperature was defined as the onset of the rapid decrease in the surface temperature and the re-wetting temperature as the temperature at which actual liquid-solid contact occurs. To better understand the dynamics of the quench process an experimental facility has been designed and built as part of this study to measure the surface temperature and visualize the two-phase flow behavior during quench of hot horizontal tubes using an array of water jets. The effect of many variables which play a role in the quench cooling has been investigated and discussed. Empirical correlations for re-wetting delay time, re-wetting front velocity, quench temperature, re-wetting temperature have been developed and provided good fit of the experimental data.

The results of this study provide novel information and an experimental database for mechanistic modeling of quench cooling of calandria tubes experiencing film boiling due to pressure tube contact after a critical break LOCA in CANDU reactors. The mechanistic modeling can be used to support safety analysis methodology that has been developed to demonstrate fuel channel integrity during LOCA in CANDU reactors.

Following are more detailed conclusions:

6.1 Water Quench Facility

A novel method of thermocouple instrumentation in the test section has been developed to accurately measure the temperature at a location on the tubes. In literature, many studies reported the existence of noise in the temperature-time profile in quench studies. The thermocouple instrumentation method in this study resulted in accurate measurement of surface temperature which allowed the differentiation between the noise created by the measurement tools and the noise created because of the two-phase flow behaviour under certain operating conditions.

The use of a high speed camera with a high framing rate provided an excellent tool to accurately determine and to introduce some variables which are highly transient in nature such as vapor film collapse, reformation of the vapor film and rebound of the re-wetting front. This tool also helped in accurately locating the edge of the re-wetting front as it moves on the surface.

6.2 Re-wetting delay time

The re-wetting delay time at the stagnation region greatly depends on water subcooling. The delay time increases with increasing water temperature. Also, it increases with increasing initial surface temperature and decreasing jet velocity. It also greatly depends on the solid material. As the solid thermal conductivity increase the delay time increases. The delay time increases by increasing the surface curvature (decreasing the diameter). Also, as the thickness of the material decreases the delay time decreases. Jet orientation was found to have a negligible effect on the delay time at the stagnation region. Number of jets applied to the surface slightly decreased the delay time at stagnation.

A correlation was developed for estimating the delay time. The correlation parameters are jet velocity, water subcooling, initial surface temperature, solid material and tube diameter. The correlation provided good fit of the experimental data collected in this study and was in good agreement with data available from literature.

6.3 Re-wetting front velocity

The re-wetting front position during quenching always follows the quench position. The re-wetting front velocity was found to increase with decreasing water temperature, increasing initial surface temperature and increasing jet velocity. Therefore, the front velocity slows down as the temperature difference between the heated tube and the liquid applied decreases. Increasing surface curvature was found to decrease the re-wetting front velocity. Also, as the solid thermal conductivity increases, the re-wetting front velocity decreases especially

in the early stages of the formation of the wet patch. The number of jets applied to the surface slightly increased the re-wetting front velocity. Jet orientation had a negligible effect on the re-wetting front velocity in the axial direction of the tube. Finally, increasing the thickness of the tube decreases the re-wetting front velocity.

Under some conditions, the re-wetting front was found to rebound just after the formation of the wet patch. The rebound increased by decreasing water temperature and decreasing jet velocity.

6.4 Boiling region size

Few studies investigated the size of the transition and nucleate boiling region. This size was found to increase with water temperature and with decreasing initial surface temperature. The size also increased as the solid thermal conductivity increased.

6.5 Quench temperature

Determining the quench temperature is important for reactor safety and most quench theoretical models require knowledge of the quench temperature. It was found that the quench temperature is mainly affected by water subcooling and the location on the test tube. A water subcooling range exists beyond which the dependence is weak and the concept of critical water subcooling has been introduced in this study. A correlation of the quench temperature as a function of water subcooling was developed based on the experimental data collected in this study.

6.6 Re-wetting temperature

The re-wetting temperature is always lower than the quench temperature. However, the two temperatures approach each other for high water subcoolings. The re-wetting temperature is mainly affected by water temperature and the location on the test tube. A correlation of the re-wetting temperature as a function of water subcooling was developed. The correlation provided good fit of the experimental data and was in good agreement with empirical correlations available from literature.

6.7 Cooling rates

It was found that, in general, increasing water temperature slightly decreases the cooling rates in vapor film and nucleate boiling. Also, the cooling rates increase by increasing jet velocity. The cooling rates were found to decrease by moving towards the tube bottom point. The stagnation point shows the maximum cooling

rates. There exists a combination of jet velocities and water temperatures for which the nucleate boiling cooling rate unexpectedly increases by increasing water temperature.

Chapter Seven

Recommendations

The results of this study showed that the quench process is a very complicated process and involves several sub-processes. Many variables affect the different sub-processes during quenching and therefore it is hard to investigate all these variables in one study. This work provided many details of some aspects of the phenomena. A primary foundation was also provided for other aspects which may lead to better understanding of the phenomena by future studies. Some directions for future work are depicted here and it is recommended to:

1. Investigate the quench phenomena using an array of tubes.

2. Use large scaled tubes.

3. Study the effect of the pressure on the quench process as high pressures are usually encountered in the reactor core.

4. Determine the heat flux at the surface during quenching. This could be done by theoretical modeling.

5. Further study the new parameter "boiling width" which may contribute to the better understanding of the quench cooling.

6. This study showed that there is not much dependence of the quench temperature on water temperatures exceeding a value around 81°C. However, it is still recommended to increase the water temperature to values close to the saturation temperature.

7. Further study the effect of wall thickness on the quench process.

8. Study the effect of surface roughness on the quench process.

9. Study the effect of surface oxidation on the quench process.

10. Study the effects of jet impingement locations on the horizontal tube.

11. Study the effect of jet size and type.

12. Study the effect of jet-to-surface distance.

13. Study the effect of using a two-phase water jet in the quench process.

Bibliography

[1] A. Satapathy and R. Sahoo, "Rewetting of an infinite tube with internal heating", International Journal of Numerical Methods for Heat & Fluid Flow, Vol. 11,No. 3, pp. 200-212, 2001.

[2] J. Jiang and J. Luxat, "Modeling the Quenching of a Calandria Tube following a Critical Break LOCA in a CANDU Reactor," Proc. Canadian Nuclear Society 29th Annual Conference, Toronto, Ontario, Canada, June, 2008.

[3] J. Luxat, "Mechanistic Modeling of Heat Transfer Process Governing Pressure Tube-To-Calandria Tube Contact and Fuel Channel Failure", Proceedings CNS Annual Conference, June 2-5, 2002.

[4] A. Abdul-Razzak, M. Shoukri and A.Chan "Rewetting of hot horizontal tubes", Nuclear Engineering and Design, Vol. 138, 3, pp.375-388, 1992.

[5] M. Sawan and M. Carbon, "A Review of Spray-Cooling and Bottom-Flooding Work for LWR Core", Nuclear Engineering and Design 32, pp. 191-207, 1975.

[6] V. Dhir, "Phase Change Heat Transfer – A Review of Purdue Research", Purdue Heat Transfer Celebration, West Lafayette, IN, 2002.

[7] B. Piggott, E. White and R. Duffey, "Wetting Delay due to Film and Transition Boiling on Hot Surfaces", Nuclear Engineering and Design, 36, pp.169-181, 1976.

[8] P. Woodfield, M. Monde and A. Mozumder, "Observations of High Temperature Impinging-Jet Boiling Phenomena", International Journal of Heat and Mass Transfer, 48 (10), 2032-2041, 2005.

[9] A. Mozumder, "Thermal and Hydrodynamic Characteristics of Jet Impingement Quenching for High Temperature Surface", PhD Thesis, Saga University, 2006.

[10] J. Carbajo, "A Study of the Rewetting Temperature", Nuclear Engineering and Design 84, pp. 21-52, 1985.

[11] S. Aldaihan and A. Alhbaib, "Reflooding and Rewetting in Light Water Reactor: A Review of Mathematical Models", The Fourth Saudi Engineering Conference, November, 1995-Volume V.

[12] F. Gunnerson and A. Cronenberg, "On the Minimum Film Boiling Conditions for Spherical Geometries", Trans. ASME, Journal of Heat Transfer 102, 335-341, 1980.

[13] J. Hammad, "Characteristics of Heat Transfer and Wetting Front during Quenching High Temperature Surface by Jet Impingement", PhD Thesis, Saga University, 2004.

[14] F. Kaminaga and H. Uchida, "Reflooding Phenomena in a Single Heated Rod- Part 1, Experimental Study", Bulletin of the JSME, Vol. 22 No. 169, pp. 960-966, 1979.

[15] A. Kim and Y. Lee, "A Correlation of Re-wetting Temperature", Lett. Heat Mass Transfer, 6, 117, 1979.

[16] B. Piggot and D. Porthouse, "A Correlation of Rewetting Data", Nuclear Engineering and Design, 32, pp. 171-181, 1975.

[17] T. Lübben, F. Frerichs, F. Hoffmann and H. Zoch, "Rewetting Behavior during Immersion Quenching", New Challenges in Heat Treatment and Surface Engineering Conference, Dubrovnik, Croatia, June, 2009.

[18] D. Hall, F. Incropera, R. Viskanta, "Jet Impingement Boiling From a Circular Free-Surface Jet During Quenching: Part 1—Single-Phase Jet", Journal of Heat Transfer, 123 (5), 901-910, 2001.

[19] M. Maniruzzaman and R. Sisson, "Heat Transfer Coefficients for Quenching Process Simulation", Journal of Physics, IV France 120, 521-528, 2004.

[20] K. Oyakawa, K. Hanashiro, S. Matsuda, M. Yaga and M. Hiwada, "Study on Flow and Heat Transfer of Multiple Impingement Jets", Heat Transfer—Asian Research, 34 (6), 419-413, 2005.

[21] Y. Mitsutake, M. Monde, "Heat Transfer during Transient Cooling of High Temperature Surface with an Impinging Jet", Heat and Mass Transfer, 37 (4-5), 321-328, 2001.

[22] H. Jouhara and B Axcell, "Film Boiling Heat Transfer and Vapor Collapse on Spheres, Cylinders and Plane Surfaces", Nuclear Engineering and Design, 239, pp. 1885-1900, 2009.

[23] H. Jouhara and B Axcell, "Forced Convection Film Boiling on Phyrical and Plane Geometries", Institute of Chemical Engineers, Trans IChem, Vol. 80, Part A, pp. 284-289, 2002.

[24] P. Woodfield, A. Mozumder and M. Monde, "On the Size of the Boiling Region in Jet Impingement Quenching", International Journal of Heat and Mass Transfer, 52, 460-465, 2009.

[26] R. Reid, "Rapid Phase Transitions from Liquid to Vapor", Advances in Chemical Engineering, Vol. 12, pp. 105-208, 1983.

[27] M. Cum, "Notes on Droplet Heat Transfer", Chemical Engineering Progress Symposium Series 65 Vol. 92, pp. 175-187, 1969.

[28] M. Akmal, A. Omar and M. Hamed, "Experimental Investigation of Propagation of Wetting Front on Curved Surfaces Exposed to an Impinging Water Jet", International Journal of Microstructure and Materials Properties (IJMMP), Vol. 3, No. 4/5, 2008.

[29] K. Takrouri, M. Hamed, A. Hassan and J. Luxat, "Two-Phase Flow and Heat Transfer during Quenching of Hot Horizontal Cylindrical Tubes", Proceedings of the Fourth International Conference on Thermal Engineering: Theory and Applications January 12-14, 2009, Abu Dhabi, UAE.

[30] T. Ueda, M. Inoue, Y. Iwata and Y. Sogawa, "Rewetting of a Hot Surface by a Falling Liquid Film", International Journal of Heat and Mass Transfer, 3, Vol. 26, pp. 401-410, 1983.

[31] C. Liu and T. Theofanous, "Film Boiling on Spheres in Single- and Two-Phase Flows", Advanced Reactor Severe Accident Program, Center for Risk Studies and Safety, University of California, Santa Barbara, 1996.

[32] P. Woodfield, A. Mozumder and M. Monde, "On the Size of the Boiling Region in Jet Impingement Quenching", International Journal of Heat and Mass Transfer 52, pp. 460-465, 2009.

[33] J. Hammad, Y. Mitsutake and M. Monde, "Movement of Maximum Heat Flux and Wetting Front during Quenching of Hot Cylindrical Block", International Journal of Thermal Sciences, 43 (8), 743-752, 2004.

[34] A. Hauksson, D. Fraser, V. Prodanovic and I. Samarasekera, "Experimental Study of Boiling Heat Transfer During Subcooled Wtaer Jet Impingement on Flat Steel Surface", Ironmaking and SteelMaking, Vol. 31, No. 1, 2004.

[35] N. Hatta, J. Kokado and K. Hanasaki, "Numerical Analysis of Cooling Characteristics for Water Bar", Transactions ISIJ, Vol. 23, 1983.

[36] A. Cokmez-Tuzla, K. Tuzla and J. Chen, "Characteristics of Liquid–Wall Contact in post-CHF Flow Boiling", International Journal of Heat and Mass Transfer
Vol. 43, Issue 11, pp. 1925-1934, 2000.

[37] F. Xu, M. Gadala, "Heat Transfer Behavior in the Impingement Zone under Circular Water Jet", International Journal of Heat and Mass Transfer, 49, 3785–3799, 2006.
[38] J. Stevens and L. Witte, "Transient Film and Transition Boiling from a Sphere", International Journal of Heat and Mass Transfer, Vol. 14, pp. 443-450, 1970.

[39] www.omega.ca.

[40] Jason Jianxin Xu, "Flow Boiling Heat Trader In The Quenching Of A Hot Surface Under Reduced Gravity Conditions", PhD Thesis, University of Toronto, 1998.

[41] S. Cheng, P. Lau and K. POON, "Measurements of True Quench Temperature of Subcooled Water under Forced Convective Conditions", International Journal of Heat and Mass Transfer, Vol. 28, No. 1, pp. 235-243, 1985.

[42] G. Hewitt, J. Delhaye and N. Zuber, "Post-Dryout Heat Transfer-Multiphase Science & Technology", CRC Press, 1992.

[43] K. Fung, S. Gardiner and D. Groeneveld, "Subcooled and Low Quality Flow Film Boiling of Water at Atmospheric Pressure", Nuclear Engineering and Design 55, pp. 51-57, 1979.

[44] A. Mozumder, M. Ullah, A. Hossain and M. Islam, "Sessile Drop Evaporation and Leidenfrost Phenomenon", American Journal of Applied Sciences, 7 (6), pp. 846-851, 2010.

Appendix

Main Components of the Experimental Setup

Component	Type	Company	Model / Notes	Specifications
Water Handling & Circulating Section				
Water Heater	Electric	Bradford White	45 kW	www.bradfordwhite.com
Pump	Centrifugal	mcKeough	750 rpm, ¾ hp GOULDS	www.mckeoughsupply.com
Flowmeter	Turbine	Simark Controls	6.2000	www.simarkcontriols.com
Valves	Ball	Boshart	-	www.boshart.com
Valves	Gate	Boshart	-	www.boshart.com
Material for: Collct. tank Head tank	S. Steel	Metal Supermarkets	Three sheets: 4×8 ft^2 each	Wall: ~ 0.32 cm
Pipes 2.0 in. 2.5 in.	S. Steel	Metal Supermarkets	-	 SCH 40 SCH 40
Hoses	High temperature PVC	TT Liquid	To minimize vibrations	2 in.
Hose-end clamps	S. Steel	TT Liquid	-	2 in.
Strainer	Y-strainer	Sure Flow	Mesh # 165	www.sureflowequipment.com
Elbows	S. Steel	TT Liquid	-	2 in.
Tee connectors	S. Steel	TT Liquid	-	2 in.
Nozzles	Rectangular	Metal Supermarkets	1× ½ in.	
Specimen Section				
Specimens (Brass Tubes)	1 in. 2 in.	Canadian Brass Co.	-	www.canadianbrass.ca
Thermocouples	K-Type	Omega	KMQSL-040U-24	www.omega.com
T.C Extension Wires	K-Type Extension	Omega	PR-K-24-SLE	www.omega.com
Specimen holder	1 in. steel pipe	McMaster Carr	-	www.mcmaster.com
Motorized motion system	3 m/s max. speed	Velmex	-	www.velmex.com

Data Acquisition System				
DAS	64 Channels	NI	SCXI	www.ni.com

High Speed Imaging System				
Camera	FASTCAM-X PCI 1024	Fastec Imaging	-	www.hsi.com
Lenses	External	HIS	-	www.hsi.com
IR cut off filter	Absorptive Reflective	Sunex Inc.	IRC21-50R IRC30-50x50	www.optics-online.com
Lights	Halogen	Lowel	-	www.lowel.com
General Items				
Stands & Supports	Steel square tubes	Metal Supermarkets	Steel	1 ½ in.×1 ½ in.× 0.1 in.